STABILITY ENHANCEMENT OF HVAC GRIDS USING HVDC LINKS

Sharlene M'Builu-Ives

10 March 16

A dissertation submitted to the School of Engineering, University of KwaZulu-Natal, Durban, in fulfilment of the requirements for the degree of Master of Science

As the candidate's supervisor, I have approved this dissertation for submission.

Signed……..…….. Date……..

Name: Dr. Andrew Swanson

COLLEGE OF AGRICULTURE, ENGINEERING AND SCIENCE

DECLARATION 1 - PLAGIARISM

I, Sharlene M'builu Ives declare that:

1. The research reported in this thesis, except where otherwise indicated, is my original research.
2. This thesis has not been submitted for any degree or examination at any other university.
3. This thesis does not contain other persons' data, pictures, graphs or other information, unless specifically acknowledged as being sourced from other persons.
4. This thesis does not contain other persons' writing, unless specifically acknowledged as being sourced from other researchers. Where other written sources have been quoted, then:
   i. Their words have been re-written but the general information attributed to them has been referenced
   ii. Where their exact words have been used, then their writing has been placed in italics and inside quotation marks, and referenced.
   iii. This thesis does not contain text, graphics or tables copied and pasted from the Internet, unless specifically acknowledged, and the source being detailed in the thesis and in the References sections.

Signed

……

COLLEGE OF AGRICULTURE, ENGINEERING AND SCIENCE

DECLARATION 2 - PUBLICATIONS

Details of contribution to publications that form part and/or include research presented in this thesis (include publications in preparation, submitted, *in press* and published and give details of the contributions of each author to the experimental work and writing of each publication)

Publication 1: S M'builu Ives, A Edwards, AG Swanson, and N Parus, STABILITY ENHANCEMENT OF HVAC NETWORKS USING HVDC LINKS, South African Universities Power Engineering Conference, January 2015.

Publication 2: S M'builu Ives, A Edwards, AG Swanson, STABILITY ENHANCEMENT OF HVAC NETWORKS USING HVDC LINKS, Eskom Power Plant Engineering Institute Student Workshop, June 2015.

Signed:

Abstract

Eskom is facing challenging times where the national power grid is placed under extreme pressure, therefore, the long existing poorly damped low frequency inter area oscillations affects the stability constraints thus reducing the power transfer capacity. Consequently new power stations are being built in remote locations to reduce the short fall of generation capacity and the HVDC technology has become appealing to transport large amount of power over long distance. This research aims to prove that stability enhancement of parallel AC systems can be achieved with the use of HVDC schemes.

The HVDC system has the rapid ability to control the transmitted power during transient disturbances and this power system control has a significant effect on the dynamic performance of the system after a disturbance therefore the dynamic performance is related to the small signal stability, where the rotor oscillations are minimised and the system is brought back to steady state after an event or disturbance.The fundamentals of small signal stability in terms of observability, controllability, residues, network sensitivities and mode shape are explained together with a dominant oscillation path definition for HVDC links location selection. The key importance in controlling the power of the HVDC link to affect stability requires that the oscillation is observable and controllable. Simulation results on a simple four-generator, two-area test system are presented, with a view to benchmark the results and develop a fundamental understanding of how using HVDC links for power transfer can stabilise the grid.

The eigenvalue analysis of the system indicates the frequency of oscillations in the system and the generator's participation factors, together with the controllability and observability of the inter area mode (mode of interest). There are a number of test simulations results from a LCC-HVDC system (First Cigrê benchmark model) integrated into a test network where the influence on the small signal stability is analysed. Various literature has been reviewed which supports the basic principles, promoting the benefits of using HVDC systems to enhance stability of a parallel AC system (Hybrid) and then integrating supplementary control.

This research investigates the use of the HVDC system to enhance the small signal stability with supplementary control which is termed predictive control. Power Oscillation Damping (POD) control through LCC HVDC links is studied to ensure secure operation of power systems. The Power oscillating damper is expressed as a transfer function whereas the MPC (Model Predictive Controller) is expressed as cost functions of a feedback signal which is a measured quantity. Two feedback signals are selected and their effectiveness with regard to

their contribution to the damping of the system is investigated. The controller feedback signals are real power and voltage difference across the AC tie lines. Bode plots, root locus plots and time domain simulation results show the comparison between the different selected controller inputs and supplementary controls. The voltage angle difference is most effective as it is more sensitive to changes in the system and assists the controller in bringing the system to steady state in a shorter period of time when compared to the controller input that uses real power across the AC tie line.

The controllers with the HVDC integrated, do improve the damping of the system and it is related to shorter mode decay time, the MPC however has been investigated to reduce the change of loading levels of the AC tie lines following a change in system operating conditions. Simulation responses from the research show that this method is more promising and does not require prior knowledge of the possible contingencies due to its ability to handle complex multi variable systems with constraints, by using cost function algorithms to perform predictions of future plant behaviour and calculating the suitable corrective control actions needed to take the predicted output as close as possible to the target value which is the steady state. This research however demonstrates the fundamental principle which proves that the HVDC together with supplementary control can enhance stability of a parallel AC system.

Acknowledgements

This dissertation would not have been completed without the encouragement, support, guidance and keen intuition of my academic (dissertation) supervisor, Dr A. Swanson. I wish to thank him for his patience and dedication as a supervisor. Because mentoring goes beyond research, I also want to thank him for his continuous advice for my academic aspirations and professional life. Working with him has been a true privilege and a great source of inspiration. I would also like to thank A. Edwards for the support and advice as an Industrial mentor. I would also like to thank Eskom and the Eskom Power Plant Engineering Institute as well as Brian Berry for the knowledge and guidance provided during my research period.

I also wish to acknowledge the support of N. Parus and S. Mvuyana, from Eskom, who always were willing to help despite their busy schedules. I will like to thank the Lord Jesus Christ for giving me the strength through my studies. I will like to thank my close family: Yves (Husband), Jehedon and Liam, I thank my Mum, for her lifelong support and encouragement. I would have never accomplished my goals without their sacrifices. I wish to thank my friends for their friendship and encouragement during my studies. I will like to thank my Power Station Manager: Mr Gersh Bonga for the giving me this opportunity to further my studies. The support of my colleagues at the Grootvlei Power Station, especially the C & I department is truly appreciated. A very special thank you goes to Jolandie Krugar for her love, understanding, and for always assisting with my travel arrangements.

Contents

Acknowledgements ..... **vi**

Contents ..... **vii**

List of Figures ..... **x**

Symbols/Abbreviations ..... **xiii**

1 INTRODUCTION **1**

1.1 Problem Statement and Hypothesis 2

1.2 Importance of Study and Contribution 2

1.3 Structure of Dissertation 3

1.4 Scope and Limitation of the Research work 3

2 HIGH VOLTAGE DIRECT CURRENT TRANSMISSION: LINE COMMUTATED CONVERTER (LCC) **5**

2.1 Type of HVDC Transmission Technologies 5

2.2 HVDC Network Topologies 6

2.2.1 Monopolar link 6

2.2.2 Bipolar link 7

2.2.3 Homopolar link 8

2.2.4 Back to back link 8

2.3 LCC HVDC System and Components 8

2.3.1 Thyristor valve 9

2.3.2 Smoothing reactors 10

2.3.3 DC filters 10

2.3.4 AC circuit breakers 10

2.3.5 Earth electrodes 10

2.3.6 Reactive power supply (AC Filters) 10

2.4 LCC HVDC Converter operation 10

2.4.1 Thyristor controlled converter 10

2.4.2 Inverter operation 12

2.4.3 Reactive power in HVDC system 12

2.5 HVDC Control 13

2.5.1 Basic control principle 13

2.5.2 Advanced control characteristics 15

2.5.3 Control hierarchy and operations of an HVDC system 16

2.6 Performance Enhancements: Control for AC Systems 18

2.6.1 Power frequency control 18
2.6.2 Power oscillation damping 19
2.6.3 Step changes in power 19
2.6.4 HVDC system in parallel with an AC transmission line 20
2.7 Cigré Benchmark Model 22
3 ROTOR ANGLE STABILITY OF A POWER SYSTEM WITH HVDC 24
3.1 Transient Stability 24
3.2 Small signal stability 25
3.2.1 Linearised power system model 25
3.2.2 Eigenvalue and stability 26
3.2.3 Eigenvectors 28
3.2.4 Participation factors 28
3.2.5 Observability and Controllability 29
3.2.6 Residues 29
3.2.7 Identification of Power System Oscillations paths in Power System Networks 29
3.2.8 Mitigation of Small Signal Instability 30
4 IMPLEMENTATION OF A TWO AREA AC SYSTEM WITH HVDC INTEGRATION 32
4.1 Introduction 32
4.2 The two area system network: Base network 32
4.2.1 Base network system analysis 32
4.3 Additional Tie Line 38
4.4 LCC HVDC integrated in the network 39
4.5 Conclusion 47
5 SUPPLEMENTARY CONTROLLER DESIGN 48
5.1 Introduction 48
5.2 Power Oscillation Damping Control 50
5.2.1 POD Design Criteria 51
5.3 Model Predictive Control 52
5.3.1 The MPC controller 52
5.3.2 Types of signal used 53
5.3.3 Model and Horizon 54
5.3.4 Cost Function 54
5.3.5 Tuning/Weighting of the MPC controller 55
5.4 Results 55

5.4.1 Analysis of the Base network with HVDC integrated 56
5.4.2 Analysis of the Base network with a POD integrated 59
5.4.3 Analysis of the Base network with a MPC integrated 64
5.5 Conclusion 72
6 CONCLUSION 74
7 REFERENCES 76
8 Appendix A – State Space Model Details 83
9 Appendix B – Controller Design Code 84

List of Figures

Figure 1: Monopolar with ground return [2] 6
Figure 2: Bipolar HVDC link [6] 7
Figure 3: Typical LCC HVDC System 9
Figure 4: Voltage at the rectifier 11
Figure 5: Voltage waveforms and valve conduction periods - Inverter ($\alpha > 120^{o}$) 12
Figure 6: Steady state V-I characteristics [2] 14
Figure 7: Practical V-I characteristics 15
Figure 8: Basic control scheme [2] 17
Figure 9: A structure for a Power oscillating Damper controller for HVDC [11]. 19
Figure 10: A simple parallel AC/DC transmission system [2] 21
Figure 11: Cigré HVDC Benchmark Model [14] [12] [13] 23
Figure 12: Modes of oscillation representation [5] 25
Figure 13: Two Area Network [2] [32] 34
Figure 14: Mode shape of generator speeds - Inter-area mode G1G2/G3G4 35
Figure 15: Mode shape of generator speeds - Local Mode G1/G2 35
Figure 16: Mode shape of generator speeds - Local Mode G3/G4 35
Figure 17: Time domain of Active Power: Normal loading between bus 7 and 9 37
Figure 18: Time domain of Active Power: Heavy loading between bus 7 and 9 (600MW) 37
Figure 19: Time domain response after a fault with an additional AC line 39
Figure 20: Two area network integrated with the LCC HVDC link [32] 40
Figure 21: Mode shapes of generator speeds with HVDC – Inter-area mode 41
Figure 22: Mode shapes of generator speeds with HVDC – Local mode G1/G2 41
Figure 23: Mode shapes of generator speeds with HVDC – Local mode G3/G4 42
Figure 24: The time domain response with HVDC after an injected self-clearing fault 42
Figure 25: Time domain response of the Rotor angle displacement after a fault 43
Figure 26: Time domain response of Active Power between buses 9-10 44
Figure 27: Time domain response of DC link Voltage 44
Figure 28: Time domain response of DC Link Active Power 45
Figure 29: Time domain response of firing angle 45
Figure 30: Time domain response of Extinction angle 46
Figure 31: Time domain response of the scenarios: with and without HVDC integrated 46
Figure 32: MPC Structure 53
Figure 33: Eigenvalue analysis of the unstable network 56
Figure 34: Bode plot of the unstable network 57
Figure 35: Root locus with negative feedback 58
Figure 36: Root locus with POD – Real Power signal 60
Figure 37: Eigenvalue analysis of the network with POD - Power signal 60
Figure 38: Impulse response with POD - Power signal 61
Figure 39: Impulse response with and without POD - Power signal 61
Figure 40: Root locus with POD - Voltage angle difference signal 62
Figure 41: Eigenvalue analysis with POD - Voltage angle difference signal 63
Figure 42: Impulse response with POD - Voltage angle difference control signal 63
Figure 43: Impulse response with and without POD - Voltage angle difference signal 64
Figure 44: The MV and UD response Real power (top) and voltage angle difference (bottom) 66

Figure 45: Plant outputs time domain response: Real power (top) and Voltage angle difference (bottom)..... 68
Figure 46 : The HVDC voltage: Rectifier and Inverter of the Real power..... 69
Figure 47: The HVDC voltage: Rectifier and Inverter of the voltage angle difference..... 70
Figure 48: A Comparison of the two feedback signals input response..... 71
Figure 49: A Comparison of the two feedback signals real power output response..... 71

List of Tables

Table 1: Generator parameters in per unit with the rated MVA 33
Table 2: Generator units loading [2] 33
Table 3: Damping ratios and frequencies for the inter-area mode 36
Table 4: Damping ratios and frequencies for local and inter-area modes -additional tie line..... 38
Table 5: Damping ratios and frequencies for local and Inter-area mode with an HVDC link.... 40
Table 6: Comparative analysis of the residue of the inter area mode 58
Table 7: POD transfer function details..... 59
Table 8: The parameters of the MPC 65
Table 9: The Output code descriptions as per Figure 20..... 67
Table 10: Mode decay times of the feedback signals..... 72
Table 11: State Space Model Inputs and Outputs 83

Symbols/Abbreviations

AC – Alternating current

CC-Constant current

CCC- Capacitor commutated converter

CEA-Constant Extinction angle

CFC-Converter Firing controller

CIA-Constant Ignition angle

CV- Controlled variable

DC – Direct current

DPF-DIGSILENT Power Factory

ESKOM-South African electricity public utility(Electricity Supply commission-ESCOM)

HVDC – High voltage direct current

VDCOL-Voltage dependant current limiter

WAMS – Wide area measurement signal

ZESA-Zimbabwe electricity supply authority

LCC – Line commutating current

UD- Unmeasured disturbance

Lmod-Load modulation

MIMO-Multiple inputs multiple outputs

MPC – Model predictive controller

MV-Manipulated variable

PSS-Power system stabilisers

SCR-Short circuit ratio

SISO- Single input Single output

TCC-Thyristor controlled converter

VSC – Voltage source converter

SVC- Static Var compensator

1 INTRODUCTION

Eskom is one of the largest power utilities in the world supplying power to Southern Africa, this power house with an installed generating capacity of approximately 45 000MW is currently under extreme pressure to supply electricity, that is stable and sustainable due to a number of issues and therefore not operating at full capacity [1]. The transmission asset base is approaching its mid-life cycle and this challenge contributes significantly to the low short circuit ratio (SCR) which indicates that the South African grid is weak [1]. Stability is a term used to indicate that the grid is operating normally, but due to the constraints, any disturbance could cause the grid to go unstable [2]. The operating conditions that may cause this can be analysed through stability analysis, specifically small signal stability, which is the capability of the grid to remain stable after small disturbances [2].

South Africa currently has a single High Voltage Direct Current (HVDC) system which is the Cahora Bassa HVDC link that connects the hydroelectric scheme at the Cahora Bassa dam in Mozambique to the Apollo Station in South Africa. The scheme is rated to transmit 1920 MW at ±533 kV over a distance of 1420 km and is predominantly used as a bulk power transmission tool into the South African grid [3].

HVDC technology has become more appealing because of its ability to transfer large amounts of power over long distances. This would be used to transmit power directly into the load centre [3]. The HVDC system is characterised by the rapid ability to control the transmitted power during transient disturbances, the HVDC controls can ramp the DC power rapidly to reduce generation or unbalanced loads on both sides and the DC power can be ramped up rapidly to support system stability by using the short term overloading capability of the LCC HVDC system [2] [3].

There is some indication that due to the fast acting converters of the HVDC system, small signal stability enhancement is possible. Kundur has shown that a HVDC system in the path of the oscillation with a supplementary controller can be used to enhance stability [2]. This dissertation investigates the use of the HVDC system with or without supplementary control to enhance the small signal stability of a simple two area study system in order to gain a fundamental understanding which can be extended to large scale practical systems [2] [4].

1.1 Problem Statement and Hypothesis

The Southern African power systems have various modes of oscillations due to the many interactions of different components as the number of machines is represented as a number of masses connected by a network of springs. The masses of the generators' rotors swing relative to one another creating these rotor oscillations and hence these inter area mode of oscillations can cause the system to be excited and lead to black outs if the protections activate [5].

Eskom is currently only using the HVDC link for power transmission while forfeiting the benefits of the HVDC controls which can contribute positively to the Southern African power system stability. The large AC interconnected system can be unstable thus leading to overloads and stability problems. Eskom would prefer to use the HVDC link to stabilise the grid thus preventing a dangerous break down of system security. The unstable network can be overcome by placing HVDC schemes strategically, taking advantage of the fast controllability of the DC power, damping and timely overloading capabilities available. Supplementary controllers would need to be developed on a simple network with steady and dynamic requirements to test for power system stability enhancement capabilities. The HVDC link has a high performance control technology tool that is well adapted for oscillation damping and this contingency should be explored to validate its worth to the power system with regard to stability enhancement.

The hypothesis of the research stipulates that the integration of a parallel LCC HVDC link in an AC network does enhance small signal stability.

1.2 Importance of Study and Contribution

The following lists the contributions of the study to industry:

- Investigating the small signal stability in relation with the application of a parallel LCC HVDC link onto a simple network for fundamental understanding.
- The development of supplementary controllers in terms of predictive control for small signal stability enhancement.

1.3 Structure of Dissertation

Chapter 2: The fundamentals of the HVDC system are presented which include the different types of HVDC technologies, HVDC topology layouts, HVDC control characteristics and components functionality. Graphical representation of topology configurations and HVDC control characteristics are outlined.

Chapter 3: The fundamentals of small signal stability in terms of observability, controllability, residues, network sensitivities and dominant oscillation path are explained.

Chapter 4: The chapter presents the eigenvalue analysis of the system which indicates the various frequency of oscillations in the system and the generator's participation factors together with the controllability and observability of the inter area mode. This chapter includes a number of test simulations on the LCC HVDC system integrated into the network and the impact on the small signal stability.

Chapter 5: The fundamentals of controller design specifications are presented in this chapter including a review of literature supporting the use of supplementary control to damp out power oscillations. A full representation of a network model in terms of its state space equivalent is used, in order to test the concept of supplementary control through HVDC links for stability enhancement in power systems. The Power Oscillation Dampers and Model Predictive Controllers are the supplementary controllers designed and are used in simulation studies where the responses are analysed for discussion.

Chapter 6: This chapter concludes the dissertation and provides recommendations for further work applicable in the field.

1.4 Scope and Limitation of the Research work

The investigation of voltage and frequency stability is excluded and all time domain studies are performed on a small test network

2 HIGH VOLTAGE DIRECT CURRENT TRANSMISSION: LINE COMMUTATED CONVERTER (LCC)

HVDC power transmission is used minimally by Eskom and the added benefits of the HVDC control technology does not contribute to the Southern African power system stability. This chapter will provide the basic principles of HVDC transmission including the operating principles, control and topologies so that an understanding of its advantages and applications can be holistically appreciated.

2.1 Type of HVDC Transmission Technologies

There are three different types of HVDC transmission technologies [3] [6] [7]. These are [3] [6] [7]:

- Line commutated converter or LCC HVDC
- Voltage source converters or VSC HVDC
- Capacitor commutated converter or CCC HVDC

Thyristors with a high current rating and thyristor banks with voltages up to 1000 kV are being developed. Due to the high voltage and high current rating, the LCC HVDC is the most suitable for bulk power transmission [8].

VSC HVDC appears to the AC network as a controllable load and generator without the need of an independent AC voltage source. This functionality promotes black start capabilities and delivers power into a passive AC network. VSC HVDC is more suitable as a power rating up to 800 MW permits low power connections of wind farms and the connection to a weak grid as it does not need compensation for reactive power [8].

The Capacitor commutated converter (CCC) is characterised by having capacitors inserted in series to the leakage impedance of the converter transformers and the main converter valves. The capacitor provides a force commutated facility and compensates for reactive power demand. However the CCC offers a more costly and complex operational alternative to the line commutated converter (LCC) [8].

Eskom has a need for bulk power transmission and as a result the dissertation focusses on using the LCC HVDC schemes for stability enhancements. This will therefore save Eskom time and money into the future.

This HVDC technology displays the following applications and advantages [2]:

- Asynchronous link between two AC systems with system stability problems or a difference in nominal frequencies.
- For underwater cables longer than 30 km because AC transmission is not practical, this is due to the high capacitance of the cable resulting in the need for direct compensation stations.
- Transmission of bulk power over long distance in excess of 600 km.
- Stabilisation of power flow in an integrated Power system [2] [3].

2.2 HVDC Network Topologies

HVDC systems are divided into four main topologies namely Monopolar, Bipolar, Homopolar and Back to Back schemes [2] [6]. The most commonly used topology configurations will be shown below .i.e. Monopolar and Bipolar.

2.2.1 Monopolar link

Figure 1 shows a Monopolar link with only one pole of either polarity. The return path is usually an earthed, metallic return (conductor at low voltage) or water and it may be used for cable transmission. It is also considered the first stage of development of the bipolar system. Metallic return can be used in an area where the ground resistivity is too high or there is likely corrosion of underground or water metallic structures [2] [6]. The 350 kV, 300 MW Caprivi link between Namibia and Zambia is an example of a Monopolar system [9] [10].

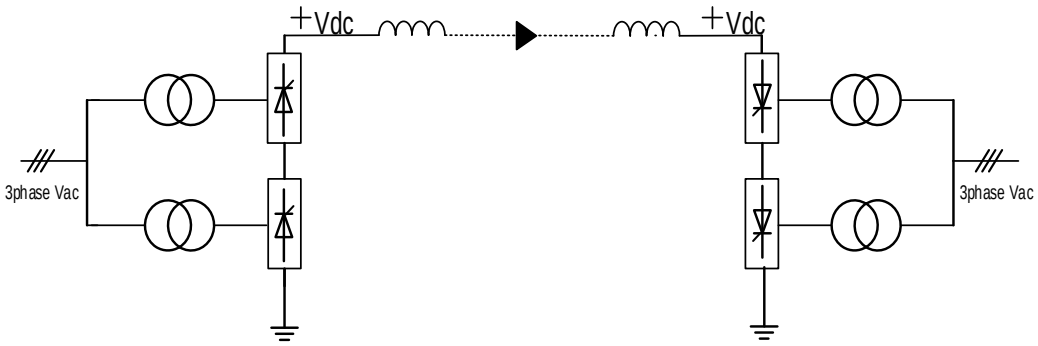

Figure 1: Monopolar with ground return [2]

2.2.2 Bipolar link

The bipolar link is seen in Figure 2. It has two poles, one positive and one negative. Each terminal has two converters with the same rated voltage, which are coupled in series on the DC side. There are no earth currents because the junctions between the converters are earthed, resulting in both poles operating independently. This is ideal during outages and maintenance activities when one pole can be out of service and the power can be still transferred. One pole can operate on its own with the use of the earth return, transporting the rated load or more by using the converter's overload capabilities and the DC line. The advantage of the bipolar link is that it will create less harmonic interference on the neighbouring facilities. Due to the high power levels associated with HVDC transmission, it is important to maintain reduced levels of AC current harmonics and DC voltage ripples of the converter. The actual level of harmonics produced by an AC/DC converter is a function of the period over which a phase brings unidirectional current to the load.

Therefore, the higher the "pulse number" of the converter (twelve pulse bridge configuration of the bipolar topology), the more switching between phases of cycle exists. This generates lower harmonic distortion in the AC line current and the DC terminal voltage [10]. A third conductor can be used as a metallic neutral and is used as a return path if one pole is out of service or when there is an imbalance during bipolar operation. It usually needs low insulation and also serves as a shield wire for overhead lines [6] [2]. The Cahora Bassa HVDC is an example of a bipolar system with each pole running on a separate tower [3].

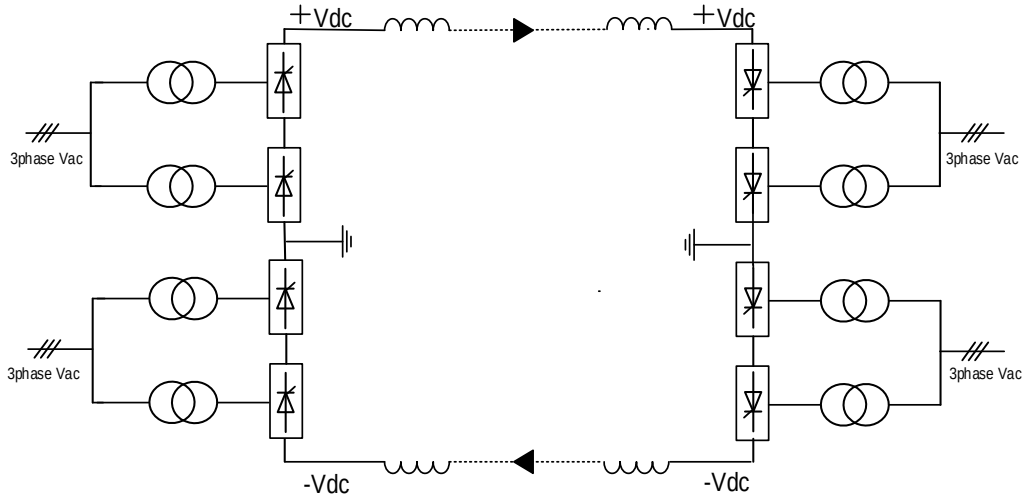

Figure 2: Bipolar HVDC link [6]

2.2.3 Homopolar link

The system configuration consists of two or more poles with the same polarities and an earth return. Negative is the more common choice due to the fact that corona under negative polarity causes less radio interference [2] [6].

2.2.4 Back to back link

The transmission distance between the rectifier and the inverter is very short and when connecting two asynchronous AC networks, the converters can be on the same site or building [6] [2].

2.3 LCC HVDC System and Components

HVDC schemes converts AC power into DC power at the rectifier terminal (sending end) and then it is converted back to AC power at the inverter terminal (receiving end) as seen in Figure 3. AC power is sent to a converter functioning as a rectifier. The rectifier outputs DC active power therefore it is not affected by the AC supply frequency and phase. The power is transmitted through overhead lines, cables or short lengths of bus bars to the second converter. This second converter (inverter side) is run as a line-commutated inverter and permits the DC power to move into the receiving AC network. Conventional HVDC transmission uses line-commutated thyristor technology [10].

When a gate pulse is introduced, the thyristor will conduct current. Conduction continues without additional gate pulses with the current flowing in the forward direction. Thyristor “turn-off” occurs only when the current reverses and a thyristor converter requires AC voltage to function as an inverter. As a result the thyristor-based converter topology used in HVDC systems is referred to as a line-commutated converter (LCC). The typical HVDC system and its components are illustrated in Figure 3.

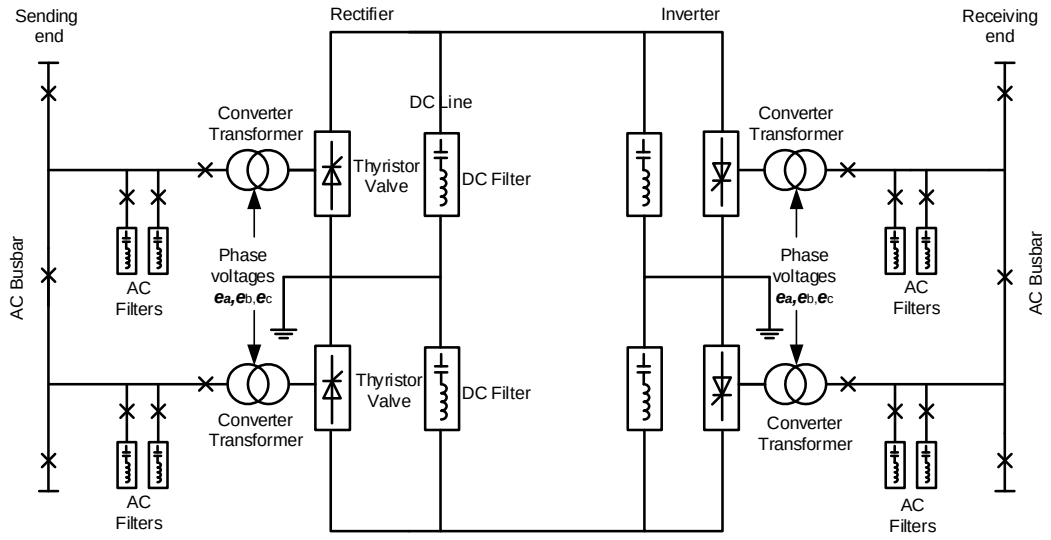

Figure 3: Typical LCC HVDC System

The thyristor based converter topology consists of thyristor valve bridges and converter transformers. The conversion from AC to DC is performed with the arrangement of high voltage valve bridges in a twelve or six pulse configuration according to the required output voltage. The converter transformer is used to provide a commutating voltage to the thyristor valves bridge at the appropriate level. The converter circuit of an HVDC converter is a three phase full wave bridge which is known as a Graetz bridge. The Graetz bridge configuration is commonly used for HVDC converters as it makes better use of the transformer and reduces the voltage drop across the valve when it is not conducting [2]. The components of the LCC HVDC system are briefly described below:

2.3.1 Thyristor valve

A thyristor is an electronically controlled switch also referred to as a valve. When a positive voltage is applied at the gate of the valve, the current is conducted in the forward direction. There is a small voltage drop across the valve when it is conducting. When the current attempts to reverse direction, making the cathode positive relative to the anode, the current is blocked by the valve as it will turn off and appear as high impedance. After conduction initiation, the current through the valve continues until it reaches zero and a reversed voltage appears across the valve. The valve can conduct current in one direction after the control pulse triggers it into conduction, subsequently the current is blocked until the next control pulse trigger [3].

2.3.2 Smoothing reactors

These are big reactors coupled in series with each pole of individual converter stations with an inductance as high as 1.0 H [2]. The reactors prevent commutation failures on the inverters, inhibit current from being irregular at low loads, restricts the rectifier's crest current for the duration of the DC line fault, and decreases harmonics on the DC line [3] [10].

2.3.3 DC filters

These harmonic filters are used to decrease harmonics which have detrimental effects on infrastructure such as transformers, especially harmonics that may cause interference with telecommunication systems [2] [3] [10].

2.3.4 AC circuit breakers

The AC circuit breaker clears faults in the transformer and forces the DC link out of operation. The converter control is used for clearing DC faults [2] [3] [10].

2.3.5 Earth electrodes

Electrodes are conductors which are connected to earth and may be used as part of the earth return in a monopolar system or for short periods of time in a bipolar system [2].

2.3.6 Reactive power supply (AC Filters)

The HVDC converters absorb reactive power therefore reactive power sources are connected closer to the converters. The reactive power used is approximately 60 % of the power transferred during nominal operating conditions and much higher under transient conditions. The AC filters are often designed to account for this [2] [3].

2.4 LCC HVDC Converter operation

2.4.1 Thyristor controlled converter

The mean direct voltage (Vd) is changed by controlling the instant at which the thyristors are switched on and the thyristor controlled converter (TCC) is responsible for this control action. The firing delay angle, α, (also referred to as the ignition delay angle) is referred to as the angle between the time when the thyristor is fired and the phase voltage crossing over the valve-winding voltage as seen in Figure 4. This firing delay angle determines when the commutation process (the transfer of current from one valve to another) begins and therefore the magnitude of

mean direct voltage (Vd). Vd is proportional to the cosine of the firing delay angle therefore the larger the delay angle results in a smaller Vd [10]. The steady state operation of the converters are directed by the standard converter equation relating direct voltage (Vd), direct current (Id), converter transformer valve winding emf (E_{L_L}) and commutating reactance (Xc) with the firing delay angle to which the converter is controlled. The converter equation is seen below [8]:

$$Vd = \frac{3\sqrt{2}}{\pi} E\text{L\_L} \left(Cos\ \alpha - \frac{Id Xc}{2} \right) \quad (1)$$

Equation 1 shows that the given Vd will require a smaller EL_L if Xc is decreased hence the transformer cost will increase however similarly the EL_L will reduce if the firing delay angle at the rectifier (or γ at the inverter) is decreased [8]. After analysing the emfs of phase A, *ea*, as the firing delay angle is increased, the phase displacement between alternating voltage and alternating current in a supply phase also changes [2]. The angle, α, shifts the current wave and its fundamental element by an angle ϕ = α, with α =0, the fundamental current element is in phase with the phase voltage, *ea*, the active power (Equation 2) is positive and the reactive power (Equation 3) is zero. As α increases 0 ° to 90 °, the active power (Pa) decreases reactive power (Qa) increases. The setting of the firing angle of the thyristor valves defines the size and polarity of the direct output voltage after rectification.

$$Pa = eaIa\ Cos\phi \quad (2)$$

$$Qa = = eaIa\ Sin\phi \quad (3)$$

Due to the commutation reactance, the phase currents cannot change instantly therefore the time taken to transfer the current from one valve to the other is referred to as the overlap angle or commutation angle and is denoted by μ as per Figure 4. When operating in the rectifier mode, the following angles are described: firing delay angles, α, overlap angle, μ, and extinction delay angle, δ (μ + α). A graphical explanation is seen below in Figure 4

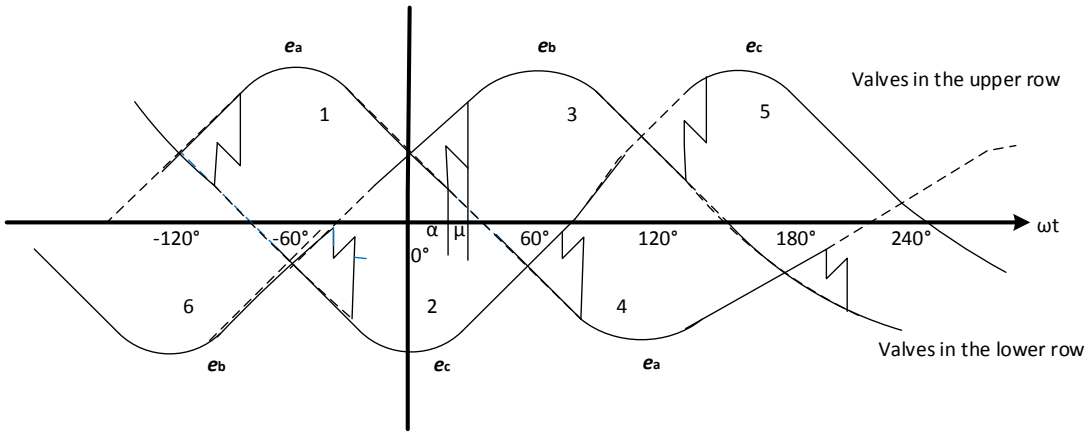

Figure 4: Voltage at the rectifier

2.4.2 Inverter operation

When relating Figure 5 and Equation 1 and 2, At 90°, Pa is zero hence zero voltage is reached and Qa is maximum, as α increases from 90° to 180°, Pa becomes negative hence the DC terminal voltage is negative and increases in size, Qa remains positive and decreases in magnitude. At 180° Pa is negative maximum and Qa is zero.

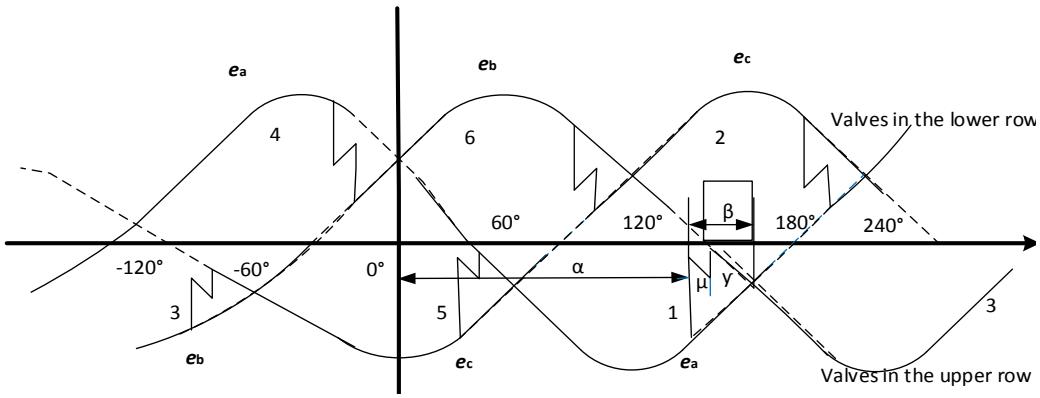

Figure 5: Voltage waveforms and valve conduction periods - Inverter (α >120°)

Beyond 90°, the firing delay angle (α) of the TCC is usually referred to as the "extinction angle" or "gamma" (γ) as seen in Figure 5. This extinction angle characterises the period between the end of the overlap period and the instant when the phase voltage related with the existing valve becomes more positive/negative than that of the succeeding valve in sequence as seen in Figure 5, and it is expressed mathematically as seen in Equation 4:

$$\gamma = = 180 - \mu - \alpha \tag{4}$$

Control of the output voltage of a six-pulse bridge is only accomplished by the firing delay angle (α). The extinction angle, γ, is the existing turn-off time for the thyristor valve following the time when the valve is fired. With the inverter operation, α and δ are defined in the same way as in the rectifier but with values of 90° and 180°. It is common practice to use the ignition advance angle, β, and the extinction advance angle, γ, to describe the inverter's performance. These angles are defined by their advance with respect to the instant when the commutating voltage is zero and decreasing as seen in Figure 5 [2] [7].

2.4.3 Reactive power in HVDC system

The converter absorbs reactive power from the AC system whether it operates as an inverter or as a rectifier. They are seen as reactive power loads as they operate in situations where the current lags the voltage because of the firing delay angle. The converter transformer impedance

however brings a further lag in the current (referred to as the overlap angle) as described earlier through equation 1 and 2. [10] [2]. The AC harmonic filters are considered the main sources of capacitive reactive power in a HVDC station. They reduce the harmonics added into the AC system and generating reactive power. An AC filter is composed of capacitances, inductances and resistances but the HV-connected capacitor is the main supplier of the reactive power generated at fundamental frequency [9].

2.5 HVDC Control

HVDC control is the most important part of the HVDC system as it has fast acting controls which are more advanced than controls on an AC system (such as the control of generators) [3]. It is very important that the HVDC control is designed correctly as this fast acting control system can assist the weak AC network to recover from faults in order to avoid AC system voltage instability or voltage collapse [2]. The control requirements for HVDC power transmission related to control functionality is determined from the HVDC system objectives and varies between different projects [3]. The control requirements include the following attributes [7] [2]:

- Flexibility in the control of power.
- Fast control response.
- Stability under all operating conditions.
- Good transient recovery.
- Promote AC system performance.
- Robustness in the ac system events.
- Maintaining symmetrical valve firing in the steady state.
- Prevention of repetitive commutation failure in inverters.
- Reactive power control.

2.5.1 Basic control principle

HVDC bridges convert AC power into DC power at the rectifier terminal and the inverse at the inverter terminal to allow power flow to the AC network. The advanced controls keep the direct voltage at specific levels for the transfer of power from or into the AC network. The rectifier's output voltage differs to the inverter's input voltage due to a volt drop caused by the resistance of the transmission line [7] [3]. The basic HVDC control characteristics are graphically illustrated below as seen in Figure 6. [10] [2]

The rectifier has two segments, Line AB and Line FA as per Figure 6 Line FA, limits the DC voltage to an acceptable magnitude in an incident of a control failure at the inverter or a communication system failure. Line AB relates to the constant current characteristic with the rectifier controlling Id in normal steady state conditions. Line FA relates to the minimum ignition angle (firing delay angle) and represents the CIA (constant ignition angle) control mode as shown in Figure 6. The constant current, CC, characteristics may not be truly vertical as seen in Figure 6, depending on the current regulator and its finite gain. The rectifier complete characteristic at normal voltage is defined by FAB and with reduced voltage, it moves as indicated by F'A'B as seen in Figure 6. The inverter complete characteristic intersects the rectifier's characteristic at point E (normal operating point) for normal voltage but not for reduced voltage at F'A'B.

This sudden reduction in voltage could cause the current and power to reduce to zero and this is avoided by setting the set point of the inverter current controller to a lower setting than that of the rectifier. The complete inverter characteristic is related to AGH consisting of the constant extinction angle (CEA) and the constant current (CC) as seen in Figure 6. [2]. The current margin as indicated by Im in Figure 6 is defined as the difference between the inverter current order and rectifier current order and is set to 10 - 15 % of the rated current to avoid crossing each other due to errors in measurements [2]

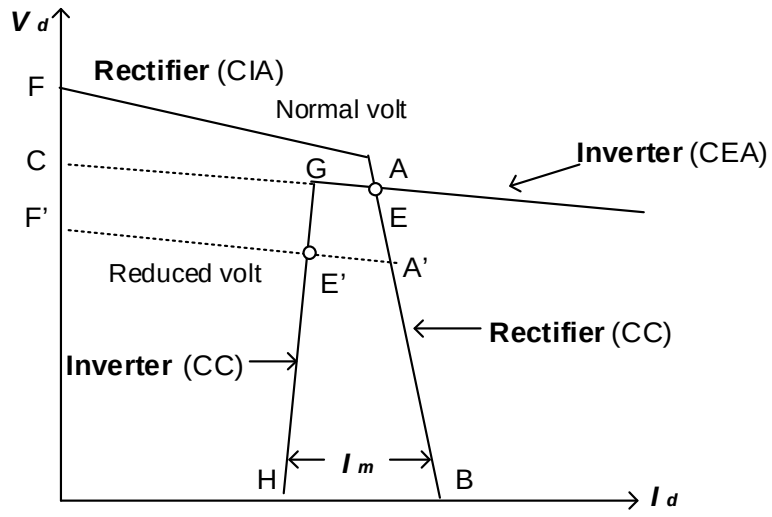

Figure 6: Steady state V-I characteristics [2]

At point E as seen in Figure 6, normal operating conditions, the rectifier controls the direct current and the Inverter controls the direct voltage but at point E', with reduced rectifier voltage

caused by a nearby fault, the inverter takes over direct current control and the rectifier controls the voltage i.e. reversed roles. The change from one mode to the other is called mode shift and happens frequently in this dynamic system [7] [2].

2.5.2 Advanced control characteristics

In Industry, there are limits for the firing delay angle and the current as seen in Figure 7, these advance control characters assists in avoiding system events on HVDC system. Hence when the rectifier maintains constant current by varying α until αmin is reached (as seen in Figure 7). The rectifier firing delay angle α is prevented from going below a fixed value αmin by its control action. The value of αmin is 3^{o} to 5^{o} and ensures that there is sufficient positive voltage across the valve before it is fired. At this point a further voltage increase is not possible with control action as the direct voltage maximum is set and the rectifier will operate in constant ignition control. There is a constant operating line (CEA as per Figure 7) for the inverter (γ line) which prevents the inverter from operating below the minimum extinction angle with control action.

The inverter operates with an extinction angle of 15^{o}-19^{o} under steady state conditions and at constant extinction angle during fault conditions within a receiving AC network. Hence, the smaller value of γ causes the inverter to be exposed to commutation failure. The current order Io on the other hand is determined by an outer power control loop and is subject to minimum and maximum limits. The minimum limits is to avoid problems at low DC currents and the maximum limits is determined by the overload capability (depends on the operating temperature of the thyristor valves). The steady state V-I characteristics with voltage dependant current order limiter, (VDCOL), minimum current limit are shown below in Figure 7.

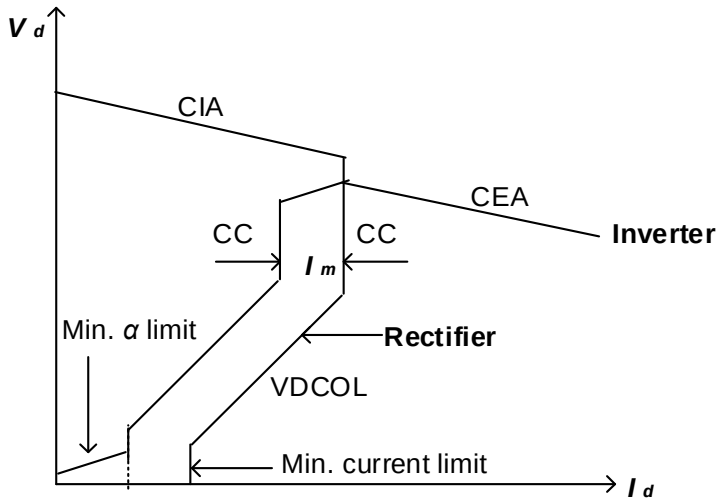

Figure 7: Practical V-I characteristics

These advance control actions are used together with associated control loops. These control actions are explained as follows [2]:

Minimum Current limit: The current is interrupted 12 times per cycle in a 12-pulse action therefore high voltages are induced in the transformer windings and the DC reactor, by the high rate of change of current at the time of current interruption. Low values of DC voltage, creates small overlap angles even though the current is continuous. This commutation period from start to finish being so close together causes stress on the valves due to voltage excursions. A minimum current limit is therefore needed as seen in Figure 7 [2] [3].

Voltage Dependent current order limit (VDCOL): When the AC bus voltage drops at one of the HVDC converters resulting in a DC voltage drop, then a higher voltage at the remote converter is demanded to control the current [2] [7]. There is definitely a risk of commutation failure and voltage instability due to the drop in AC voltage caused by system faults. The VDCOL has a disadvantage as it may clash with the AC overvoltage (Vacmax) control loop. If there is AC system over voltage, the converter reactive power consumption increases by decreasing the α at the inverter which reduces the Vd and the VDCOL control action operates by limiting Id thus preventing the effective reactive power consumption [3] [7].

The inverter characteristic duplicates the rectifier VDCOL to maintain the current margin. Implementation of the VDCOL includes a simple time lag transfer function. The measured direct voltage is sent through a first-order time lag, which is designed differently for increasing and decreasing voltage conditions. For falling voltages, fast VDCOL action is required; hence a short time constant is employed. The time lag is made larger when the DC voltage is recovering, to avoid control oscillations and possible system instability. The break points are between 30% and 80% of the DC voltage and higher break points can be used if the AC system requirements demands, it is evident that a higher breaking point can assist a receiving AC network which is sensitive to disturbances thus reducing the risk of large voltage oscillations [2] [3].

2.5.3 Control hierarchy and operations of an HVDC system

The HVDC control loops are layered in terms of hierarchy with different speeds of response and time precision. A basic control scheme is shown in Figure 8 and the control hierarchy changes from one DC scheme to another but the basic concepts are the same. The HVDC control scheme is divided into four levels [4] [2] [3]:

- bridge or converter unit control,
- pole control,

- master control and
- overall control

The bridge unit control selects the firing times of the valves within the bridge and selects α min and γ min limits. The bridge unit control is the fastest response within the control hierarchy. The pole control coordinates the control of bridges in a pole. The conversion of the current order (current set point) to a firing angle order, tap change control and certain sequence protection is managed by the pole control [3] [2]. This includes coordination of starting up, balancing of the bridge control and de-blocking. The current order and coordinated current order signals are provided by the master control to all the poles. There is an interface between the pole controls and the overall system control created so that the master control as seen in Figure 8 can interpret the broader demands of the HVDC system.

The inner loop is the fundamental converter control unit which outputs accurately timed pulses synchronised with AC system phase voltage waveforms. The input to this unit is the error signals chosen by means of a loop selector. The error signals are generated from variances between set points and measured variables such as DC current and voltages and min α (α min) and γ (γ min). The net result is the phase advance or phase retardation of the firing angle, α, and hence the valve firing pulses depending on the size and sign of the particular signal selected [2].

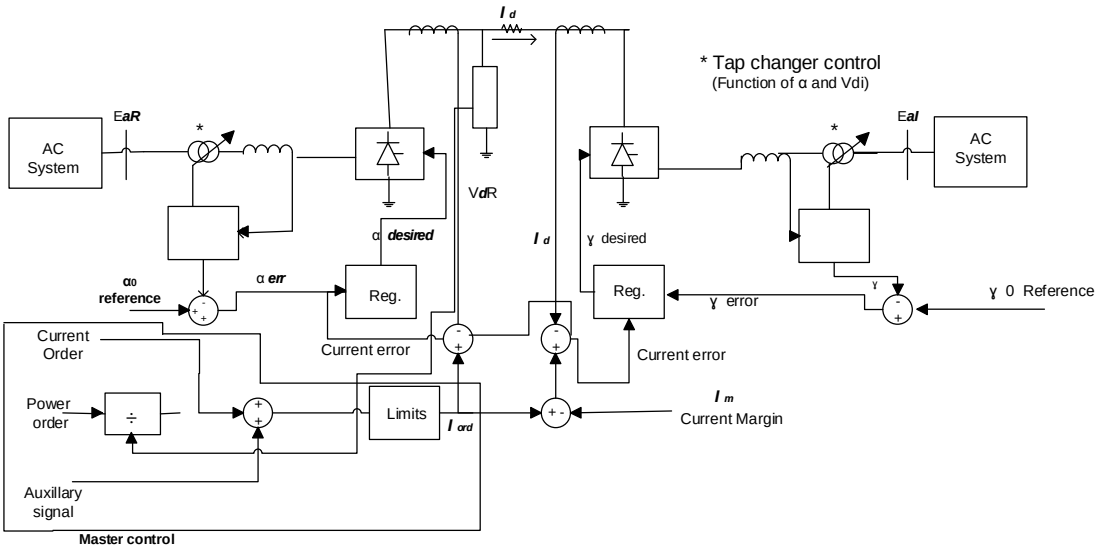

Figure 8: Basic control scheme [2]

Converter firing controller, CFC, determines the firing instants for each valve in the converter and lies at the centre of the control system. There are many control loops in a controller which are similar in structure. In industry, multiple loop controllers are used in the same controller with loop selection decision logic determining which control loop is in control at any time. CFC

essential task is to generate sequences of valve firing pulses with a delay angle, α, timed relative to the AC voltage waveforms such that the error signal of the active control loop is driven towards zero. CFC also matches all the timing information to the AC bus voltages to prevent out of sequence firing valves in relation to the zero crossings of the voltage waveforms. It also places limits on the rectification and inversion by means of control loops [2] [3] [10].

It is very important that at least one thyristor in the group has a firing pulse available to it and is ready to fire when a forward voltage appears across it. There are two methods to simultaneously generating and synchronising converter firing pulses within converter firing controller. These are Individual Phase Control (IPC) and Equidistant Firing Control (EFC). The IPC method determines the firing instants for each valve depending on the zero crossing of the AC waveforms so that a constant delay angle is maintained across all valves. The Equidistant firing control over comes some deficiencies of the IPC by using the phase lock oscillator technique. Equal time intervals are maintained between successive firing pulses under fault conditions and steady state. The phase locked and phase limited oscillator is indirectly synchronised to the AC system to provide stable operation even if the system goes out of steady state [2] [10].

2.6 Performance Enhancements: Control for AC Systems

2.6.1 Power frequency control

The frequency of both AC networks will change when the DC power order of a HVDC scheme changes, depending on the generating capacity. The frequency of only one AC system (rectifier or inverter side) can be controlled at a time. If the power order is increased to increase the receiving system frequency, then the sending frequency is reduced. The AC system frequency control by the HVDC schemes is implemented for the following purposes [2] [3]:

- Frequency control of the sending end AC system for DC transmission from remote power sources
- Frequency control of an AC system in an isolated island or a small AC system when it is interconnected to a large AC system through a DC link.
- Frequency control, when interconnected by systems with different frequencies.

AC system frequencies control is initiated when the system frequency of the controlled AC system exceeds certain limits. It can also be initiated when the AC system is islanded from the main AC network and the only means of power transfer is via the HVDC system [2] [3] [4].

Limits are applied to power variations or rate of change of power necessary to maintain the AC system voltage fluctuations within specified bands. When two AC systems with different frequencies are interconnected, a suitable dead band is implemented to compensate the effect so that only large or fast frequency disturbances are compensated by the DC power control [2] [3] [4].

2.6.2 Power oscillation damping

Power Oscillation Damping (POD) is positive damping to electromechanical oscillations between generators or groups of generators in the frequency range up to 3 Hz through the modulation of the power order current order to the rectifier. The voltage angle difference, change of real power, AC system frequency or rate of change of AC power can be the input signal for this supplementary control [3]. The small signal oscillations and the dominant oscillation path of a system are of interest in this research and will be explored in Chapter 3; the development of a controller will be explored in Chapter 5. This schematic arrangement as seen in Figure 9 shows the derivation of the power oscillation damping (POD) signal [3].

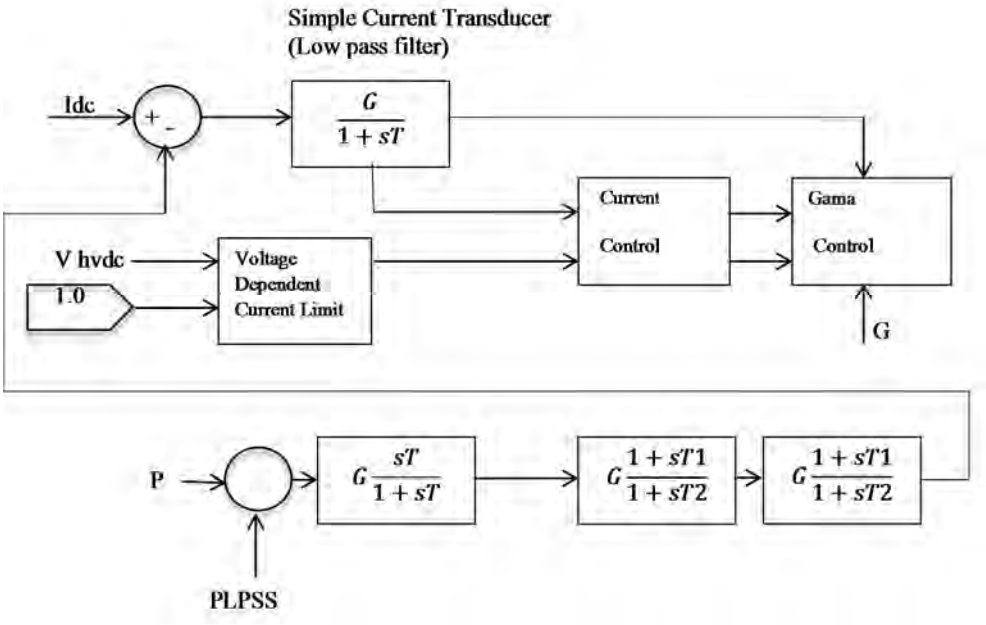

Figure 9: A structure for a Power oscillating Damper controller for HVDC [11].

2.6.3 Step changes in power

The HVDC power should be changed in steps to improve the AC system's response during and after power system disturbances. This may also involve DC power reversal under certain circumstances. An AC trip line, loss of large power supply sources or a sudden decrease or

increase in power system loads are the power system disturbances or events considered when using power step changes with HVDC power. The HVDC step power changes initiation signal is usually a large change is loading, a large frequency deviation or the tipping signal of a transmission line which is detected at the HVDC substation. There should be set priorities if there are many initiating signals for power demands with specified contingencies [2] [3] [4].

2.6.4 HVDC system in parallel with an AC transmission line

Transient angle stability difficulties exist in AC networks where a long AC transmission line linking two AC systems experiences unstable power oscillations. The HVDC system in parallel with an AC transmission line can assist in the enhancement of AC power system stability. However the DC current cannot be increased without considering the effect of transmission angle swings when the HVDC system has a parallel AC path. Figure 10 shows the simplified parallel AC/DC transmission system. The HVDC control modulates the active power transmitted to respond to changes in the phase angle between the two connected AC regions. Frequency or voltage angle difference, real power or current in the parallel AC line are possible input/feedback signals to the damping controller of the HVDC system [3].

Since the HVDC power is independent of angular difference between the AC terminals, maintaining the HVDC power flow or increasing it will strengthen the weak AC parallel transmission corridor. Careful consideration must be taken when designing the HVDC control in order to avoid inciting transient voltage instability when faults occur. The control strategy must be able to see situations when the parallel AC link is opened and the two AC networks lose synchronism. They can also provide timely and enough synchronising and damping torque to avoid voltage instability. The short term overloading capabilities of the HVDC converters should be considered as a control strategy to improve system stability [2] [3].

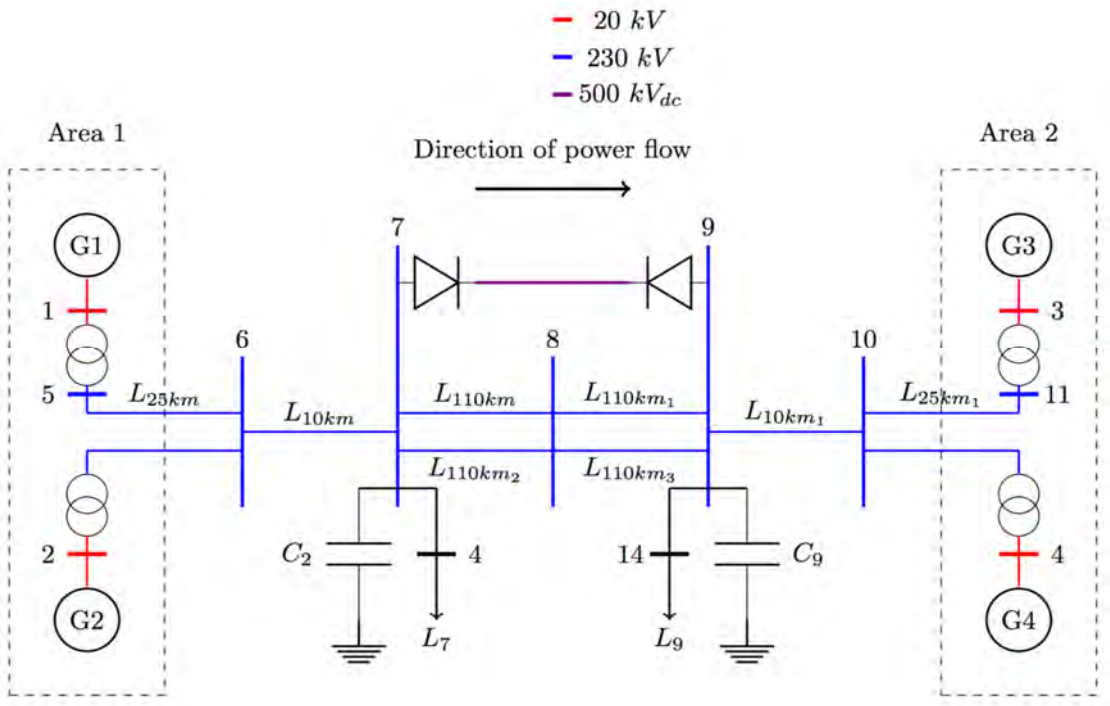

Figure 10: A simple parallel AC/DC transmission system [2]

In a weak AC transmission, where the power flow capacity is less than the HVDC system, the HVDC controls can employ a strong influence on the total power flow. Throughout transient stability swings of the AC transmission power angle, the HVDC system can effectively increase the stability margin by increasing its current order. However, if the HVDC system trips causing the transfer of power from the HVDC system into the parallel AC lines (at Bus 7 and 9 in Figure 10), the voltage collapses in the AC system. Pre-planned operational AC line-tripping schemes should be initiated on the detection of an HVDC system trip event thus preventing voltage collapse. When the AC line power flow capacity is greater than that of the HVDC system, increasing or even maintaining the DC power during transient variations of the AC transmission load angle will deny the system of the synchronising torque [3] [4].

With the increase in the DC current due to the overload capacity of the HVDC system, a drop in the power transfer capability is seen and hence synchronising torque with large values of swing angles. This is evident since AC systems operating with larger swing angles require higher synchronising torque to maintain transient stability otherwise they become unstable and cascaded blackouts occur. When both the AC and DC transmission capacity are comparable, maintaining constant DC power can become overpowering and this trend increases as the AC interconnection becomes stronger. These effects can be mitigated by using the exceptional control capability of an HVDC system and assisting in damping power oscillations. The control strategies for the HVDC system can be developed to assist the momentary synchronising torque

generated by the combined AC/DC transmission. The control signals are derived from the real power flow on the parallel AC lines. The control strategy should be validated with small signal stability studies on accurate system models which will be seen later in chapter 5 [3] [4].

2.7 Cigré Benchmark Model

A benchmark system provides a base to test new concepts and to make comparisons between the simulation results and published literature results. This Cigré model is a simple model and it was created to inspire the comparison of performance of the different DC control equipment and strategies of different manufacturers by means of HVDC simulators [12].

The first Cigré LCC HVDC benchmark model is modelled in DIgSILENT PowerFactory as shown in Figure 11. This model represents a Monopolar 500 kV, 1000 MW HVDC system with 12-pulse converters at both rectifier and inverter ends [12]. The damped filters and capacitive devices for reactive compensation exist on both sides of the converters. The DC line parameters could represent either a cable or a Monopolar equivalent of a bipolar overhead line [12]. The system parameters are shown in Figure 10 [13] [14]. The power circuit of the converter is divided into three sub circuits, i.e. AC side, HVDC side and the HVDC converter. The AC side of the HVDC system has an equivalent network, filters, and transformers which are located on both sides of the converter. The AC supply network is supplied with a Thevenin equivalent voltage source with source impedance. AC filters are added to absorb harmonics generated and provide reactive power to the converter [14] [13] [12] [15].

The DC side consists of smoothing reactors and a T-network equivalent of the DC transmission line. The converter stations are characterised by 12-pulse configuration with two six-pulse valves in series. Under normal or steady state conditions using this model, the rectifier end operates in constant current control mode while the inverter controls the voltage/extinction angle. The current order is derived from the power order using the measured HVDC link voltage. The current order at the rectifier and inverter ends determines the 10-15 % current margin. The VDCOL is enabled to reduce the current order during a fault condition (voltage drops) in order to prevent a run-away situation. The firing delay angle at the rectifier end is limited between 5º and 150º to allow reliable valve operation and mode shift i.e. inversion mode, to clear faults in the HVDC link. At the inverter end, the firing delay angle is limited between 110º and 170º to reduce the possibility of commutation failures and avoid accidental mode shift into rectification [2].

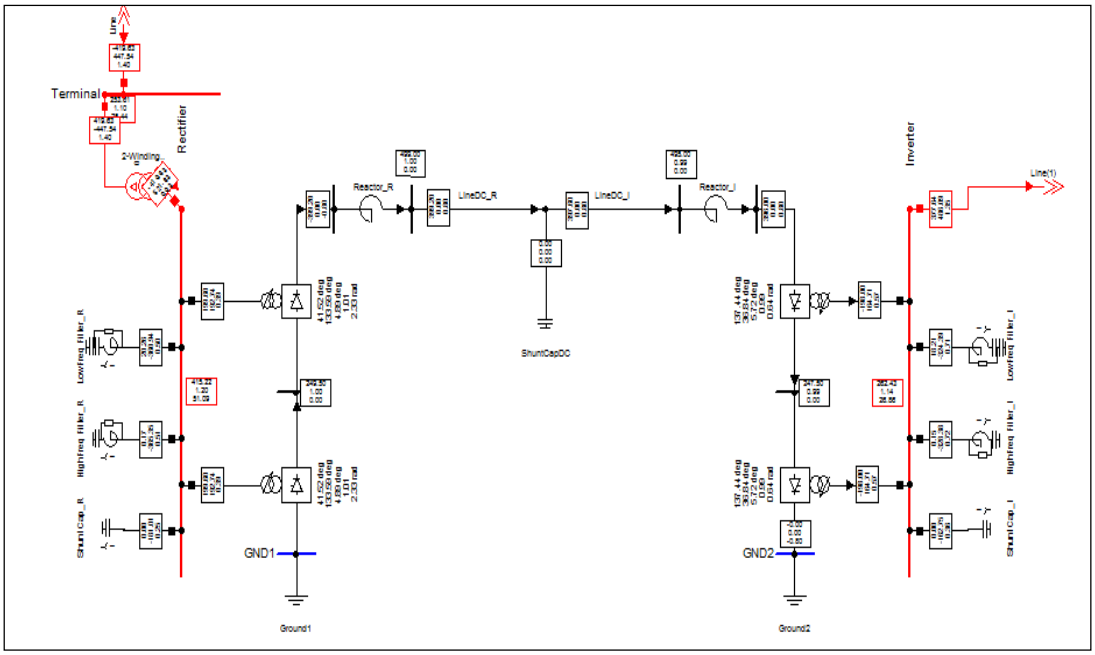

Figure 11: Cigré HVDC Benchmark Model [14] [12] [13]

3 ROTOR ANGLE STABILITY OF A POWER SYSTEM WITH HVDC

Stability of a power system refers to the ability of the system to operate in a state of equilibrium under normal operating conditions. In the event of a disturbance or event, the system should return to a state of equilibrium within a specified time [2]. Stability in power systems is related to a condition where all the generators remain in synchronism with each other. Power systems are continually subjected to perturbations or events such as switching of transmission lines or loads and faults at different points on the system. Power system control has a significant effect on the dynamic performance of the system after a disturbance therefore the dynamic performance of a system can be classified into [5]:

- Voltage stability
- Frequency stability
- Rotor angle stability - Small signal stability
  - Transient stability

3.1 Transient Stability

Transient stability (also called Large rotor angle stability or large disturbance) is the ability of a power system to remain in a state of synchronism when exposed to a large fault, on the transmission system. The loss of generation or a sudden loss of load is types of events that could cause system interruptions. Synchronism is the ability of the system to remain stable i.e. remaining within certain limits with regard to rotor angle separation between the machines in the system [2]. The stability is subjective to the non-linearity of the power system. Loss of synchronism due to the transient stability will be seen within 2-3 seconds of the initial disturbance.

Factors that influence transient stability include [2]:

- The loading of the generator.
- The generator output during the fault depending on the type and location of the fault.
- The fault clearing time.
- The post-fault transmission system reactance.
- The generator reactance as a lower reactance increases peak power and reduces the initial rotor angle.
- The generator inertia.

- The generator internal voltage magnitude and the infinite bus voltage magnitude.

3.2 Small signal stability

Small signal instability can exist after a loss of an interconnection resulting in rotor oscillations. Inter-area oscillation may occur where there are two areas of great inertia with a weak interconnection as seen in Figure 12. In large power systems small signal stability problems may be either local or global in nature. The local problem is associated with oscillations between the rotors of a few generators close to each other (local mode) and the frequency of the mode of oscillation can be in the range from 0.5 to 2.0 Hz [2] as seen in Figure 12. The global small signal stability (also called Small rotor angle stability or small disturbance) problem is associated with a group of rotors in one area operating against a group of generators in another area (inter-area mode) and the frequency of this mode of oscillation can be in the range from 0.1 to 0.5 Hz [2].

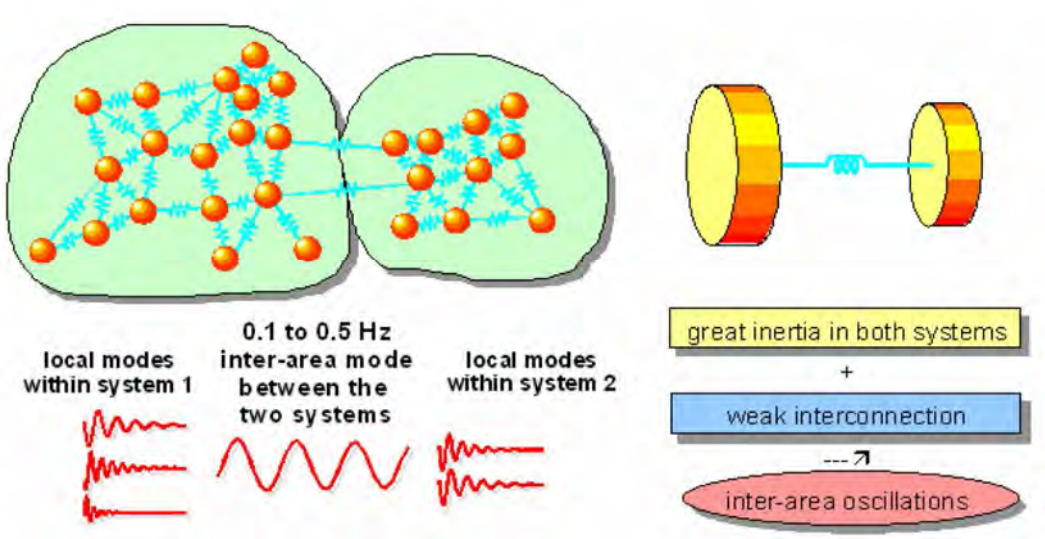

Figure 12: Modes of oscillation representation [5]

Small signal stability analysis is based on the eigenvalue technique which shows the small signal behaviour of the power system. This technique is used to investigate the problems related to oscillations with regard to their mode shape and relationship with different modes [2].

3.2.1 Linearised power system model

Power systems can be represented by a set of algebraic and differential equations that can provide an accurate state space solution [2]. The linearised system model is given by the following equations i.e. Equation 5 and 6 [2] [16]:

$$\dot{x}_p = A_p x_p + Bu \tag{5}$$

$$y_p = C_p x_p + D u_p \tag{6}$$

Where:

$\boldsymbol{A_p}$ is the system state matrix

$\boldsymbol{B_p}$ is the system input matrix

$\boldsymbol{C_p}$ is system output matrix

$\boldsymbol{D_p}$ is the feed forward matrix

$\boldsymbol{x_p}$ is the system state vector

$\boldsymbol{u_p}$ is the system control vector and

$\boldsymbol{y_p}$ is the system output vector

A state variable is one of the variables that can be used to describe the mathematical state of a dynamical system [17]. State variables within power systems may include generator machine states such as speeds and rotor angle, exciter states, power system stabiliser states and HVDC control states [2].

3.2.2 Eigenvalue and stability

The state of a system describes enough about the system to determine its future behaviour without any external forces affecting the system [17]. However the stability of a system can be represented using the eigenvalue (λ) technique. Various software packages (such as DigSILENT PowerFactory and MATLAB) have the ability to generate the eigenvalues from a linearised state space model through a model analysis tab. The eigenvalue is reduced to the following equation:

$$\lambda = \sigma \pm j\omega \tag{7}$$

A power system has different modes because of its dynamic nature where generators or groups of generators interact in relation to each other. There are also other control modes of oscillation which are associated with the controls of the HVDC, FACTS, etc. and the frequency of oscillation is not fixed, hence it depends on controllers' parameters [18]. In the frequency domain, a mode refers to real or a pair of complex conjugate eigenvalues. In the time domain, a mode has a single frequency and damping together with other sinusoid attributes (phase angles and amplitude) which is a component in a time response. A modal analysis of a linearised system model is a perfect tool to understand the behaviour and characteristic of different modes.

If a mode has poor damping, when it is excited by a perturbation or disturbance, it can then be observed on the post- disturbance time domain response. When a system is unstable, then the individual modes are unstable. A real eigenvalue corresponds to a non-oscillatory mode while a pair of conjugate eigenvalues corresponds to an oscillatory mode. However, one can say that the time dependant characteristic of a mode relates to an eigenvalue as seen in Equation 7 [19]. Therefore, the stability of the system is identified by the eigenvalues.

A negative real eigenvalue ($-\sigma$) represents a decaying mode (i.e. damped oscillation) and a positive real (σ) part represents an oscillation of increasing amplitude. The larger the value, the faster the oscillation decay and positive real eigenvalue represents aperiodic instability [2].

The real component ($-\sigma$) of the eigenvalues delivers the damping, and the imaginary component ($\pm j\omega$) delivers the frequency of oscillation as seen in Equation 7 and Equation 8. The frequency of the mode is the given by:

$$f = \frac{\omega}{2\pi} \tag{8}$$

The damping ratio is the rate of decay of the amplitude of oscillation and for an oscillatory mode of eigenvalues represented by a complex conjugate as seen in Equation 9 where the damping ratio is given by:

$$\zeta = \frac{-\sigma}{\sqrt{(\sigma^2+\omega^2)}} \tag{9}$$

The mode decay time ($\boldsymbol{\tau}$) is the time constant of amplitude decay in which the amplitude of oscillations decays to 37% of its initial amplitude in τ seconds or as seen in Equation 10.

$$\tau = \frac{1}{\zeta 2\pi f} \tag{10}$$

The damping ratio is more fitting when expressing degree of damping rather than the time constant since oscillatory modes have a wide range of frequencies. Since the mode decay time is related to the damping ratio as seen in Equation 9 and 10, the mode decay time or settling time can also be used to express controller's effectiveness in terms of the degree of damping after an event or disturbance. As a result the comparison of the two types of supplementary controllers used in this study will be using the mode decay time after a disturbance or event, to establish effectiveness in terms of damping.

The damping ratio is an important index relating to the small signal stability of a system where the type of system response depends significantly on the damping ratio of the individual modes. The minimum acceptable limits of damping in which a power system can operate sufficiently

well is not really established but situations where local modes and inter area modes with a damping ratio of below 0.02 should be accepted with caution. In addition to the absolute value of the damping ratio, the sensitivity of the dynamic responses to operating conditions and system parameters is significantly important.

According to reference [20] frequency and damping of inter-area modes are highly dependent on the system operating conditions and tests were conducted showing the strength of an AC-tie. The two weak operating conditions produced an unstable network and required further damping control actions to achieve stability of the network.

3.2.3 Eigenvectors

The eigenvalues of the state matrix given by A can be calculated from the scalar parameter λ, a solution exists that satisfies Equation 11. The right eigenvector (as seen in Equation 11) for each mode defines the relative distribution of the modes during the system dynamic state, which. is actually the mode shape of a particular mode of interest. When the simulation results are dominated by a single mode, the ratio of amplitude of any states (changes of the speed variable) to another in the simulation will correspond to the ratio of the magnitudes associated with eigenvector linked with that mode. The formulation of the power system model depends on the selection of states made. This makes them dimensional and indicates that there is no specific importance of a state to a mode. The left eigenvector (as seen in Equation 11) be taken as giving the distribution of the states within a mode. It has a direct effect on the amplitude of the mode excited on by a specific input. The different components of the left eigenvector contribute to the controllability of the mode of interest with respect to the component of interest [2].

$$A\phi = \lambda\phi \tag{11}$$

Where ϕ is an n×1 column vector , for any eigenvalue λj, the n×1 column vector ϕj, which satisfies Equation 11 is called the right eigenvector of A, but associated with λj, in the form ϕ_{ij}. ψ_{ij} is seen as the left eigenvector after mathematical manipulation and transformation to be used in Equation 11.

3.2.4 Participation factors

Eigenvectors are dependent on units and scaling factors linked with different state variables therefore the negative impact of using the left and right eigenvectors to determine stability and the relationship between the state variables and the oscillation modes of interest are evident. The participation factors are defined by the element, through element multiplication of the right and

left eigenvectors as seen in Equation 12. This is avoided by introducing the participation matrix P, which combines the left and the right eigenvectors as follows:

$$P_{ij} = \phi_{ij}\,\psi_{ij} \tag{12}$$

It is a measure of the sensitivity of the i^{th} eigenvalue to a change in the j^{th} diagonal of A. The participation factors are non-dimensional and it provides an impartial indication of the effects of the state variables of the system to a mode.

3.2.5 Observability and Controllability

Observability and controllability factors are defined to provide a measure of how effective the choice of input signal is (controllability) and how effective the choice of feedback signal is (observability) [2] [21]. According to Mhaskar, modal controllability, observability, and transfer function zeros play a major role in the selection of location and feedback signals for flexible AC transmission systems (FACTS) based power swing damping controllers [22]. If the observability factor for a certain mode is zero, then the mode cannot be seen in the selected feedback signal. An input signal to a damping control should have high observability. If the controllability factor is zero, the mode is not controllable with the selected feedback signal.

A large HVDC scheme controller mode may be observable in the active power and frequency of the system whereas the small SVC controller mode may be observable in bus voltage values in the adjacent transmission lines. Frequency is one parameter that is measurable at every point of the power system. Frequency measured at low voltage levels will provide oscillation mode measurements that are observable in the high voltage bus of that area [18]. According to Farsangi et al, different output controllability analyses is useful for determining the correct feedback signals for damping of inter-area modes. They used two case study networks using various methods to determine the best location and the stabilising signal for FACTS devices [23].

3.2.6 Residues

Residue is the sensitivity of the corresponding mode to feedback of the transfer function output to its input. Transfer functions, poles, zeros and residues give information for control design [24]. Since the residue is a normalised product of the corresponding observability and controllability, it will provide valuable information regarding the influence of the mode to feedback. A higher value of residue suggests a higher sensitivity of the corresponding eigenvalue to controller gain. [22]

3.2.7 Identification of Power System Oscillations paths in Power System Networks

Mvuyana presented a summary of works related to the identification of power system oscillation paths in power system networks [25]. An understanding of the path that the oscillation energy travels within a power system indicates the correct location of the appropriate measurement and control action. The HVDC link may be installed in parallel to the path and the power transfer is controlled following a disturbance. Mvuyana identifies the dominant oscillation path for a known two area network power system together with other literature sources [2] [26] [27] [21] [25]. According to Hauer the interaction paths is the main path along which generators, controllers and loads interact with one another in the exchange of oscillation energy [28].

In practical examples of interaction paths, the active power signal used at one important line relates to all the important lines in the network. This study showed that the interaction of the distantly located transmission lines assisted in identifying the location of transmission corridors thus providing oscillatory content in the measured signals passing through them [28] [27]. It is then assumed that the propagation of most visible inter-area oscillations occurs along a certain path and the main path can be determined [29] [30]. This path is referred to as the dominant inter-area path and it is the pathway that contains the highest content of the inter-area oscillation [27]. The HVDC scheme with supplementary control can then be correctly placed according to the identified dominant inter-area oscillation path for effective control thus bringing enhanced stability to the power system after an event.

3.2.8 Mitigation of Small Signal Instability

Devices that may be used for economic design and improvement of system stability without compromising system performance include the Static VAR Compensator (SVC), Power System Stabiliser (PSS) and HVDC [2].

- **Static VAR Compensator with supplementary control**

SVC has the ability to influence the voltage profile of a power system thus affecting the reactive and active power [4]. By accurately controlling the voltage and the reactive power, the SVC can enhance power system stability. The primary mode of operation is voltage regulation which improves transient and voltage stability. The SVC contribution to the damping of system oscillations is however small and a supplementary control (POD) is needed to achieve significant damping. The location of the SVC depends on the feedback signals used and the controller design [2]. The feedback signals used for the supplementary control must be responsive to the modes of oscillations to be damped. This can be determined by the residues and observabilities of various feedback signals for both pre-fault and post-fault conditions [2] [24].

- **Power System Stabilisers**

The PSS function is to increase the damping to the generator's rotor oscillations. This is achieved by modulating the generator's excitation thus developing a component of electrical torque in phase with the rotor speed deviations [2] [4]. Power system stabilisers are inexpensive and simple in design, it can be the most effective power system damping controllers if setup correctly. The PSS must have phase lead requirements which are easily defined. The PSS phase lead characteristics are chosen to eliminate the lag between PSS input into the exciter and the generator rotor electrical torque with the generator at constant speed [2] [4].

The performance of a PSS with regard to local modes is influenced slightly by the location of the PSS and the characteristics of the load. The PSS does however damp inter-area oscillations significantly by modulating the system loads. It is therefore evident that the mechanisms in which the PSS adds damping to local and inter-area modes are different [31].

- **HVDC links with supplementary control**

The HVDC links are commonly used to damp system electromechanical oscillations. The HVDC control is the heart of the HVDC scheme as it is fast acting with controlled dynamics [3]. The correct design of HVDC control allows the fast acting control system to assist the weak AC network to recover from faults and as such avoiding voltage instability or voltage collapse as well as optimising the power flows within the network.

However modal damping plays no part in their performance specification therefore only certain modes can be damped using HVDC line controls. Low level oscillations are related to small signal stability and according to literature; the use of HVDC links together with supplementary control, to reduce modes of oscillations has been demonstrated successfully [32].

4 IMPLEMENTATION OF A TWO AREA AC SYSTEM WITH HVDC INTEGRATION

4.1 Introduction

In this chapter, modelling of a simple AC network with an integrated LCC-HVDC link using DigSILENT PowerFactory (DPF) is demonstrated. The first Cigrê LCC HVDC benchmark model is selected and the primary controls of certain components are adjusted to certain values,(e.g. filters) in order to adapt this HVDC link for this particular study system. Dynamic performance of the LCC-HVDC link will be simulated in DPF and validated against reported results for faults on the inverter buses. An AC system comprising of 4 generators and 11 buses spread over two geographical areas will be the study system considered and modelled [2].

Kundur's study system is well known and is used by many researchers in simulation based studies. The modal analysis and simulation results from DPF will be analysed to locate the modes of oscillations for interpretation and validation against those reported in literature [2]. An LCC-HVDC link will then be integrated into the AC network in parallel with an AC corridor connecting the two areas. Different scenarios related to the study system are simulated. The dynamic performance of the AC-DC system are observed, analysed and interpreted. The responses of the simulations provide answers to questions relating the ability of parallel HVDC links in stabilising AC systems, after an event.

4.2 The two area system network: Base network

4.2.1 Base network system analysis

The network consists of two similar areas connected by weak parallel AC ties, as shown in Figure 13. Each area consists of a set of coupled generator units, each having a rating of 900 MVA [2]. The generators, transformers and transmission system parameters are seen in Table 1 below [2]. The generator parameters in per unit on the rated MVA and kV base are as follows:

Table 1: Generator parameters in per unit with the rated MVA

Generator parameters				
$X_d = 1.8$	X_q = 1.7	X_l =0.2	$\dot{X}_d = 1.8$	$\dot{X}_q$ = 0.55
$\ddot{X}_d = 0.25$	$\ddot{X}_{q0}$=0.25	R_a =0.0025	$\dot{C}_{d0} = 8.0$	$\dot{T}_{q0}$ =0.4 s
$\ddot{T}_{d0}$ =0.03	$\ddot{T}_{q0}$ =0.05	A_{sat} =0.015	B_{sat} =9.6	Ψ_{T1} =0.9
H = 6.5 (G1 and G2)		H = 6.175 (G3 and G4)		K_D = 0

Each step-up transformer has an impedance of 0+j0.15 per unit on 900 MVA and 20/230kV voltage base. The transmission system nominal voltage is 230 kV. The line lengths are identified in Figure 13. The parameters of the lines in per unit on the 100 MVA, 230kV base are: r= 0.0001 pu /km, x = 0.001 pu/km and = 0.00175 pu/km. The generating units are loaded as per Table 2 [2].

Table 2: Generator units loading [2]

Generator	Real Power	Reactive Power	Excitation Voltage
G1	P = 700 MW	Q =185 MVAr	Et = 1.03∟20.2°
G2	P = 700 MW	Q = 235 MVAr	Et = 1.01∟10.5°
G3	P = 719 MW	Q = 176 MVAr	Et = 1.03∟-6.8°
G4	P = 700 MW	Q = 202 MVAr	Et = 1.01∟17.0°

The system operating within area 1 exports 400 MW to area 2 and is electrically loaded according to reference [2]. The generators have an integrated IEEE type DC1A DC excitation system model [2]. The modulated loads of areas 1 (L_7) and 2 (L_9) are 976 MW and 1767 MW respectively.

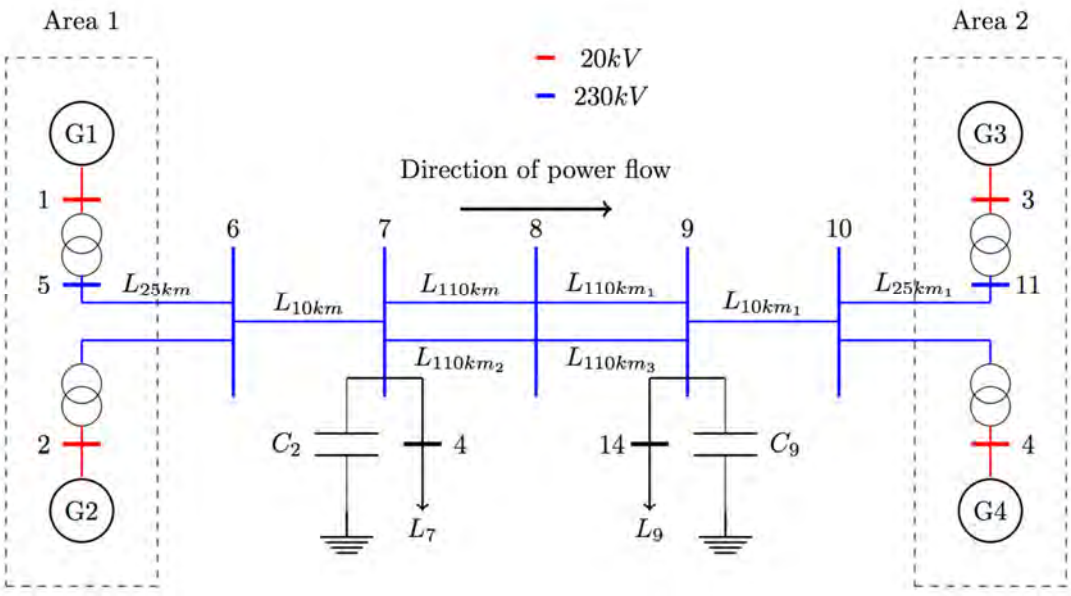

Figure 13: Two Area Network [2] [32]

The load flow and eigenvalue analysis of the power system are performed where the inter-area and local modes are identified with information about the active inter-area mode in real-time. The information includes the following [19]:

- The active oscillation modes detected.
- The damped frequency and damping of each mode.
- The amplitude of the mode of oscillations and in each measurement signal.

The modal observability, i.e. how well the relative phase in which each oscillatory mode is visible in each measurement signal. Observability (mode shape) provides an indication of which generators are oscillating with each other. The state variable chosen is speed as it allows for the identification the generators that are participating in the oscillatory modes. Their mode shapes as seen in Figure 14, 15, 16 respectively, showing the eigenvector component corresponding to the rotor speeds of the four machines. The observability of the system exhibits three rotor angle modes of oscillations:

- Figure 14, shows the inter area mode, with a frequency of 0.48 Hz, the generators G1and G2 swinging against generators G3 and G4.
- In Figure 15 and 16, shows the two local modes, with frequencies of 0.97 Hz and 0.99Hz respectively, with generators G1 swing against G2 and G3 swing against G4.

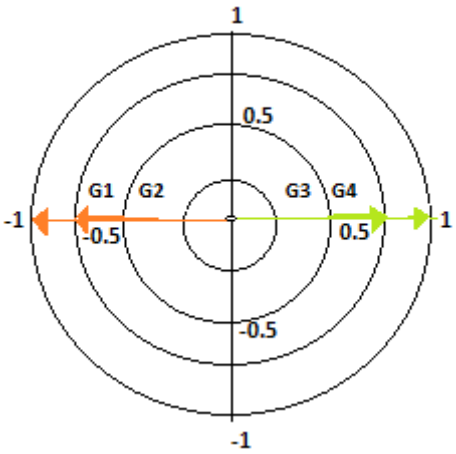

Figure 14: Mode shape of generator speeds - Inter-area mode G1G2/G3G4

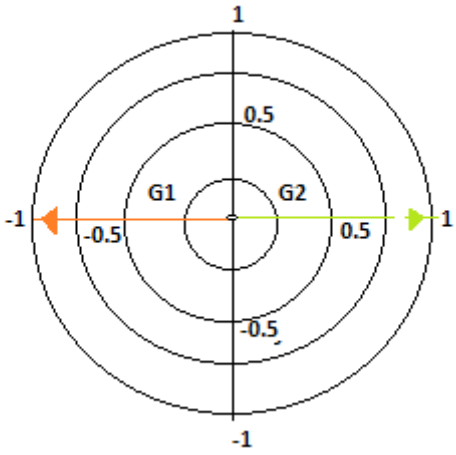

Figure 15: Mode shape of generator speeds - Local Mode G1/G2

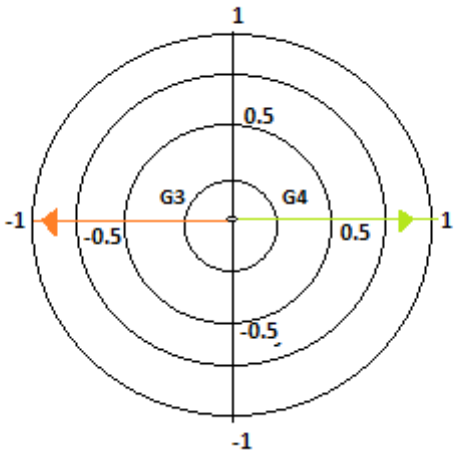

Figure 16: Mode shape of generator speeds - Local Mode G3/G4

Table 3: Damping ratios and frequencies for the inter-area mode

Base Case		Overloaded Case		
Damped Frequency (Hz)	**Damping Ratio Normal Load**	**Damped Frequency (Hz)**	**Damping Ratio Heavy Load**	**Mode shape**
0.4837	0.0256	0.3399	-0.0385	**G1G2/G3G4 Inter Area mode**
0.4837	0.0256	0.3399	-0.0385	

Modes with a damping ratio of less than 3% can be accepted but with caution as it may lead to instability [31]. It is evident that the inter-area mode has poor damping of 2.5% as seen in Table 3. The local modes have significant positive damping of 9% which make the local modes more stable compared to the inter-area mode. A damping ratio of 5% shows that in three oscillation periods, the amplitude reduces to 37% of its initial value. The smallest acceptable level of damping is not evidently known but a damping ratio which is negative causes the mode to become unstable [2] as seen in Table 3. However, it is a significant characteristic that negatively damped oscillations appear to occur when the equivalent transmission power angle between two interconnected systems are large. Large power angle occur when the loading of the AC tie lines are heavy [33]. Figure 18 shows an example of the load increasing to 600MW. Table 3 shows the negative damping of the inter area mode causing instability of the system. Time domain results are effective in confirming frequency domain results as it shows how the system nonlinearities affect the mode of oscillations [2].

Non-linear time domain simulations are performed to validate the dynamic response when a self-clearing fault is applied for a duration of 0.1 s on one of the tie lines connecting buses 8 and 9 (inverter end) on the base case seen in Figure 17. A three phase short circuit fault is simulated on the AC tie line connecting buses 8 and 9 for the duration of 0.1 s. It is monitored for 40 s to capture the damping of the power oscillation for the post-fault condition and pre-fault condition as shown in Figure 17. The response of the network to a fault is directed by how long the fault acts on the network and the location of the fault within the network. These factors have an influence on the phase characteristics of the network because they directly impact the fault impedance and network stability.

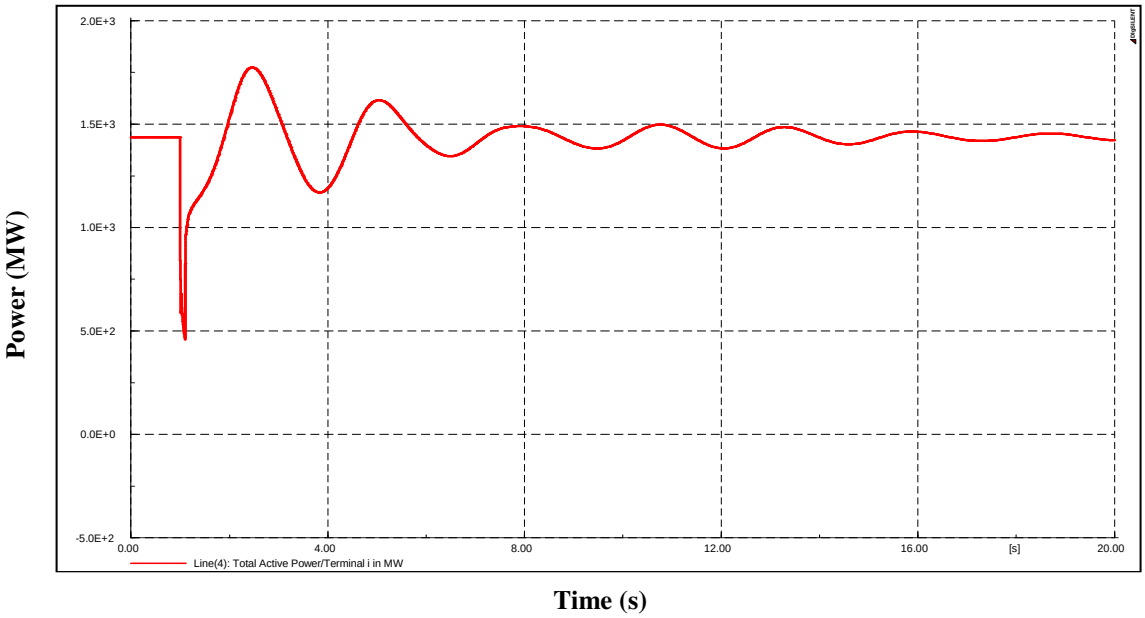

Figure 17: Time domain of Active Power: Normal loading between bus 7 and 9

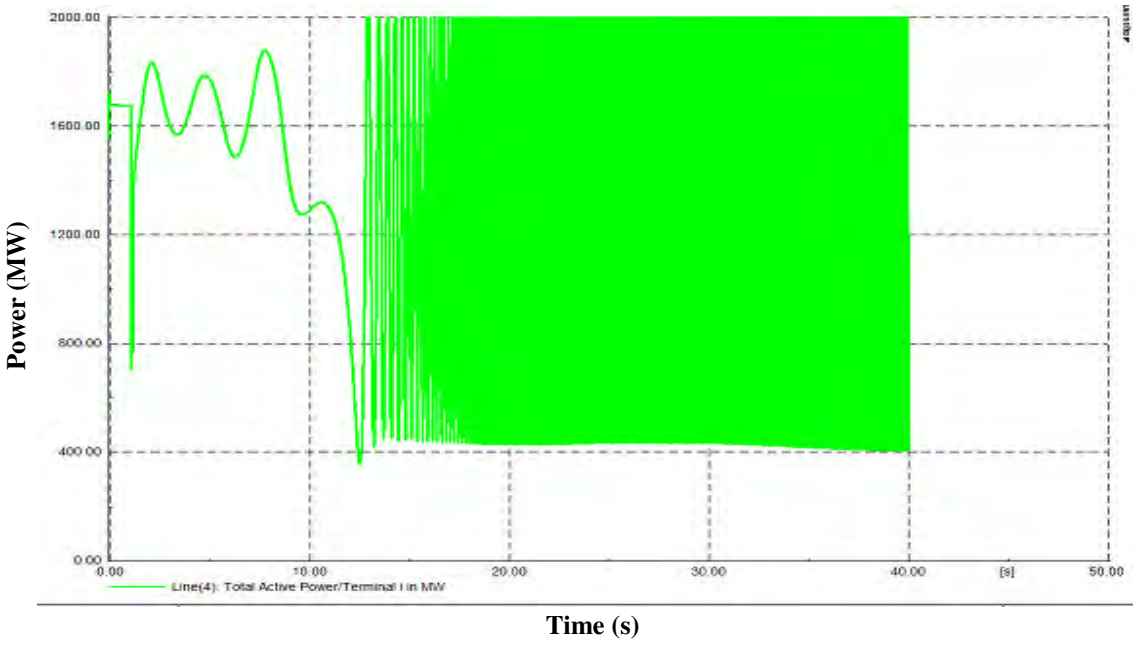

Figure 18: Time domain of Active Power: Heavy loading between bus 7 and 9 (600MW)

The active power at L10km between bus 6 and 7 is monitored for the dynamic response of the fault on the system stability. It is also evident as seen in Figure 18 that the network (without the HVDC) becomes unstable under heavy loading conditions. The system stabilised after a period of approximately 33.7 s (mode decay time or recovery time) and this is indicative of the system's natural damping.

4.3 Additional Tie Line

The more lines that are connected in parallel reduce the Surge Impedance Loading (SIL) of the network. However, an AC line with specific power loading is connected onto the base case between bus 7 and bus 9 to analyse the system's behaviour. The three mode shapes that were seen in Table 1 are present in all the case scenarios as seen in Table 4 but with different damped frequencies, however, this scenario shows a damping ratio (inter area mode) of 3.2% which is an improvement from the base case. It is then noted that the transmission power angle decreases as the load is distributed across the AC tie transmission lines thus improving the damping ratio faintly.

Table 4: Damping ratios and frequencies for local and inter-area modes -additional tie line

Base Case		**Additional AC Tie Line**		**Mode shape**
Damped Frequency	**Damping Ratio**	**Damped Frequency**	**Damping Ratio**	
Hz		**Hz**		Local mode
0.9889	0.0935	0.9957	0.0915	G3/G4
0.9889	0.0935	0.9957	0.0915	
0.9614	0.0939	0.9664	0.0923	Local mode
0.9614	0.0939	0.9664	0.0923	G1/G2
0.4837	0.0256	0.5776	0.0317	G1G2/G3G4
0.4837	0.0256	0.5776	0.0317	Inter Area mode

The nonlinear simulation shows that the AC line experienced oscillations and the active power recovered after 30.4 s (recovery time or mode decay time). It can be seen in Figure 19 that the additional AC line is also affected by the fault with a sudden reduction in active power but the generated oscillations stabilises with the system's natural damping.

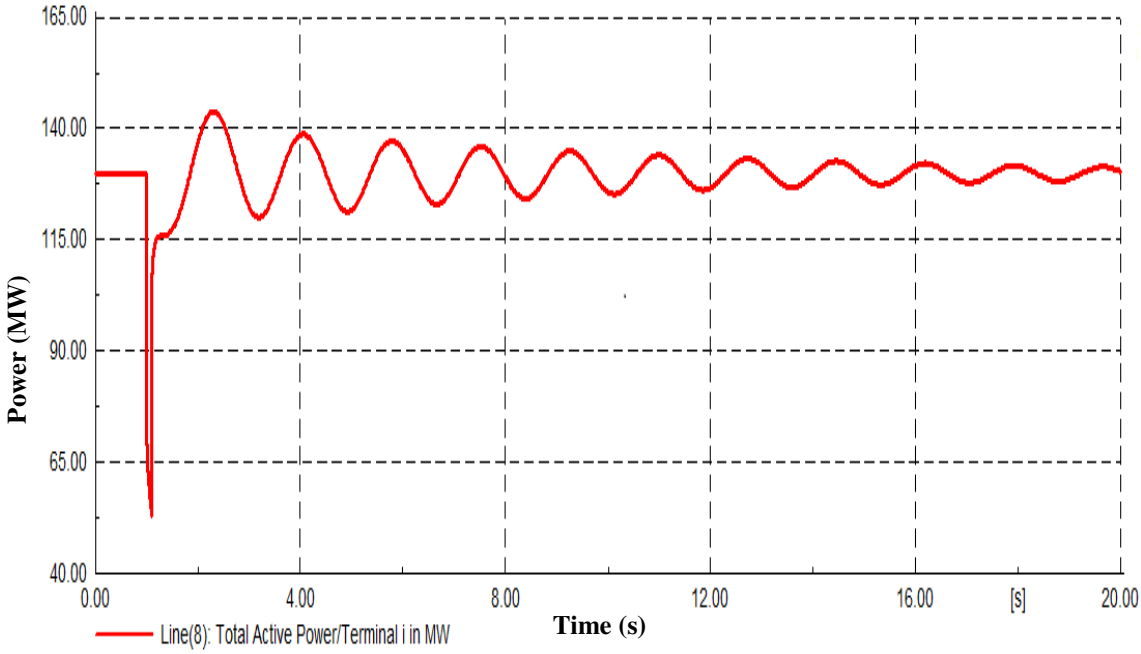

Figure 19: Time domain response after a fault with an additional AC line

4.4 LCC HVDC integrated in the network

The LCC HVDC link is integrated into the base case between bus 7 and bus 9 as shown in Figure 20. The modal analysis and simulation results are validated against certain parameters of components (e.g. for filters, capacitors, etc.). Some adjustments are made to adjust the power loading of the HVDC link rating to 0.45 A (to transmit 200MW). An LCC HVDC link is separately introduced into the AC network in parallel with the AC corridor, connecting the two areas in the power system.

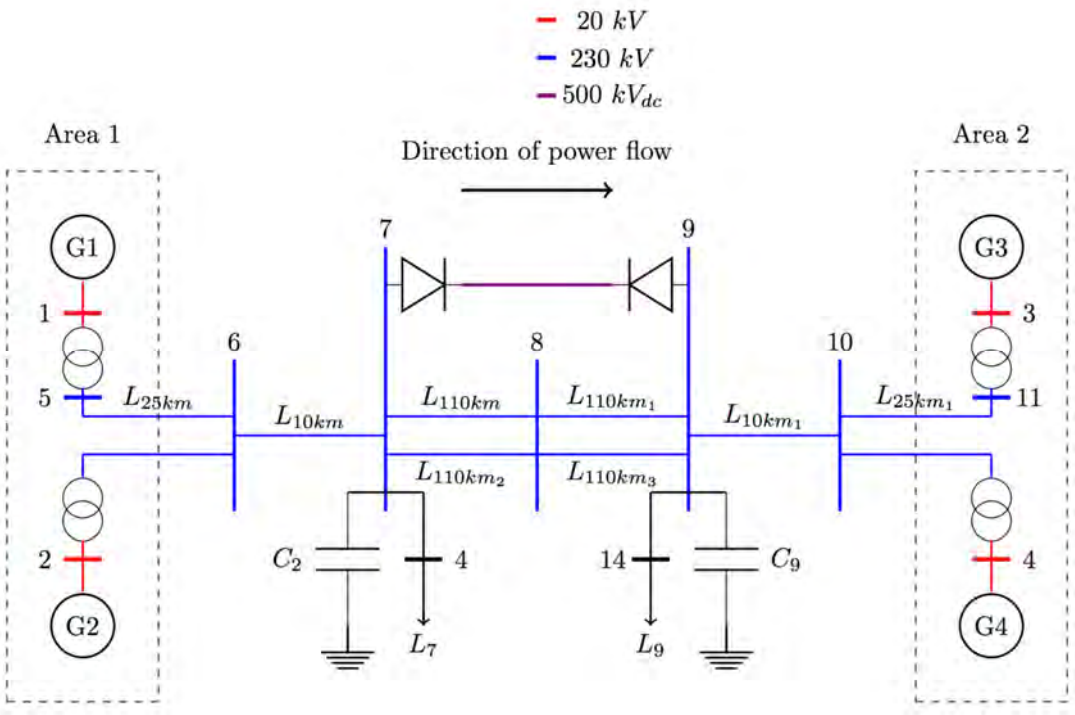

Figure 20: Two area network integrated with the LCC HVDC link [32]

Table 5: Damping ratios and frequencies for local and Inter-area mode with an HVDC link

Base Case		**Integrated HVDC Line**		**Mode shape**
Damped Frequency	**Damping Ratio**	**Damped Frequency**	**Damping Ratio**	
Hz		**Hz**		
0.9888	0.0935	1.0492	0.0587	Local mode G3/G4
0.9888	0.0935	1.0492	0.0587	
0.9614	0.0939	1.0284	0.0595	Local mode G1/G2
0.9614	0.0939	1.0284	0.0595	
0.4837	0.0256	0.5594	0.0496	G1G2/G3G4 Inter Area mode
0.4837	0.0256	0.5594	0.0496	

The modal analysis is performed and the three mode shapes are also identified but at different damped frequencies. The local modes now represent a reduced damping ratio of 6% and 5% respectively while the inter-area mode represent an improved damping of 5% as seen in Table 5. The mode shape is visible for all three oscillation modes as seen in Figures 21, 22 and 23. The integration of the HVDC link has increased the damping ratio of the inter-area mode as the AC

tie lines are left to carry only 200 MW (instead of 400 MW) while HVDC link carries the other 200 MW. With a decrease in power over the AC tie line, the transmission power angle across the corridor decreases which results in an increase in synchronising torque and therefore the frequency of oscillation [2].

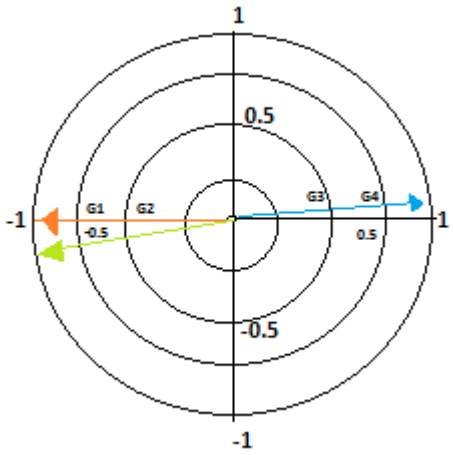

Figure 21: Mode shapes of generator speeds with HVDC – Inter-area mode

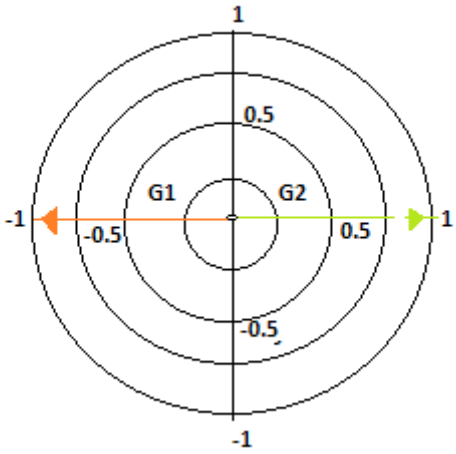

Figure 22: Mode shapes of generator speeds with HVDC – Local mode G1/G2

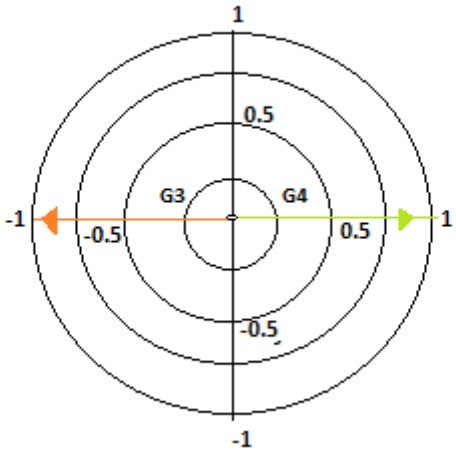

Figure 23: Mode shapes of generator speeds with HVDC – Local mode G3/G4

If the network is heavily loaded, the inter-area mode will become unstable and the HVDC link will relieve the AC tie lines from carrying more power thus stabilising the inter area-mode. Changing the loading conditions has little impact on the local modes as they are faintly affected by line power flow [32]. The base case network with HVDC integrated layout is used with the same fault and in the same location and monitored at L10km (Line4), i.e. midway along the line. Figure 24 indicates the results of this study.

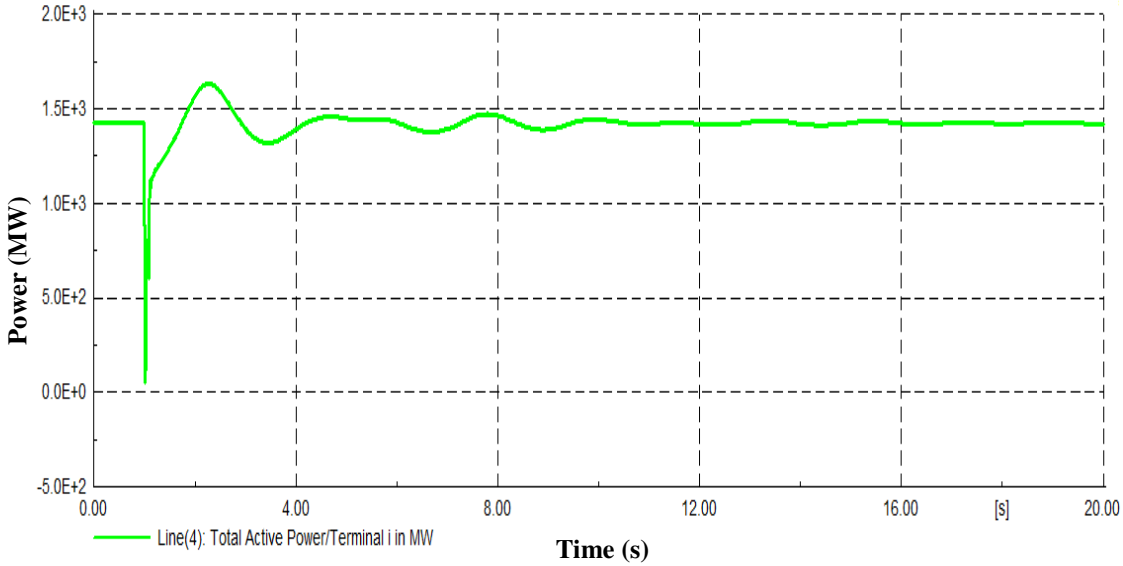

Figure 24: The time domain response with HVDC after an injected self-clearing fault

The active power did spike for the duration of the fault but the damping ratio is higher therefore the active power recovered quicker when compared with the study without the integrated LCC HVDC scheme. The mode decay time or recovery time for the post fault condition is shortened to 19.5 s which correlates with the increased damping ratio as seen in Table 5. The control action as seen in the responses is very fast and aims to maintain the accuracy of the controlled

variable i.e. constant dc current and constant extinction angle. The presence of poorly damped inter-area mode is evident from the angular separation between G1 and G3 (G1 is the slack bus) and the power flow in the line connecting buses 9 and 10 as seen Figure 25and 26 respectively.

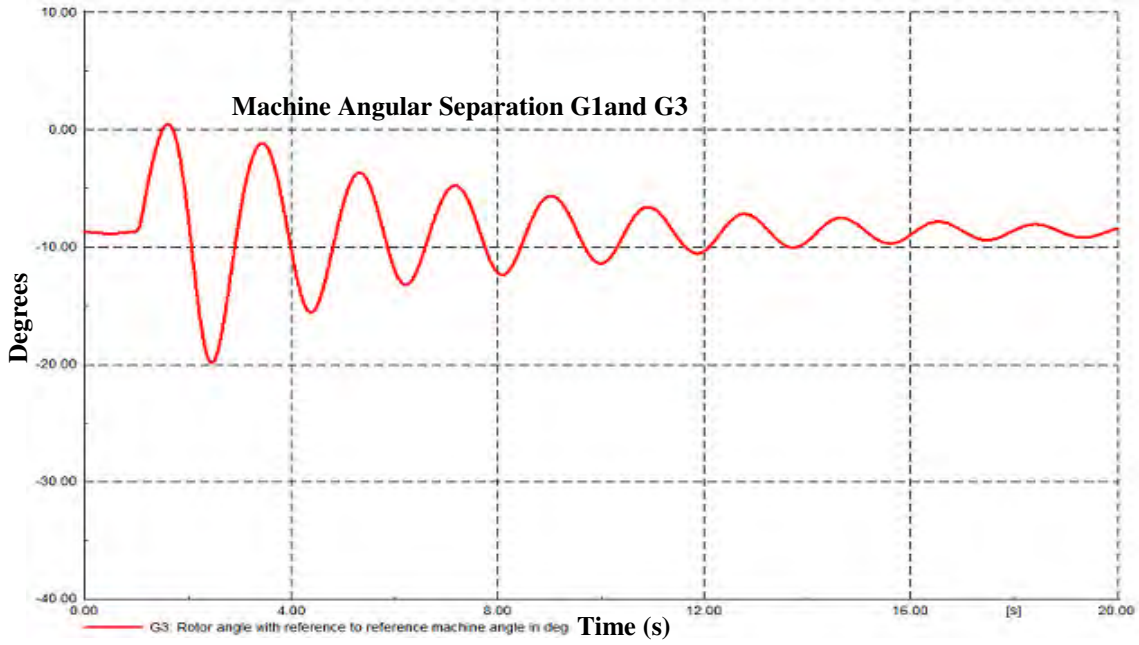

Figure 25: Time domain response of the Rotor angle displacement after a fault

As seen in Figure 27, the LCC HVDC link voltage drops sharply during the fault due to the reduction in inverter end AC voltage.

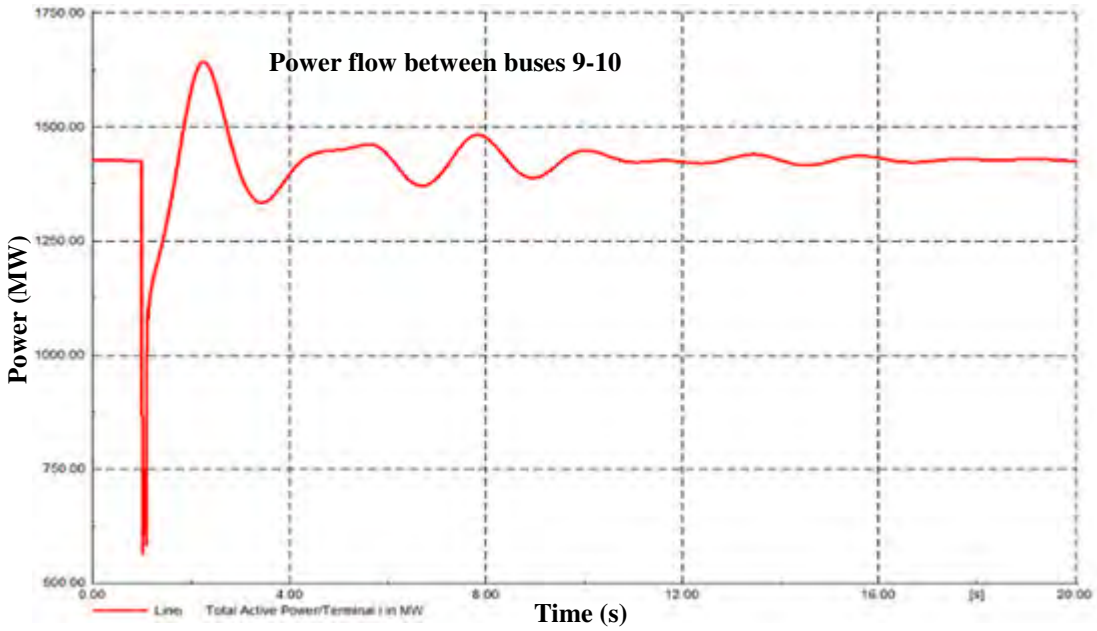

Figure 26: Time domain response of Active Power between buses 9-10

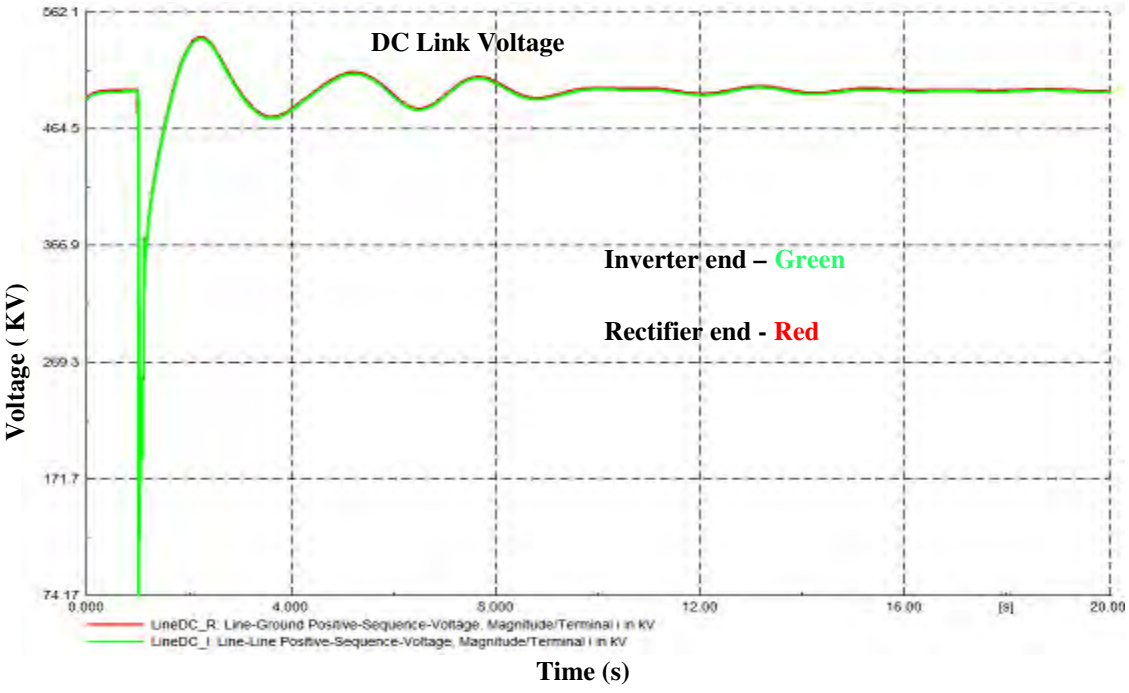

Figure 27: Time domain response of DC link Voltage

When monitoring the inter-area oscillation during the fault condition, the rectifier switches between constant current and constant firing angle control which is performed by the advanced controls (mentioned in chapter 2) as seen in Figure 29 and the power through the DC link drops during the fault as anticipated (as seen in Figure 28). The inverter moves to constant extinction

angle control which is the measure of gamma, this is basically the period when the thyristor valve voltage is negative

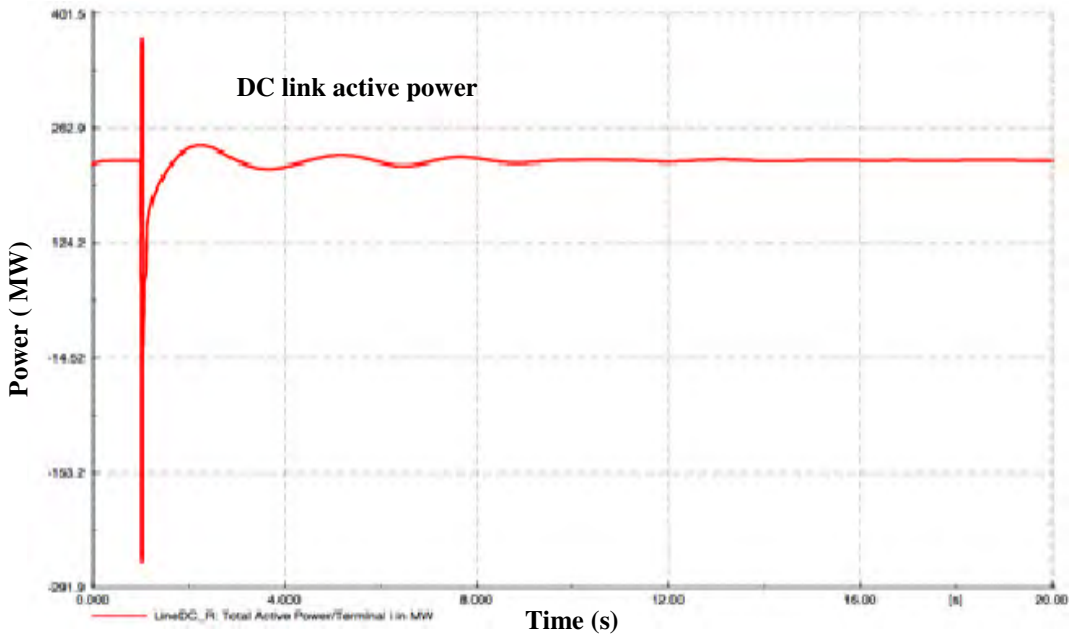

Figure 28: Time domain response of DC Link Active Power

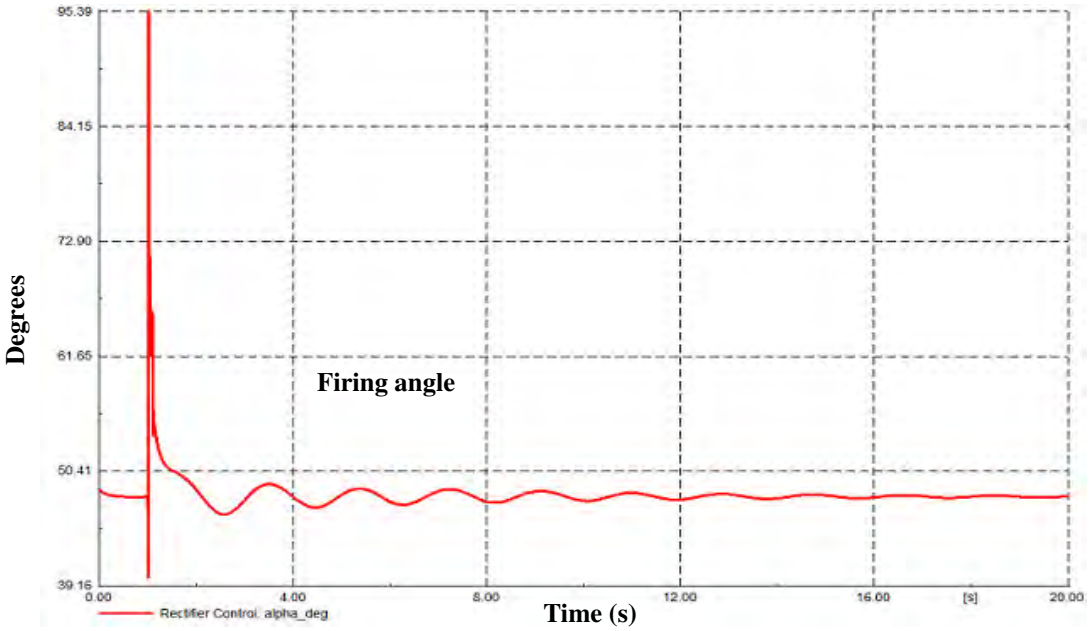

Figure 29: Time domain response of firing angle

As seen in Figure 30, the gamma control element increases sharply during a fault but the controller reduces the value of gamma and operates in minimum extinction angle control thus reducing reactive power consumption and assisting in improving stability [32].

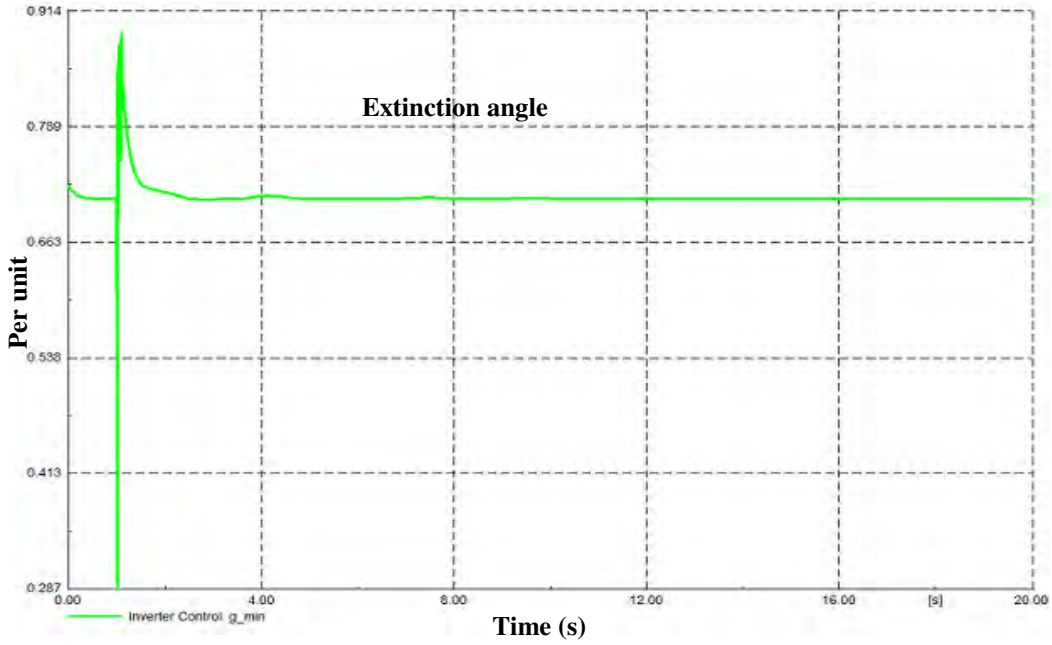

Figure 30: Time domain response of Extinction angle

Figure 31 shows a comparison of the active power swing responses, after a fault is applied, with and without the HVDC integrated. The behaviour of the active power and the rate of decay of the oscillations after the fault condition are visible. Red indicates the power swing with no HVDC link integrated and the green indicates the power swing with an LCC HVDC link integrated. It can be clearly seen that the HVDC link enhanced the stability of the network with the introduction of damping to the inter area mode of oscillation.

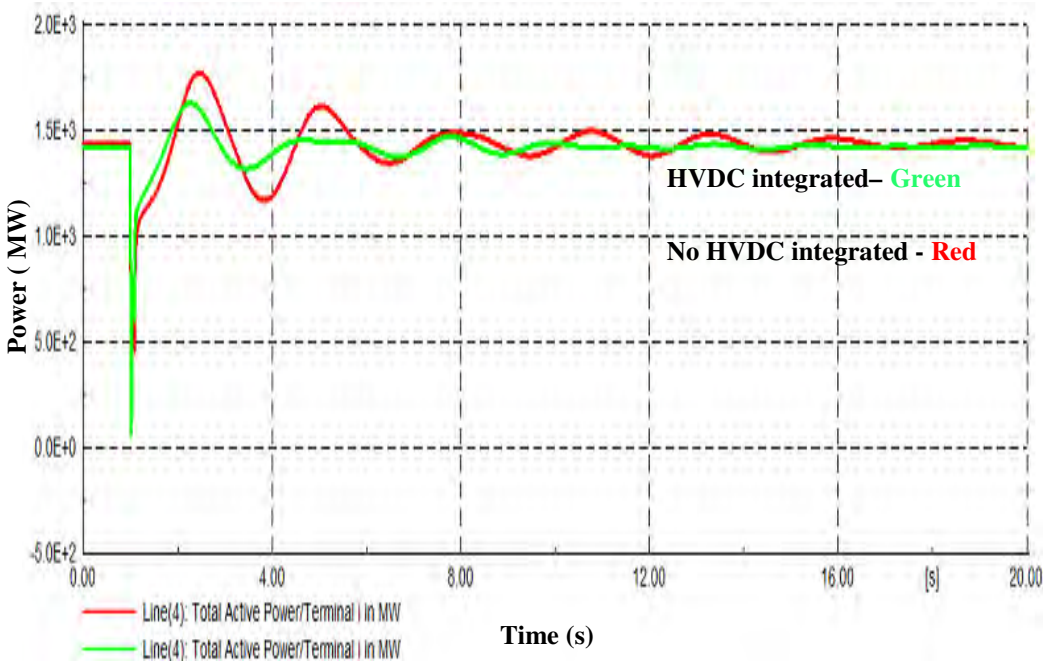

Figure 31: Time domain response of the scenarios: with and without HVDC integrated

4.5 Conclusion

This chapter presented a power system modelling study of a two area AC network with an imbedded LCC HVDC scheme. The work was done in order to study the validity of published literature with regard to power system stability enhancement through the use of parallel HVDC connections. The results obtained were consistent and in good agreement with literature. Although the two area AC network modified with an additional AC line became more stable with a slight increase in the damping ratio of the inter-area mode, the value was not big enough to contribute significantly to system stability. This slight increase in damping ratio is due to the additional AC tie line which creates a 'stronger' network and the transmission power angle across the corridor decreases.

With the integration of parallel HVDC links, a reduction of power over the AC tie line is visible therefore the transmission power angle across the corridor decreases thus resulting in an increase in synchronising torque coefficient. According to the responses, the inter area mode of the system will become unstable if the system is heavily loaded resulting in the HVDC link relieving the AC tie lines from carrying more power as a result stabilising the inter area-mode. Hence, the integration of the parallel HVDC link has increased the damping ratio and decreased the mode decay time or recovery time of the inter-area oscillation mode. With regard to inter-area oscillations during fault conditions, the rectifier switches between constant current and constant firing angle control. As expected, the power through the DC link drops during the fault. The simulation studies have also shown shorter recovery times of 19.5s from 3.7s after a fault or disturbance. The study system simulations set up the foundation for studying supplementary control through HVDC links which will be elaborated in the next chapter.

5 SUPPLEMENTARY CONTROLLER DESIGN

5.1 Introduction

HVDC schemes through the modulation of their power can be used to dampen fluctuations in voltage in an AC transmission network. Inter area oscillations are a typical phenomenon in large interconnected systems and HVDC schemes can serve as powerful tools to damp these oscillations [19] [34]. According to Witzmann, the damping of inter area oscillation between (Zimbabwe Electricity Supply Authority) ZESA and Eskom is demonstrated showing the improved damping with the introduction of a POD. This supplementary controller assists by taking advantage of the quick change in HVDC power flow modulation and overload capability which improves the damping of the inter area oscillations thus making better use of the installed capacity [35]. However the voltage maintenance ability from the AC tie line can assist the HVDC link to recover from short term commutation failures or single/bipolar blocking faults as mentioned in reference [36]. Rabbani et al show the effectiveness of the SVC and the HVDC control schemes in a simplified model; the results show that there is a reduction in reactive power during a fault with the addition of the LCC HVDC POD control system and that the decrease in overshoot and settling or mode decay time are similar to the SVC and PSS. The simplified model in the research shows the interaction of the various elements in the power system before implementation on Great Britain's (GB) transmission network [11].

According to Fuchs [34], HVDC links are not used in a systematic manner therefore his research aims to develop a framework for power system control using HVDC links with the results from conventional AC networks. The research presents operation approaches, network planning with dynamically controlled HVDC links. The identification of the HVDC location for power system control adds to the effectiveness of the HVDC link in the surrounding AC network and even a small HVDC link capacity in a power system can bring about a large benefit from the coordinated control of power injections. The primary concern for HVDC links location selection depends on the load flow congestion mitigation and economic gain but Fuchs provides a novel criterion to relate a HVDC link location to the dynamic power system control with a performance measure [34]. Reference [37] proposed a Wide Area Measurement Robust Controller which uses a sliding mode control to handle the model inaccuracy of a standard HVDC model and the area centre of inertia signals are chosen as the feedback signals. The effectiveness of this control are verified with simulations on a two area-four machine AC/ DC power system and a real large scale AC/DC power system.

Cresap et al also illustrates the operating experience and benefits of using the Pacific HVDC intertie to damp out oscillations on the parallel Pacific intertie however he uses a more practical approach to the theory with studies performed on the Pacific HVDC intertie [33]. Shi et al demonstrates the effective damping of supplementary control on AC/DC power system but based on the Hamilton energy function theory which uses the oscillation energy of the interconnected system and the Lyapunov function to study the stability [36]. Tomiyama et al describe power swing damping control by HVDC power modulation where the characteristics of the power swing in an AC system are related to the eigenvectors of typical generators in inter-area power swing [38].

From the conclusions made by Hammad, the conventional HVDC scheme in parallel with an AC intertie can promote instability by reduced synchronising torque during a disturbance. Therefore by deviating from the conventional power controls and adopting advanced signal control strategies, the dynamic performance of the parallel AC/DC transmission can be greatly enhanced, providing more damping and synchronising torque to damp out oscillations after faults or events. These advanced controls can also increase the transient stability of the AC transmission without the need of reactive power support [39].The POD cannot be depended on entirely to maintain the stability of a power system after a large disturbance or changes in system operating conditions. These damping controllers are designed around a linearised state space model for a nominal operating condition. The inter area mode is the dominant mode and is perceived as the mode of interest to assess POD effectiveness.

The Model predictive controller (MPC) is another type of supplementary controller that uses a model to perform predictions of future plant behaviour and the calculation of suitable corrective control actions needed to take the predicted output as close as possible to the desired target value [40]. According to reference [41], [42], [43], Model Predictive control (MPC), can manage control constraints and therefore has proven to be valuable for adapting the reference settings for FACTS and HVDC links to avoid transients. The MPC is usually represented as cost functions which penalises the deviations of the output over a time horizon. These strategies can maintain an acceptable system response without any prior knowledge of the disturbance [44]. The main advantage of a MPC is that it considers the constraints on the control effort while calculating the predicted control action [45].

Azard et al further investigated the damping of inter-area oscillations using a MPC as the supplementary controller with the HVDC system [46]. They compared the performance of various controllers with the MPC on a 9 bus and 14 bus system. The study showed that the

MPC had a superior performance to the other controllers for damping poorly damped oscillatory modes of the test system [47].

This chapter incorporates the application of power modulation control including the study of the POD and MPC performance. Although, DigSILENT PowerFactory was useful in understanding the problem of small signal stability and the integration of the LCC HVDC into the network, it is, however, limited due to the complexity of extracting the state space model. Power Systems Toolbox (PST)-MATLAB is considered the most appropriate tool in investigating and designing the controllers as the state space model is directly accessible. In additional to the MATLAB tools used to design the controller, a number of design analysis tools are provided within the Power System Toolbox itself [24] [48]. A two area network with an integrated HVDC system is investigated. The model is similar to the model used in the previous chapter and that used by Rogers in reference [24]; however, the model was purposely made unstable to allow a study of the effectiveness of the controllers. Further details of the study system are found in reference [24] and in Appendix B.

5.2 Power Oscillation Damping Control

The POD is a damping controller that is designed around a linearised state space model for a nominal operating condition with some non-linearities but at the same time, it is faster than conventional controllers and improves the reactive power of the system, it is represented as a transfer function. The configuration of a POD controller comprises of the gain block, the washout filter block, and double stage lead-lag phase compensators. The output of the POD controller provides further damping by shifting oscillation modes to the left side of the plane thus improving stability [49].

Many corrective control strategies have been proposed to adapt the power order of HVDC links following a disturbance. The basic proportional-integral (PI) controllers is the simplest [50] together with more advanced control strategies, this will maintain acceptable system performances for a wider range of working conditions. The PI controller comprises of one pole and one zero. The single pole is seen as the integrator and eliminates steady-state error while the zero improves the stability margins.

A PD controller comprises of one zero, and is used in systems with integration to offer better stability margins with the addition of phase lead and a faster step response thus improving damping [51]. A causal PID controller consists of two poles and two zeros between them. The one pole is an integrator and the other is at high frequency which prevents increasing noise and extremely large step signals. The PID is a simple controller up to second order where the

parameters are tuned for optimum results. This controller is frequently used in industry and it is closely related to the lead/lag compensator [51] [52].

A lead/lag controller is represented with a lead and a lag compensator connected in series, consisting of two poles and two zeros, with the zeros between the poles. The lag compensator adds phase lag, slows down the response and improves disturbance rejection. The lead compensator has the zero before the pole and adds phase lead, improves damping, improves the phase margin and speeds up the response [52]. For that reason, the lead/lag controller was selected to be used in the POD transfer function as this study focuses on improving damping hence, enhancing stability.

5.2.1 POD Design Criteria

There are a number of criteria that must be accounted for in the designing a POD controller including:

- Pole-placement: The closed-loop poles related to the inter-area modes should be placed in the left half of the complex s-plane in order to confirm their stability and shorter recovery time [4]. The root locus method with the sensitivity calculated using the residues is also effective, as it shows the sensitivity of the scalar feedback between output and input and provides the overall picture of the modes in the system so one can analyse the system holistically [24]. Chilali et al [53] and Ramos et al [54] describe regional pole placement criterion as a design objective which provides sufficient damping for all oscillation modes of interest.

- Damping ratio: A minimum damping ratio must be sustained for critical modes but different utilities have different minimum values (Australian utilities with a damping ration of 0.05). But low frequencies inter-area modes (related to small signal stability) require higher damping ratios of greater than 0.1. [55].

- Settling or mode decay or recovery time: The oscillations must settle out in a chosen time specified by the operating guidelines of a certain utility. The settling time in some countries are specified as damping criteria in the time domain. [55]

- Robustness: Robust control handles uncertain system parameters and disturbances outside the nominal operating point therefore making the controller more flexible [56].

- Control effort: Minimisation of control effort is essential to effectively utilise the dynamic range available for the highly expensive power electronic HVDC actuators with

very limited short-term overload capacity. Since the performance of the HVDC modulation controllers depends on its parameters and different feedback signals to effectively minimise faults [43].

- Controller structure: If there are multiple HVDC links in a system with individual PODs, it is important that the PODs are designed in a coordinated way to achieve the overall design specifications effectively; since there is a risk that the controller would not work in unison requiring larger control effort. The HVDC controllers of different devices must not interact unfavourably. The multi variable approach to control design can solve this problem much better than sequential design [55].

The choice of technique is situation specific and one technique cannot address all the design specifications therefore a detail analysis needs to be performed.

5.3 Model Predictive Control

Model predictive control is based on the optimisation of a plant model by using a cost minimising technique. It predicts the operation of the plant for a finite time horizon and manipulates the necessary input variables to achieve the set points of the plant.

It is suitable for power systems due to its complex nature as it makes use of multiple variables to optimise the output. This MPC considers the constraints on the control effort while calculating the predicted control action which will have a positive contribution to stability enhancement especially with a constraint network [45].

5.3.1 The MPC controller

The basic MPC controller has set-points and a feedback signal from the plant as illustrated in Figure 32. The controller predicts the most optimised input to the plant so that the feedback signal can return to its set-point while predicting future events [57] . However the MPC has additional benefits which are outlined below:

- It can be used to handle a multivariable system.
- Permits constraints to be enforced on both the manipulated variable in order to operate closer to constraints.
- Permits time delays, inverse response, difficult dynamics, changing control objectives and sensor failure (predictive) [40].

The number of each subclass of signals specifications such as manipulated variables and unmeasured disturbance is seen in Figure 32.

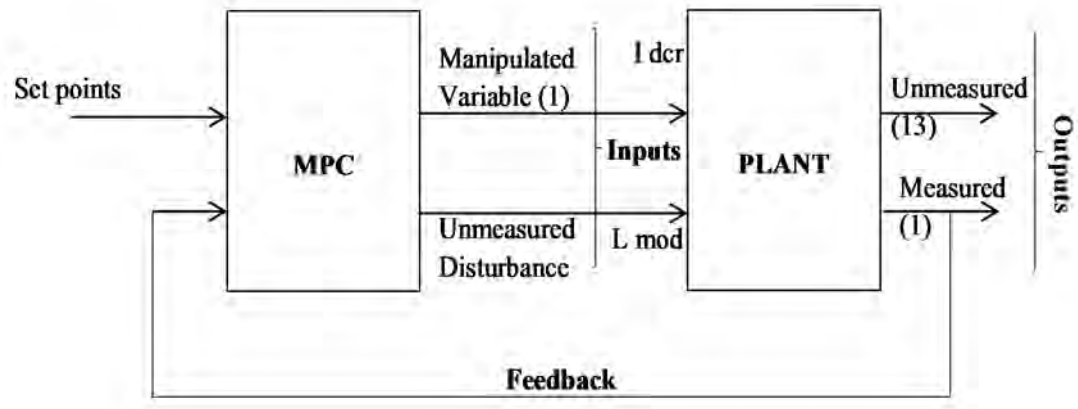

Figure 32: MPC Structure

5.3.2 Types of signal used

The descriptions of the signals used in the model predictive controller are:

5.3.2.1 Input signals

The MPC supports three types of input signals [58] but this design only incorporated two types of input signals .i.e. the Manipulated Variables and Unmeasured Disturbances. The controller uses changes in the load on bus 9 (Figure 20) as the unmeasured disturbance and the rectifier current at the manipulated variables. The manipulated variable may have plant constraints; in this case, there is a limit on the amount power (20 MW) that the converter can produce. The MPC takes account of these constraints in its prediction calculations.

5.3.2.2 Output signals

The output signals include the measured outputs, which are used as the feedback signal, and the unmeasured outputs.

- Measured outputs: The controller uses the real power measured on the AC tie line and the voltage angle difference between bus 7 and bus 9 (as per Figure 20).
- Unmeasured outputs: The unmeasured outputs are the outputs of the system that are not used by the controller to main stability, but are useful in understanding the impact on the system.

5.3.3 Model and Horizon

The control interval (or time-step), the control horizon and the prediction horizon are important for the controller, where the:

- The control interval sets the duration between changes of the manipulated variable.
- The prediction horizon is the number of control intervals for which the outputs must be optimised over a time duration.
- The control horizon is the number of control intervals for which the manipulated variable must be optimised over a time duration [58].

The ability of the controller to ensure stability is based on the length of the predictive horizon and the constraints which drives the state to a certain value at the end of the prediction horizon.

5.3.4 Cost Function

The cost function penalises deviations of the predicted control output from a reference trajectory and it predicts the deviations of each output over a predicted horizon. This cost function as seen in Equation 13, calculates the weighted sum of squared deviations from its reference. The goal of the controller is to minimise $\boldsymbol{Vy(k)}$ in Equation 13. Bemporad et al defines the cost function used in the MPC prediction to be [58]:

$$Vy(k) = \sum_{i=1}^{P} \sum_{j=1}^{ny} \{ j [rj(k+i) - yj(k+i)] \}^2 \quad (13)$$

Where

k is the current sampling interval

$(k + i)$ is a future sampling interval (within the prediction horizon)

P is the number of control intervals in the prediction horizon

ny is the number of plant outputs

j is the selected output

The term $[rj(k + i) - yj(k + i)]$ is a predicted deviation for output j at interval k + 1. On every discrete time instant k the MPC algorithm calculates a sequence of control actions that minimises a certain cost function over a time horizon P.

The cost function was implemented to adapt the current order of the rectifier of a LCC HVDC as the predictive control scheme. The objective is to reduce the loading of the AC tie line when exposed to various operating conditions. The current order of the LCC HVDC is the control input of the proposed controller. Two alternative cost functions are considered based on the input-output controllability analysis involving its residue and the location is based on the dominant oscillation path. The cost functions are:

$$Vy(k) = \sum_{i=1}^{P} \{ j\,[Power_{pf2}(\text{L110 km3})] - [Power_{pf2}(\text{L110 km3})_{ss}] \}^2 \quad (14)$$

$$Vy(k) = \sum_{i=1}^{P} \{ j\,[Vangdifference_{B7\text{-}B9}(k+i)] - [Vangdifference_{B7\text{-}B9\,ss}] \}^2 \quad (15)$$

Equation 14 shows the cost function where the real power across the AC tie line (L110 km3 on the receiving side of the transmission line) is selected as the output. Equation 15 shows the voltage angle difference across the AC corridor (voltage angle difference between bus 7 and bus 9).

5.3.5 Tuning/Weighting of the MPC controller

Most controllers need to be tuned correctly so that the system can return to its nominal or steady state. There are many adjustable parameters in predictive control such as weighting [59]. Weighting can be divided into three types, i.e. input weights, rate weights and outputs weights. The output weights determines the accuracy in which the selected output tracks its set point while the rate weights force the controller to make smaller more cautious adjustments of the manipulated variables, the input weight on the other hand minimises the weighted sum of the manipulated variables from its nominal value [58]. The output weights are set on the measured signal and the input weights are set such that the system can return to its nominal state. i.e. both were set to 1.

5.4 Results

The following methodology was adopted for the work:

- The two area AC network is implemented and the performance specifications of this network is established by detailed modelling to represent an unstable network with the damping of the inter area mode being negative. The studies involved time domain fault analysis and eigenvalue analysis.

- A parallel HVDC link is connected across bus 7 and bus 9 and the changes in damping are studied. This study also involved time domain fault analysis. A disturbance is introduced

and cleared in order to move the system out of steady state operating condition causing the rotors in the two areas to exchange the excess energy generated by the fault.

- A POD is introduced to the unstable base network as supplementary control and two different feedback input signals are tested for effectiveness, the results are graphical displayed and analysed.

- Two different MPC cost functions are integrated into the unstable base case network and the same two feedback signal are tested for effectiveness in terms of stability enhancements. The MPC is tuned accordingly in order to get the desired stable system. The results are graphically displayed and analysed for interpretation.

5.4.1 Analysis of the Base network with HVDC integrated

This study system with the HVDC link integrated is referred to as the base case network with the details captured in Appendix A. The base case network is manipulated (by overloading the AC tie lines) to produce an unstable network and the inter area mode is the mode of interest for the study. Figure 33 illustrates the damping ratio and frequency of the associated eigenvalues from the study. The red line on Figure 33 shows the minimum damping ratio before the mode becomes unstable. The eigenvalue conjugate of this unstable inter area mode is 0.2296 -3.7926i and 0.2296+3.7926i respectively which correlates to a frequency of approximately 0.60 Hz.

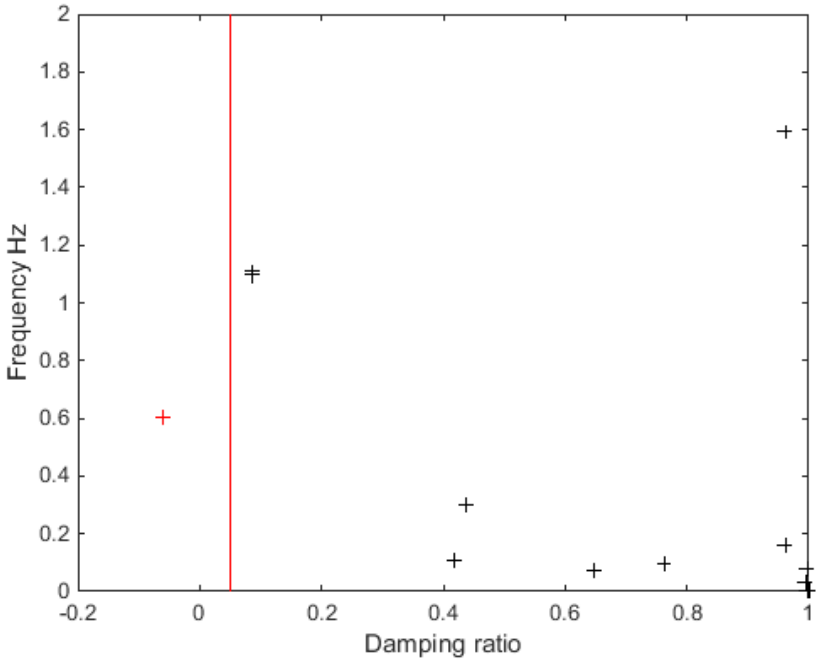

Figure 33: Eigenvalue analysis of the unstable network

Bode plots is a useful tool when designing a controller as it shows this unstable mode in the frequency domain with a peak magnitude as seen in Figure 34. The gain and phase approach is a method used in designing PODs where the inter area mode of oscillation is minimised. The gain and phase compensation required from the controller is commonly used in a single input single output (SISO) system with one dominant mode. This technique is simple, yields low order controllers and leads to exact pole-placement [60].

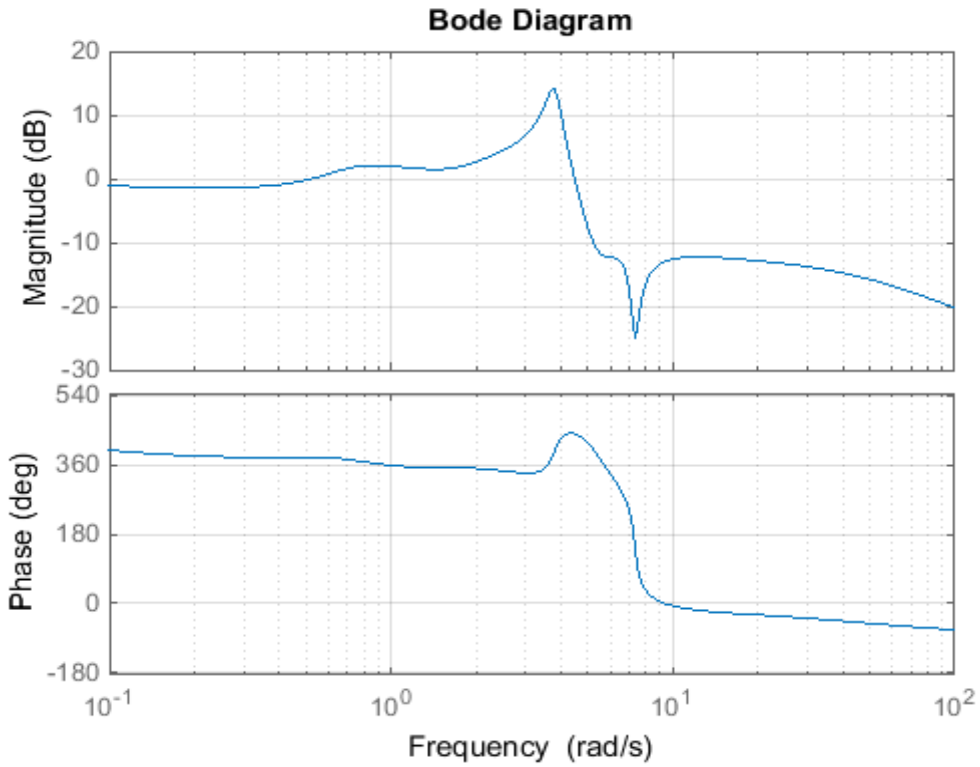

Figure 34: Bode plot of the unstable network

The root locus was, however, considered the most appropriate tool for designing a controller as this method allowed the assessment of all the oscillation modes at once. Each point on the locus represents an increase in the gain of 0.2, within the range from 0 to 10 [24]. The residues indicate the eigenvalue's movement for a small gain and good separation between critical poles and zeros is important to obtain acceptable eigenvalue movement as the gain increases. Since the residue relates the input to the output of the model. It can be used to indicate the sensitivity of the controller's output to its input/ manipulated variable. Table 6 shows different output/control signals that were tested in terms of its observability and controllability but if the residue is 0, it is either unobservable or uncontrollable or both with the input as the DC current to the rectifier.

Table 6: Comparative analysis of the residue of the inter area mode

Output Signal	Eigenvalues	Residue	Residue Angle
Speed Gen 1	0.2296 - 3.7926i	0.0005 + 0.0019i	75º
	0.2296 + 3.7926i	0.0005 - 0.0019i	-75º
Real Power Line	0.2296 - 3.7926i	-0.7713 + 0.7102i	137º
(Between bus 7 and 9)	0.2296 + 3.7926i	-0.7713 - 0.7102i	-137º
Angle Difference	0.2296 - 3.7926i	-0.1815 + 0.1579i	139º
(Between bus 7 and 9)	0.2296 + 3.7926i	-0.1815 - 0.1579i	-139º

As a result, it is evident that the real power and the voltage angle difference between bus 7 and bus 9 is more observable and controllable compared to the residue of the speed output on generator 1, which is approximately 0. The control signal selected is the power flow, however the compensator was designed for the voltage angle difference as well to illustrate the difference in effectiveness and confirm the selection of the feedback signal.

According to Rogers [24], for negative feedback, the locus leaves the pole with an angle equivalent to the complement of the residue angle. For negative feedback, the compliment of the angle of residue for real power and voltage angle difference is 43° and 41° respectively. This indicates that negative feedback cannot be used to stabilise a mode as seen in Figure 35.

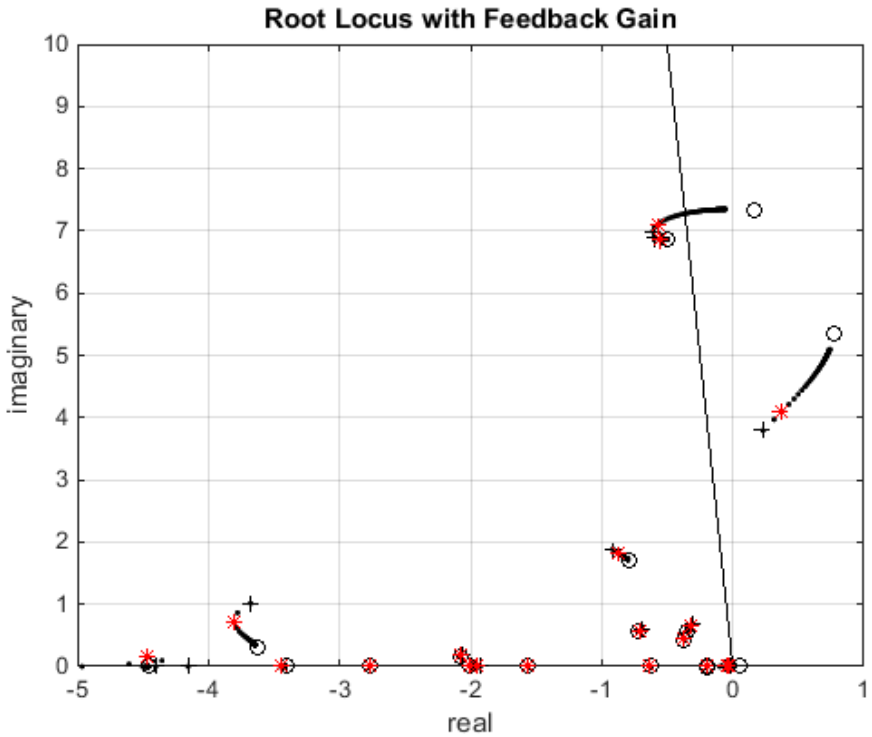

Figure 35: Root locus with negative feedback

5.4.2 Analysis of the Base network with a POD integrated

The supplementary controller was used to move the unstable mode by moving the poles to the left half of the plane. Decent separation can be attained by a suitable choice of feedback signals or by retuning existing controllers in the system [22]. The feedback control signals that were reviewed are real power on the AC intertie (L10km as per Figure 20) and voltage angle difference (between bus 7 and bus 9 as seen in Figure 20). The sensitivity of the system to dynamic feedback can be achieved through the POD where the system stability is taken back to steady state or nominal operating point.

This transfer function consists of a washout filter and a lead/lag compensator. The washout filter eliminates the effect of the steady state voltage magnitude and the control moves at high frequencies. The lead/lag compensator has the effect dragging the poles into the left half plane. The poles and zeros must be designed correctly such that they bring damping to the inter area mode. The lead compensator adds up to 90 degrees and with positive feedback at the inter area frequency; it is then used to stabilise the mode. This is seen in the following POD transfer function :

$$G(s) = K\left(\frac{Tw}{1+sTw}\right)\left(\frac{1+sT2}{1+sT1}\right)\left(\frac{1+sT2}{1+sT1}\right) \quad (16)$$

The transfer function has the following parameters for the selected signals.

Table 7: POD transfer function details

Term	Real Power	Angle
T1	0.04	0.05
T2	0.02	0.02
Tw	10	10
K	0.6	2.4

5.4.2.1 Real power control signal

The root locus plot seen below in Figure 36 shows how the POD transfer function with the real power as the feedback signal, brings stability by moving the pole from the right to the left side of the plane. The sensitivity of the output to parameter changes is visible. As a result, any slight change of the gain will cause the system to respond drastically. The damping ratio has improved to 0.36 (as seen in Figure 37) which is a significant improvement and is visible in the impulse response (time domain simulation) which relates the mode decay time of an oscillation after an event. The mode decay time in Figure 38 is approximately 26s and it is a major improvement

when compared to the unstable base case in Figure 38. Figure 39 shows the comparison of impulse response of the base case system integrated with the POD and the unstable base case. With the integrated POD, the real power signal settles about 26s after the event and the base case remains unstable.

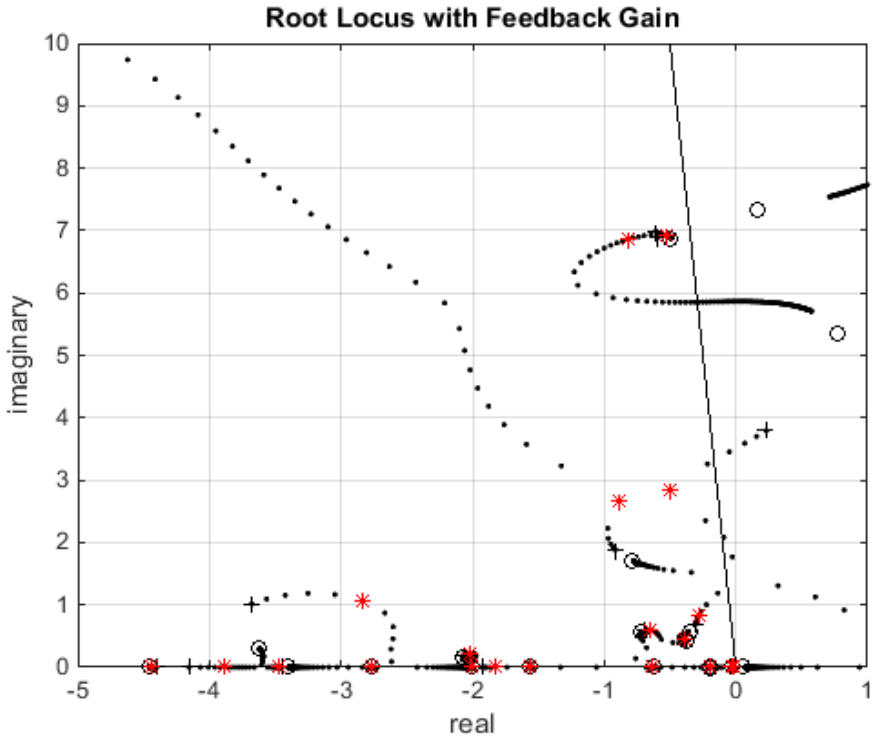

Figure 36: Root locus with POD – Real Power signal

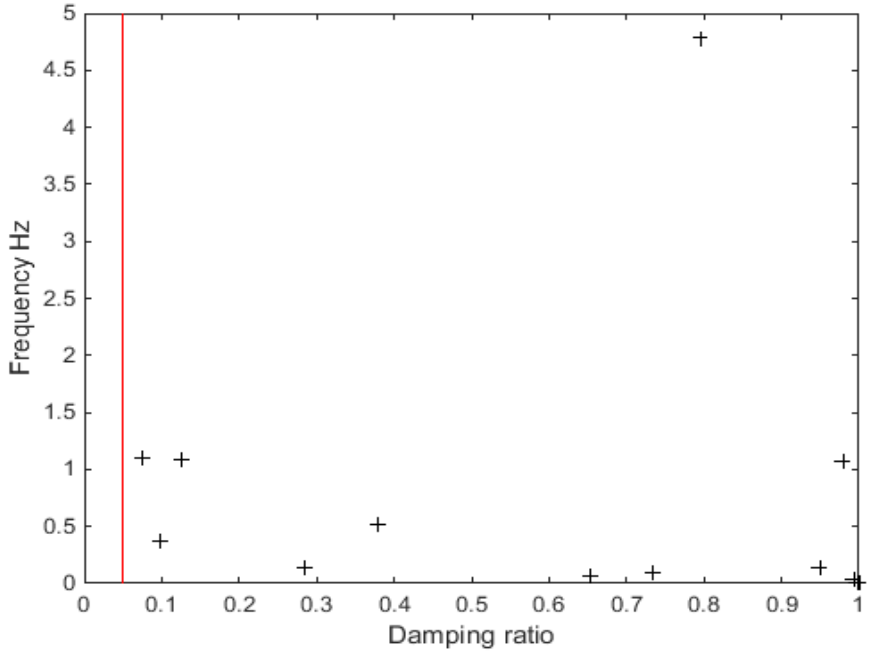

Figure 37: Eigenvalue analysis of the network with POD - Power signal

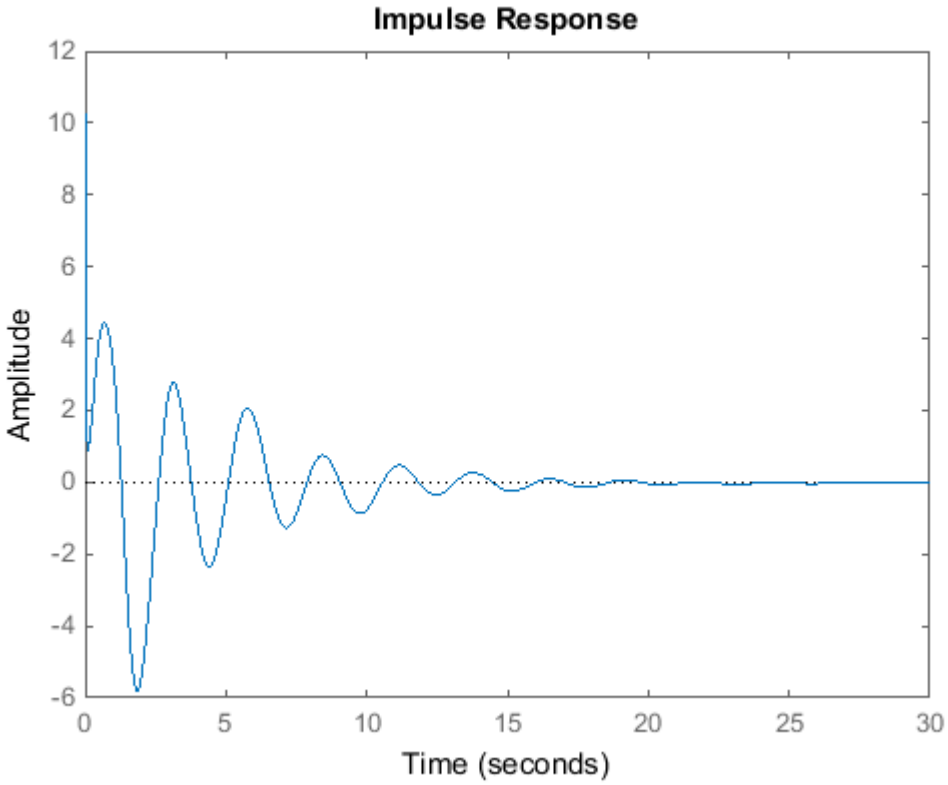

Figure 38: Impulse response with POD - Power signal

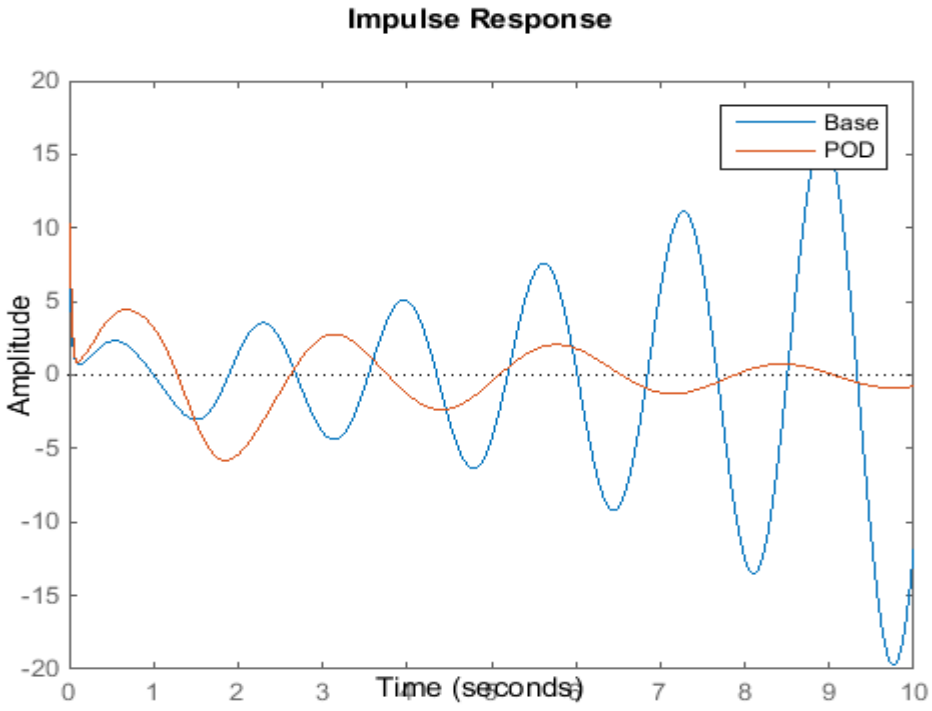

Figure 39: Impulse response with and without POD - Power signal

Hence, the effectiveness of the POD with the real power control signal does enhance the stability of the system.

5.4.2.2 Voltage angle difference

According to Figure 40, the root locus shows that the selected voltage angle difference feedback signal is less sensitive to parameter changes such as the gain. The root locus also shows the movement of the poles from the right side to left side of the plane thus bringing stability to the system. The eigenvalue analysis shown in Figure 41 shows an increase in damping ratio of 0.42 of the inter area mode which again correlates to a reduction in the mode decay time of 5s as the power of system settles in 21s after the event (fault or step change). This is seen in the time domain response plots in Figure 42. Figure 43 shows the comparison of responses of the base case system integrated with the POD and the unstable base case. With the integrated POD based on the voltage angle difference feedback signal, the real power settles about 21s after the event and the base case remains unstable.

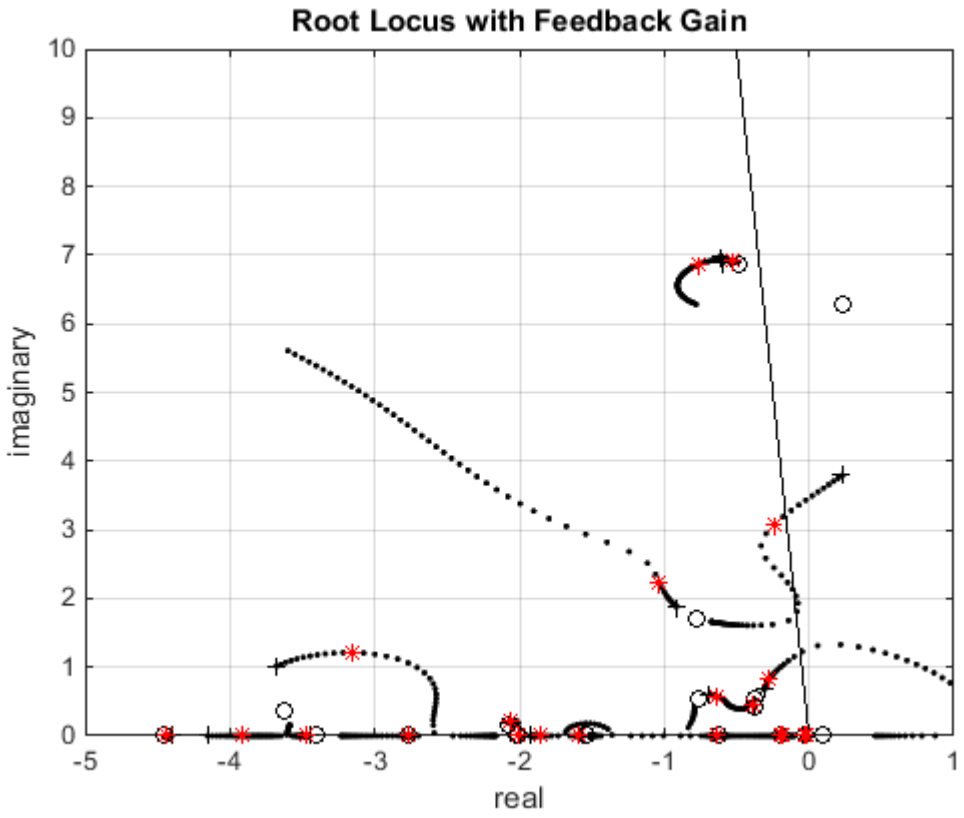

Figure 40: Root locus with POD - Voltage angle difference signal

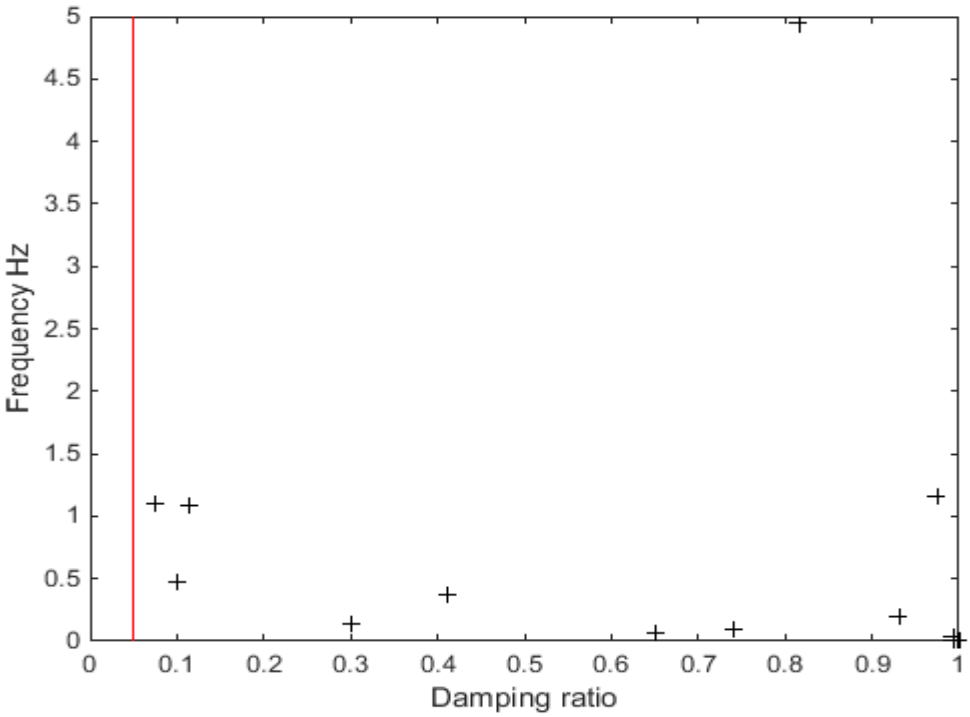

Figure 41: Eigenvalue analysis with POD - Voltage angle difference signal

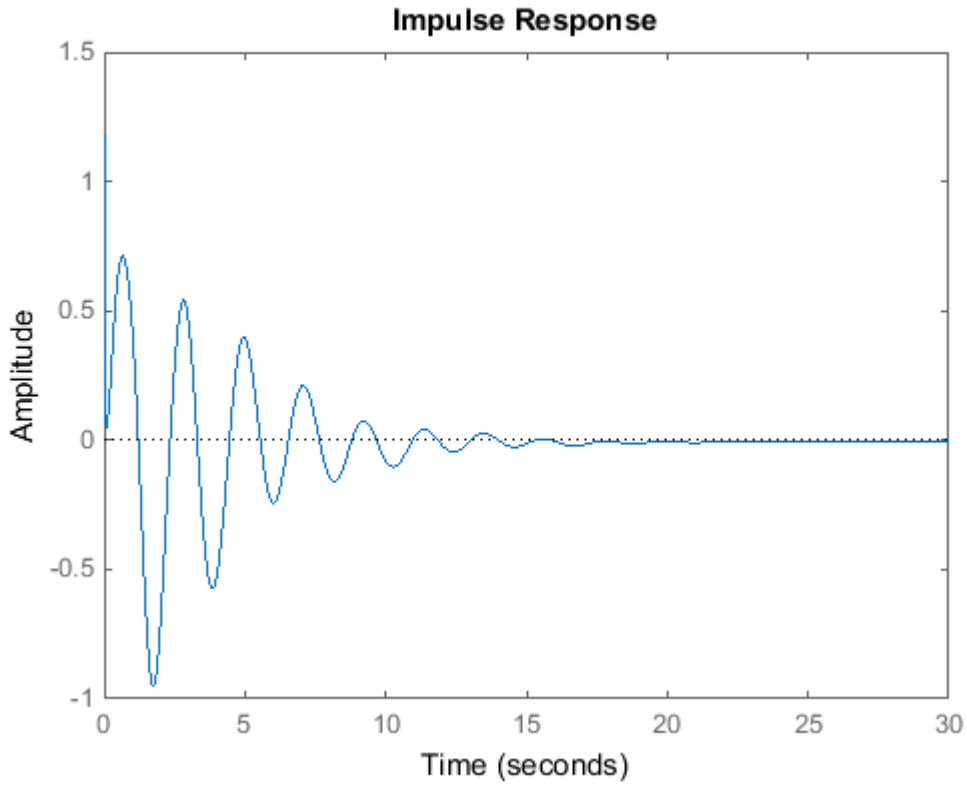

Figure 42: Impulse response with POD - Voltage angle difference control signal

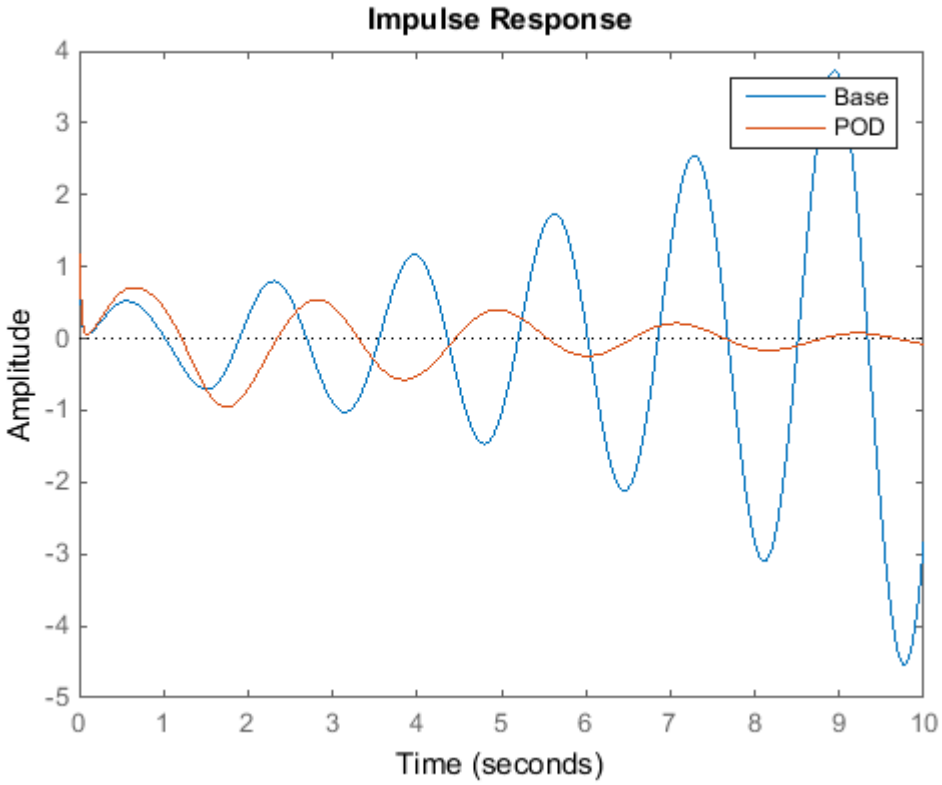

Figure 43: Impulse response with and without POD - Voltage angle difference signal

5.4.3 Analysis of the Base network with a MPC integrated

The MPC uses a code (as seen in Appendix B) with a cost function (Equation 14 and 15) to generate trends representing the responses of the modulated load (on Bus 7 in Figure 20) at 1 s for duration of 0.1s. Equation 14 and Equation 15 show the cost functions with the real power and the voltage angle difference as a feedback signal respectively in order to control it. The two cost functions are simulated and the results of the two cost functions are discussed below while the MPC parameters are tuned according to the values seen in Table 8:

Table 8: The parameters of the MPC

Parameters	Quantity
Constraints on the manipulated variable	Min = 0;Max = 20; RateMin = -1; RateMax = 1
Weighting on manipulated variable	1
Rate Weight	0.1
Prediction horizon	10
Control horizon	3
Nominal values	Appendix A

5.4.3.1 Cost function with Real Power and Voltage angle difference as the feedback signal

The current order to the rectifier is the manipulated variable and the Figure 44 shows how the current order drops due to the impulse/event but quickly moves towards the steady state set point. This impulse on the modulated load (bus 7) is referred to as the unmeasured disturbance and it is used to take the system out of steady state. This unmeasured disturbance is seen in both (top and bottom) graphs in Figure 44. Both MPC cost functions (Equation 14 and 15) have similar responses but the MPC based on the voltage angle difference shows increased performance as there is more control action observed to correct the deviation from its steady state value as seen in Figure 44 (bottom).

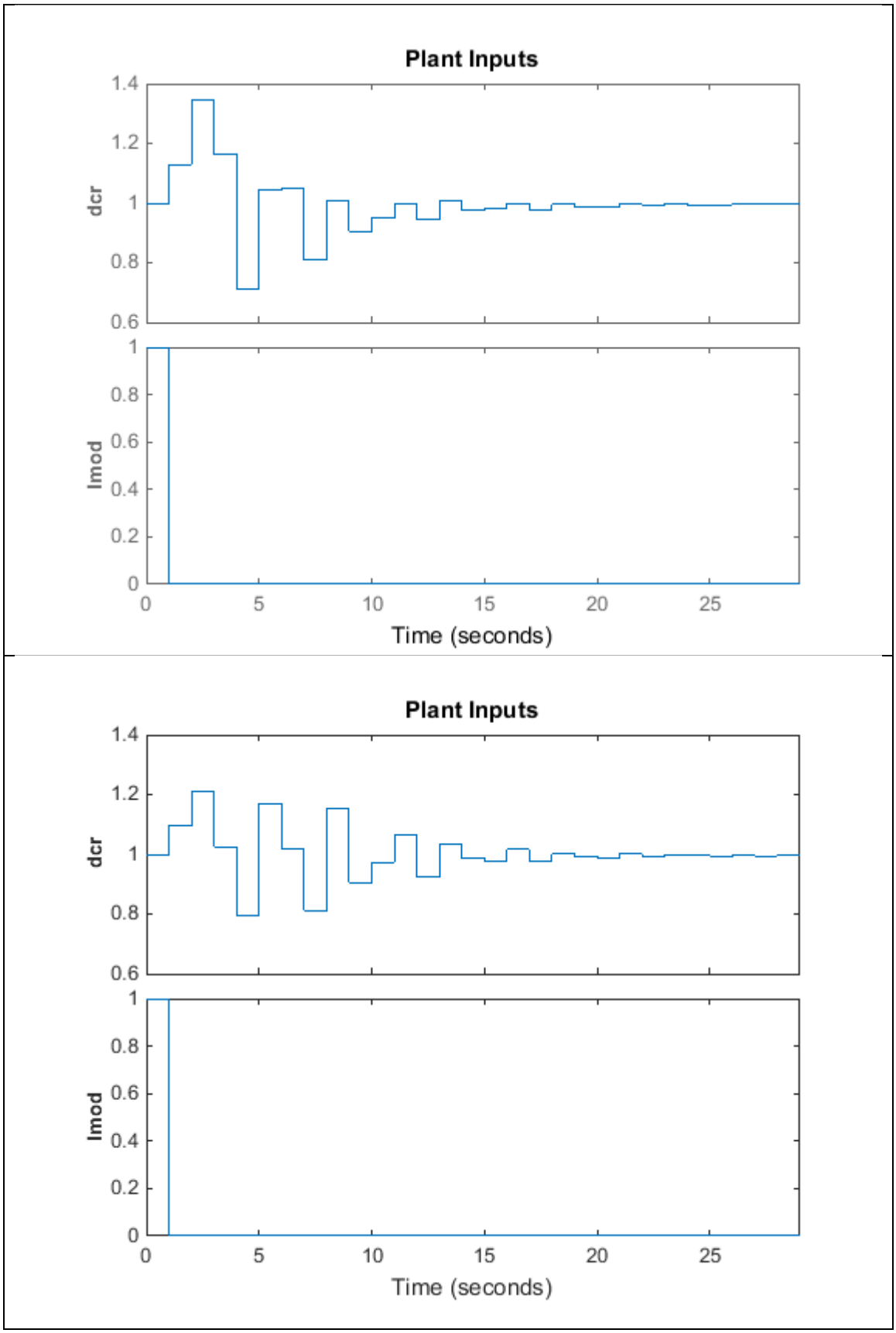

Figure 44: The MV and UD response Real power (top) and voltage angle difference (bottom)

The outputs which are described below in Table 9 show the description and the location of the observed real power.

Table 9: The Output code descriptions as per Figure 20

Location	Buses	code	Output name
Line10km	B6 to B7	Pf 1_5	Line sending Real power
Line110km	B7 to B8	Pf1_6	Line sending Real power
Line110km 2	B7 to B8	Pf1_7	Line sending Real power
Line10km	B6 to B7	Pf2_5	Line receiving Real power
Line110km	B7 to B8	Pf2_6	Line receiving Real power
Line110km 2	B7 to B8	Pf2_7	Line receiving Real power
Line110km 1	B8 to B9	Pf2_13	Line receiving Real power
Line110km 3	B8 to B9	Pf2_14	Line receiving Real power
Line10km 1	B9 toB10	Pf2_15	Line receiving Real power

These responses that are seen in Figure 45 show the effectiveness of the MPC. Both graphs shown in Figure 45 shows the quick real power (through the AC tie line) recovery to its steady state value. Similarly, the four generator speeds are observed to behave in the similar way. At every discrete time instant k, the MPC algorithm calculates a sequence of control actions that minimises the cost function (Equation 14 and 15) over a time horizon P. The real power (*pf2* L110km3*)* and the voltage angle difference (*Vangdiff B7-B9*) deviation from its steady state is reduced where the first control action of this sequence is applied at instant *k* and at the next time step the process is repeated. These two MPC cost functions with different feedback signals have similar and comparable responses therefore showing the effectiveness of the MPC.

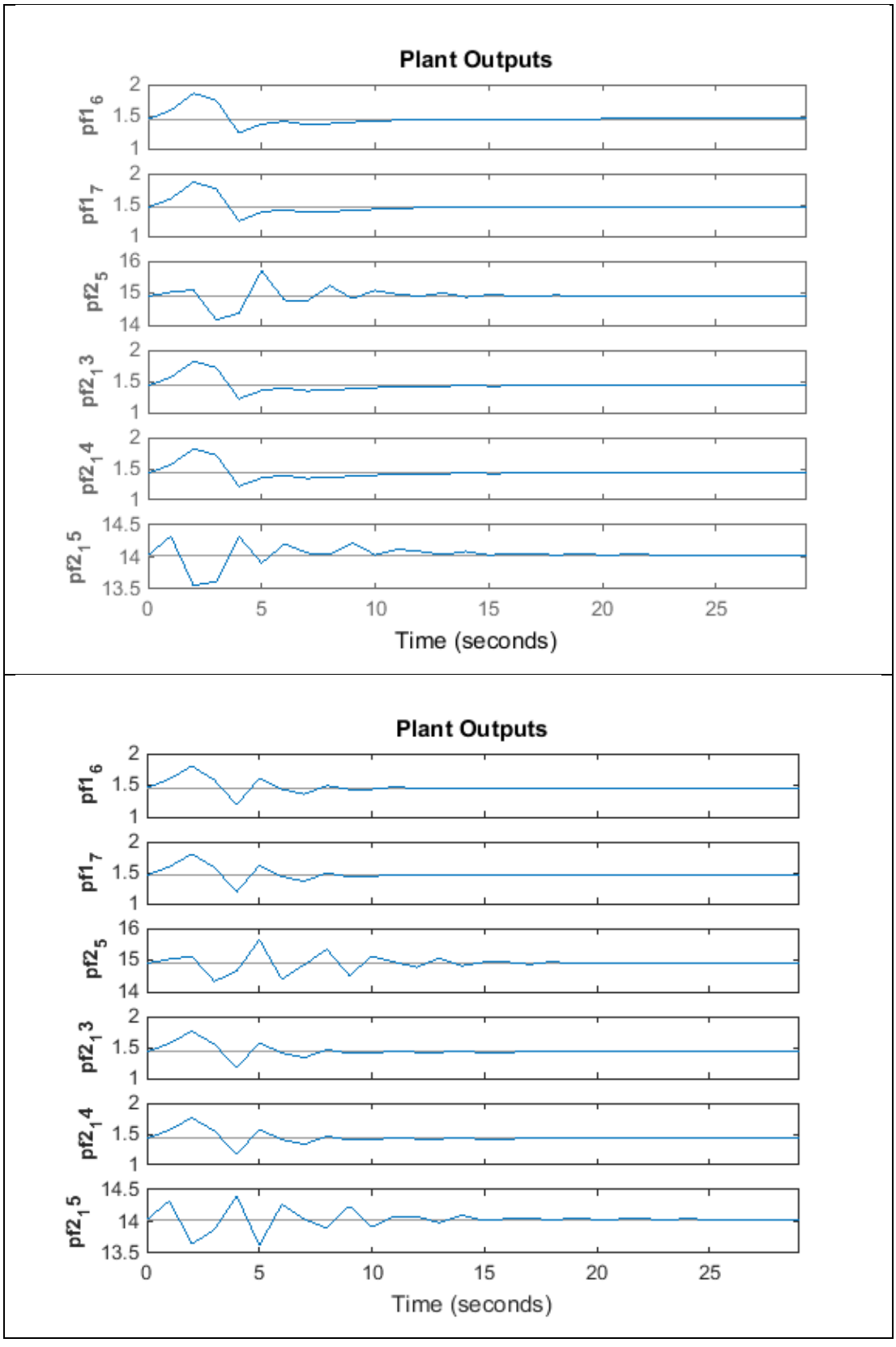

Figure 45: Plant outputs time domain response: Real power (top) and Voltage angle difference (bottom)

Figure 46, however shows the response of the DC voltage at the Rectifier (Vdcr) and the DC voltage at the Inverter (Vdci) after the event. The dynamic response of the system after the event increased the power transfer from area 1 to area 2. The first cost function (Equation 14) using real power across the AC tie has poorer performance as it does not restore the DC voltage of the rectifier to almost its pre event value (504.466 kV) but on the other hand, the second cost function (Equation 15) restores the DC voltage of the Rectifier to its pre event value (504.267 kV) in a shorter period of time (Figure 47) thus showing superior performance over the first MPC (Figure 46) based on the real power feedback signal. However, the MPC is effective in automatically relieving the burden on the AC lines by adapting the HVDC current order to rectifier after the event or disturbance. Consequently to this, the amplitude of the rotor angle oscillations of the generators decreased with MPC based predictive control therefore enhancing small signal stability.

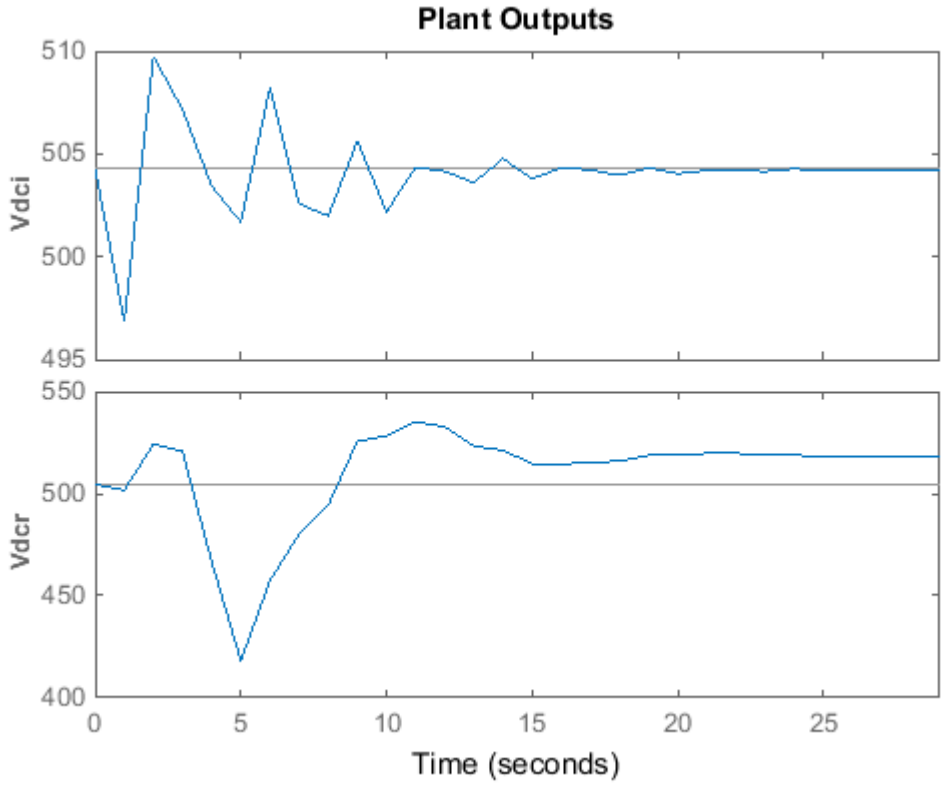

Figure 46 : The HVDC voltage: Rectifier and Inverter of the Real power

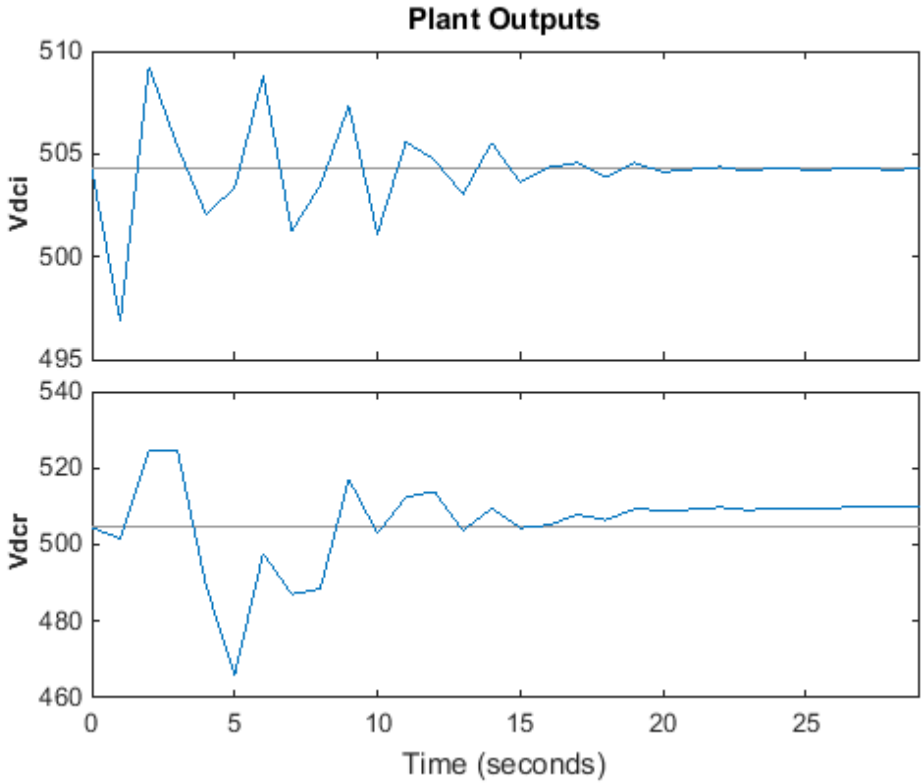

Figure 47: The HVDC voltage: Rectifier and Inverter of the voltage angle difference

Figure 48 shows the behaviour of the DC line current which is the current order to the rectifier after the event. It is clearly evident from Figure 48, that the voltage angle difference feedback signal has a lower overshoot value of 1.22 compared to the real power which is 1.35 but this control action is understood from the real power output response as seen in Figure 49 where the real power (Pf2-13) is observed and the comparison of the two feedback signals clearly show that the voltage angle difference is a more effective signal in enhancing stability as the mode decay time is approximately 18s (voltage angle difference across the AC corridor) compared to 23s (Real power across the AC tie) however the feedback signals does not really return to the exact steady value but close enough to be accepted as seen in Figure 49.The lower overshoot of the voltage angle difference feedback signal is again seen in the Figure 49 and this will prevent the premature activation of over current protections on transmission lines.

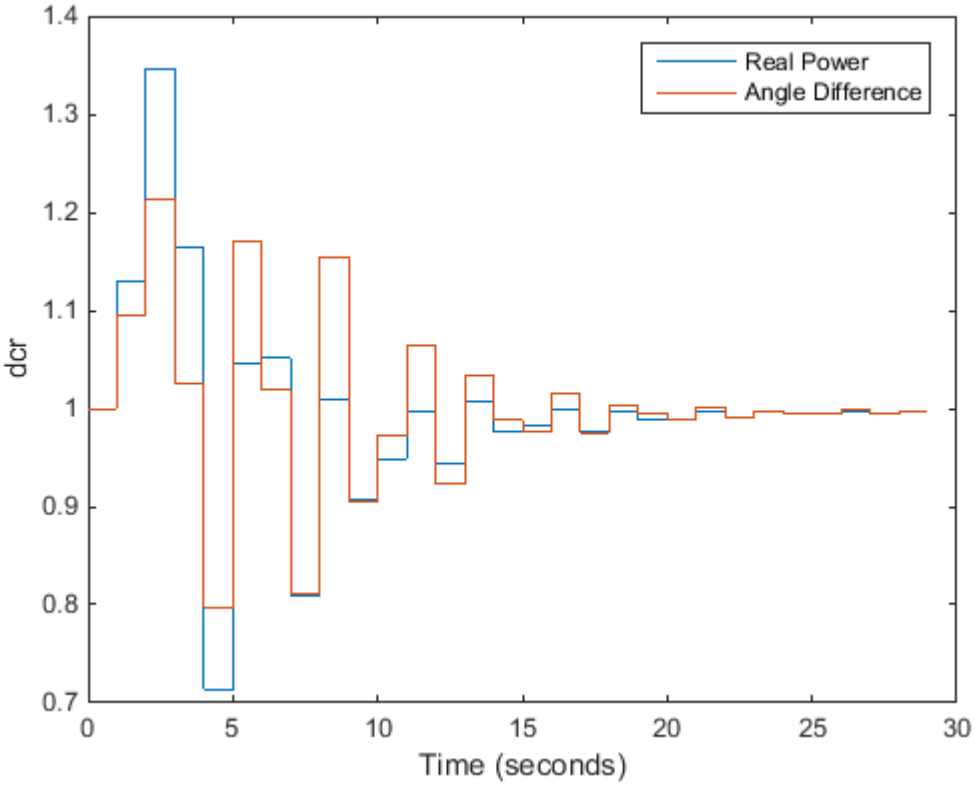

Figure 48: A Comparison of the two feedback signals input response

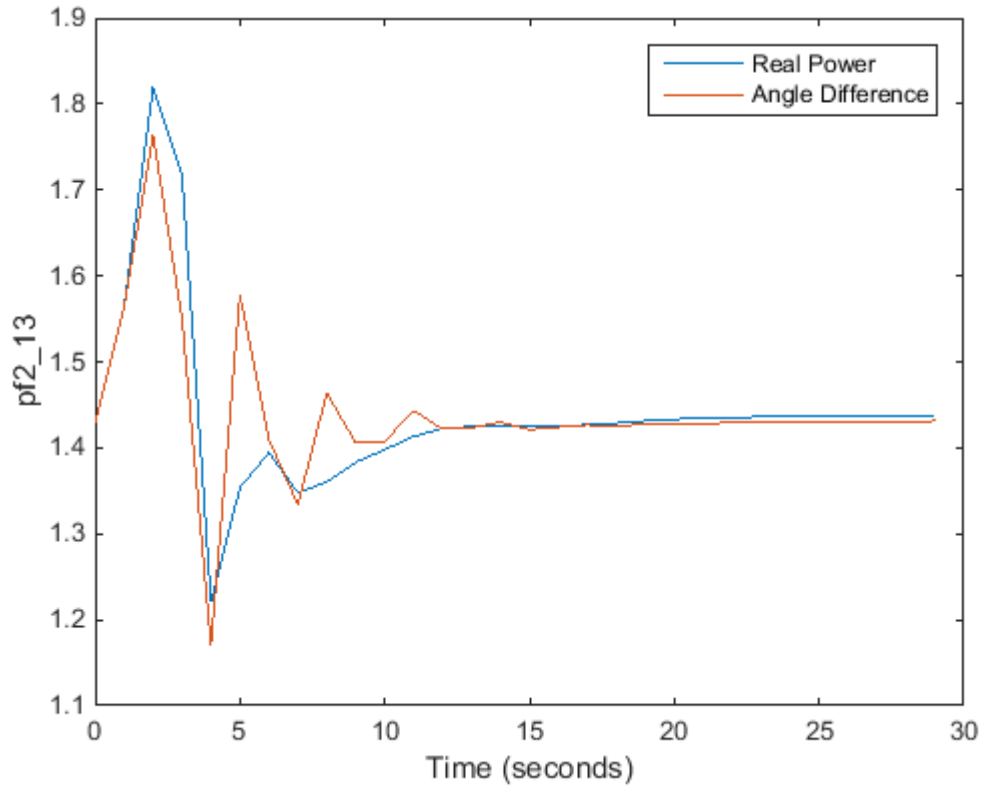

Figure 49: A Comparison of the two feedback signals real power output response

5.5 Conclusion

This chapter focused on the use of supplementary control using power oscillation damping control and predictive control through a single Monopolor LCC HVDC link integrated into a simulated unstable system (as seen with an eigenvalue conjugate of 0.2296 ∓ 3.7926i). The main design specifications were outlined together with POD controller design techniques and it was established that the choice of technique is situation specific and one technique cannot address all the design specifications. The POD design represented as a transfer function was outlined and explained with simulations studies; the two feedback control signals were demonstrated. Stability studies using root locus and time domain plots showed the effectiveness of the POD with two different feedback signals i.e. real power across the AC tie and voltage angle difference across the AC corridor. The voltage angle difference feedback signal proved to be more sensitive to changes in the system and contributed to improving system stability, hence increased damping and reduced settling/mode decay time after an event was evident. The mode decay time provides a good reflection of the controller's effectiveness therefore a comparison of the two controllers is possible despite the fact that the controller's operational characteristics differ. The mode decay times from the simulations in this chapter are outlined in the Table 10 below.

Table 10: Mode decay times of the feedback signals

Generator	**POD**		**MPC**	
Feedback signals	**Real Power at L110 km1)**	**Voltage angle difference AC corridor**	**Real Power at L110 km1)**	**Voltage angle difference AC corridor**
Mode decay time	26s	21s	23s	18s

The reduced mode decay time confirmed that the inter area mode moved to the left half of the complex plane thus making the system stable. This chapter then shows the description of the MPC characteristics and parameters together with the two cost functions using the same feedback signal that was used for the POD simulations, so that comparison studies could be conducted. Both MPC cost functions showed that the MPC is effective in minimising the change of the loading level in the AC tie-lines by adapting the HVDC current order to the rectifier. Consequently to this, the amplitude of the rotor angle oscillations of the generators decreased with MPC based predictive control in place thus enhancing small signal stability. Similar trends for the POD, showed the inter area mode moving from the right plane to the left complex plane resulting in a more stable AC system

The MPC using the feedback signal of the voltage angle difference, like the POD, also proved to contribute significantly to system stability and its adaptive functionality to system constraints contributes to its performance. The MPC allows the system to operate so close to its power constraint. The two types of supplementary controllers operate differently but with the same goal, i.e. to improve the damping of the system. This chapter shows that the MPC with the voltage angle difference (across the AC corridor) as the selected feedback signal is a more effective controller as the recovery time of 18s after an event reflect so. The conclusion from the simulations in this chapter does demonstrate that the MPC is capable due to its ability to handle complex multi variable systems with constraints, by using cost function algorithms to perform predictions of future plant behaviour and calculating the suitable corrective control actions needed to take the predicted output as close as possible to the target value which is the steady state value. Additional research is necessary to determine the effectiveness of the MPC following large events such as critical faults in larger networks.

6 CONCLUSION

The aim of this research is to investigate the small signal and transient stability for the application of a parallel LCC HVDC link onto a simple grid and then develop supplementary controllers for small signal stability enhancement. As a result fundamental understanding is achieved for further investigation on the larger Southern African network. This research provided a comprehensive literature review of the High voltage direct current (HVDC) where the basic fundamental principles of HVDC, the three different types of technologies and the control characteristics were described. Stability in power systems is related to a condition where all the generators remain in synchronism with each other and therefore the basic principles relating to small signal stability were discussed to get a basic understanding of the problem in order to determine where and how to use LCC HVDC with supplementary control for an effective solution.

Small signal stability analysis is based on the eigenvalue technique which shows the behaviour of the power system and was used to investigate the small signal oscillations including their mode shape, controllability observability and participation. Methods to determine the dominant oscillation path are reviewed in literature to establish the best location for the parallel LCC HVDC link to increase the effectiveness of the LCC HVDC link integration. With the integration of parallel HVDC links, a reduction of power over the AC tie line is shown and the transmission power angle across the corridor decreases thus resulting in an increase in synchronising torque. According to the responses of the study, the inter area mode of the system became unstable when the system was heavily loaded resulting in the HVDC link relieving the AC tie lines from carrying more power thus stabilising the inter area-mode. The integration of the parallel HVDC link has increased the damping ratio and decreased the mode decay time of the inter-area oscillation mode.

Supplementary controllers, including the POD and the MPC, were modelled and integrated into the same two area network in an unstable state. The POD was implemented through a transfer function where the system stability was taken back to steady state or nominal operating point. . Two controller feedback signals (i.e. real power across the AC tie and real power across the AC corridor) were tested for effectiveness in terms of its sensitivity, but the voltage angle difference proved to have superior performance. From Table 10, it can be seen that the POD with the voltage angle difference (across the AC corridor) as the selected feedback signal has a lower the setting time (mode decay time) of 21s after an event than the real power feedback signal, of 26s.

The first MPC cost function using real power across the AC tie has inferior performance to the MPC using the voltage angle difference as it does not restore the DC voltage of the rectifier to almost its pre event value (504,466 kV) but however the second MPC cost function restores the DC voltage of the Rectifier to its pre event value (504.267 kV) in a shorter period of time (18s) thus showing higher performance over the first MPC based on the real power (23s). These MPC Cost functions penalises deviations of the predicted control output from a reference trajectory and it predicts the deviations of each output over a predicted horizon.

Similar to the POD, increased damping ratio and a reduction in settling time after an event was demonstrated. From Table 10, it can be seen that the MPC with the voltage angle difference (across the AC corridor) as the selected feedback signal has the setting time (mode decay time) of 18s resulting in a more stable AC system. The tuning of the MPC cost functions contributed positively to its effectiveness by setting the constraints and weighting of the manipulated variables in relation to its control and prediction horizon. The MPC is therefore capable and does not require history of the possible contingencies

The MPC is demonstrating corrective action in automatically relieving the burden on the AC lines by adapting the HVDC current order to the rectifier after changes in operating conditions, thus proving its effectiveness. The amplitude of the rotor angle oscillations of the generators decreased with an integrated HVDC link and MPC based corrective control in place thus enhancing stability of HVAC grids. Additional research is necessary to determine the effectiveness of the MPC method for corrective control particularly, following large events like critical faults on a more complex network.

It is then evident that the hypothesis of this research has been proven correct and as Eskom is pursuing investing in HVDC lines at various locations, this research presented will be applied to those new cases so that all the advantages of HVDC links can be considered in the terms of the techno-economic feasibility. Eskom will then have the full advantage of transporting bulk power but at the same time mitigating the effects of small signal stability on the National grid and internationally (with the Southern African Power Pool (SAPP)).

7 REFERENCES

[1] Eskom Holdings SOC Pty Ltd, Transmission Development Plan 2015 to 2024, Gauteng: Eskom, 2015.

[2] P.Kundur, Power system stability and control, 1st Edition, McGraw-Hill, 1994.

[3] Eskom Power Series, HVDC Power Transmission , Basic principles, planning and convertor technology, Gauteng: Crown Publications, 2012, ISBN 978-0-9921781-0-9.

[4] Cigre Task Force 7 of Advisory Group 1 of Study Committee 38, "Analysis and Control of Power System Oscillation," CIGRE, Paris, 1996.

[5] B.Berry and A.Edwards, "Control shift training presentation - Dynamic stability and WAMS: Small signal stability," Eskom Holdings SOC Pty Ltd, Gauteng, 2013.

[6] T.Bayliss and B.Hardy, Transmission and Distribution Electrical Engineering, 4th ed., Gauteng: Elsevier Ltd, 2012, ISBN: 978-0-08-096912-1.

[7] J.Arrillaga, Y.Liu and N.Watson, Flexible Power Transmission: The HVDC Options, John Wiley and Sons, 2007.

[8] H.Ryan, High Voltage Engineering and Testing, 3rd ed., Institute of Engineering and Technology, 2014.

[9] ABB, "Caprivi Link," [Online]. Available: http://new.abb.com/systems/hvdc/references/caprivi-link. [Accessed 03 03 2015].

[10] C.Barker, HVDC for beginners and beyond, Gauteng: ALSTOM Grid Worldwide, 2010.

[11] R.Rabbani, A.F.Zobaa and G.A.Taylor, "Applications of Simplified Models to Investigate Oscillation damping control on the GB Transmission system," in *AC and DC Power Transmission(ACDC2012),10th IET International Conference*, Birmingham, 2012.

[12] M.Szechtman, T.Wess and C.V.Thio, "The Cigre HVDC benchmark model - a new proposal with revised parameters," *Cigre working group 02 (Control in HVDC Systems) of study committee,* vol. 14, pp. 61-66, 1994.

[13] M.O.Faruque, Y.Zhaung and V.Dinavahi, "Detailed modelling of CIGRE HVDC benchmark system using-PSCAD/EMTDC and PSB/SIMULINK," *IEEE,* vol. 21, no. 1, pp. 378 - 387, 2006.

[14] M.Szechtman, T.Wess and C.V.Thio, "A benchmark model for HVDC system studies," *Cigre working group 02 (Control in HVDC Systems) of study committee,* no. IET, pp. 55-73, 1991.

[15] V.K.Sood, K. Narendra, K.Khorasani and R.Patel, "EMTP modelling of CIGRE benchmarkbased HVDC transmission system operating with weak AC systems," *Power Electronics, Drives and Energy Systems for Industrial Growth, 1996., Proceedings of the 1996 International Conference on,* vol. 1, 1996.

[16] Y.Song, X.Wang and M.Irving, Modern Power Systems Analysis, 1st ed., Springer, 2009.

[17] W.J.PalmIII, System dynamics (2nd ed.), McGraw-Hill Science/Engineering/Math, 2010.

[18] G.Gajjar and S.Soman, "Power System Oscillation Modes Identifications: Guidelines for Applying TLS-ESPRIT Method," *International Journal of Emerging Electric Power Systems,* vol. 14, no. 1, pp. 57-66, 2013.

[19] M.Larsson, P.Korba, W.Sattinger and P.Owen, "Monitoring and Control of Power System Oscillations using FACTS/HVDC and Wide-Area Phasor Measurements," *Cigre,* vol. B5, no. 119, 2012.

[20] E.Zhou, "Power oscillation flow study of electric power systems," *International Journal of Electrical Power & Energy Systems,* vol. 17, no. 2, p. 143–150, 1995.

[21] S.Mvuyana, "Small Signal Stability Assessment of the Eskom Network based on Measurements," in *Eskom PowePlant Engineering Institute (EPPEI) - First Student Conference ESKOM Academy of Learning*, Gauteng, 2014.

[22] A.M.Kulkarni and U.P.Mhaskar, "Power Oscillation Damping Using FACTS Devices : Model Controllability, Observability in Local Signals and Location of transfer function zeros," *IEEE,* vol. 21, no. 1, 2006.

[23] M.Farsangi, Y. H.Song and K.Y.Lee, "Choice of FACTS Device Control Inputs for Damping Interarea Oscillations," *IEEE,* vol. 19, no. 2, pp. 1135 - 1143, 2004.

[24] G.Rogers, Power System Oscillations, Kluwer Academic Publishers, 1999.

[25] S.Mvuyana, J.VanColler and T.Modisane, "Identification of Power System Oscillation Paths in Power System Networks," in *22nd South African Universities Power Engineering Conference*, Kwazulu Natal, 2013.

[26] L.Vanfretti, Phasor measurement-based state estimation of electric power systems and linearized analysis of power system network oscillations, PhD Thesis, Rensselaer Polytechnic Institute, Troy, NY, 2009.

[27] Y.Chompoobutrgool and L.Vanfretti, "On the persistence of dominant inter-area oscillation paths in large-scale power networks," *Power Plants and Power Systems Control,* vol. 8, no. 1, pp. 150-155, 2012.

[28] J.F.Hauer, D.J.Trudnowski and J.G.DeSteese, "A Perspective on WAMS Analysis Tools for Tracking of Oscillatory Dynamics," in *IEEE Power Engineering Society General*

Meeting,2007,IEEE, Tampa,FL, 2007.

[29] Y.Chompoobutrgool and L.Vanfretti, "Identification of Power System Dominant Inter-Area Oscillation Paths," *IEEE Transactions on Power Systems,* vol. 28, no. 3, 2013.

[30] J.Chow, Time-Scale Modeling of Dynamic Networks with Applications to Power Systems, Springer Berlin Heidelberg, 1982.

[31] M.Klein, G.J.Rogers, S.Moorty and P.Kundur, "Analytical investigation of factors influencing power system stabilizers performance," *IEEE Transactions on Energy Conversion,* vol. 7, no. 3, pp. 382 - 390, 1992.

[32] EPRI, "Adaptive HVDC Control System and Power Oscillation Damping Methods: Theoretical Developments," *EPRI,* vol. 1024321, 2012.

[33] R.L.Cresap and W.A.Mittelstadt, "Small Signal Modulation of the Pacific HVDC Intertie," *IEEE,* Vols. PAS-95, no. 2, pp. 536-547, 1976.

[34] A.Fuchs, Coordinated Control of Power Systems with HVDC links, Austen: M.S., University of Texas, 2014.

[35] R.Witzmann, "Damping of inter area oscillation in large interconnected systems," Siemens, Erlangen.

[36] F.Shi, J.Wang and P.R.Jinan, "The HVDC Supplementary Control for AC/DC inteconnected Power Grid Based on the Hamilton energy function," *ELEKTRONIKA IR ELEKTROTECHNIKA,,* vol. 20, no. 4, pp. 1392-1215, 2014.

[37] H.Weng and Z.Xu, "WAMS based robust HVDC control considering model imprecision for AC/DC power system using sliding mode control," *Electric Power Systems Research,* vol. 95 , no. 2013, pp. 38-46, 2102.

[38] K.Tomiyama, M.Sato, K.Yamaji, M.Sekita and M.Goto, "Power Swing Damping Control by HVDC Power Modulation in an ac/dc Hybrid Transmission system," *Electrical Engineering in Japan,* vol. 124, no. 3, pp. 10-18, 1998.

[39] A.E.Hammad, "Stability and Control of HVDC and AC Transmissions in Parallel," *IEEE,* vol. 14, no. 4, 1999.

[40] None, "Model Predictive Controller," Chemical Engineering department, 2002.

[41] D.Q.Mayne and J.B.Rawlings, Model predictive control:theory and design, Madison,Wis.:Nob Hill Pub.,, 2009.

[42] J.J.Ford, G.Ledwich and Z. Dong, "Efficient and robust model predictive control for first swing transient stability of power systems using flexible AC transmission systems devices," *IET Generation, Transmission and Distribution,* vol. 2, no. 5, pp. 731-742, 2008.

[43] Y.Phulpin, J.Hazra and D.Ernst, "Model predictive control of HVDC power flow to improve transient stability in power systems," in *IEEE International Conference on Smart Grid Communications (SmartGridComm)*, Brussels, 2011.

[44] M.Glavic, D.Ernst and L.Wehenkel, "A reinforcement learning based discrete supplementary control for power system transient stability enhancement," *Engineering Intlligent System for Electrical Engineering and Communications,* vol. 13, no. 2, pp. 81-88, 2005.

[45] L.A.Wehenkel, Automatic learning techniques in power systems, Boston: Mass :London Kluwer Academic, 1998.

[46] S.P.Azad, R.Iravani and J.E.Tate, "Damping InterArea oscillation based on a Model Predictive Controller MPC HVDC Supplementary controller," *IEEE,* vol. 28, no. 3, pp. 3174 - 3183, 2013.

[47] S.P.Azad, R.Iravani and J.E.Tate, "Damping Inter-Area Oscillations Based on a Model Predictive Control (MPC) HVDC Supplementary Controller," *IEEE Transactions on Power Systems,* vol. 28, no. 3, pp. 3174 - 3183, 2013.

[48] J.H.Chow and K.W.Cheung, "A toolbox for power system dynamics and control engineering education and research," *IEEE Transactions on Power Systems,* vol. 7, no. 4, pp. 1559 - 1564, 1992.

[49] A. N.Hussain, F.Malek, M. A. Rashid and M. F. H. A. Malek, "Performance Improvement of PowerSystem Stability by Using Multiple Damping Controllers Based on PSS and the UPFC," *International Journal of Engineering and Technology (IJET),* vol. 5, no. 4, pp. 3257-3269, 2013.

[50] J.Hazra, Y.Phulpin and D.Ernst, "HVDC control strategies to improve transient stability in interconnected power systems," in *Power Tech,IEEE Bucharest*, Bucharest, 2009.

[51] None, "http://www.eng-tips.com/viewthread.cfm?qid=370916," 4 September 2014. [Online]. [Accessed 2 Oct 2015].

[52] I.Bruce, "Control Systems," in *ELEC ENG 4CL4: Lecture 15*, Prentice Hall, 2004.

[53] M.Chilali, P.Gahinet and P.Apkarian, "Robust pole placement in LMI regions," *Automatic Control, IEEE Transactions,* vol. 44, no. 12, pp. 2257-2270, 1999.

[54] R.A.Ramos, L.F.C.Alberto and N.G.Bretas, "A new methodology for the coordinated design of robust decentralized power system damping controllers," *IEEE Transaction on,* vol. 19, no. 1, pp. 444-454, 2004.

[55] B.Pal and B.Chaudhuri, Robust Control in Power Systems, New York: Springer Science+Business Media, Inc., 2005.

[56] J.Ma, T.Wang, W.Yan and Z.Wang, Design of wide-area robust damping controller based on the non-convexstable region for inter-area oscillations, Beijing: State Key Laboratory of Alternate Electrical Power System with Renewable Energy Sources,North China Electric Power University, 2013.

[57] None, "https://en.wikipedia.org/wiki/Model_predictive_control," Wikipedia, 2015. [Online]. [Accessed 18 August 2015].

[58] A.Bemporad, M.Morari and L.Ricker, Model Predictive Control Toolbox- Getting Started Guide, Natick,MA: MathsWorks, 2015.

[59] J.M.Maciejowski, Predictive control: with constraints, Harlow : Prentice Hall, 2002.

[60] I.Postlethwaite and S.Skogestad, Multivariable feedback control: analysis and design 2nd ed, Chichester: Wiley & sons, 2005.

[61] X. Huanhai; Z. Huang; K.Zhuang ; L.Cao;, "Applications of Stability-Constrained Optimal Power Flow in the East China System," *Power Systems, IEEE Transactions on,* vol. 25, pp. 1423-1433, 2010.

[62] A.Fuchs, S.MarieThoz, M.Larsson and M.Morari, "Grid stabilization through VSC-HVDC using wide area measurements," in *PowerTech,2011 IEEE Trondheim*, Trondheim, 2011.

[63] M.Glavic, D.Ernst and L.Wehenkel, "A reinforcement learning based discrete supplementary control for power system transient stability enhancement," *Engineering Intelligent System for Electrical Engineering and Communications,* vol. 13, no. 2, pp. 81-88, 2005.

[64] L.Busoniu, R.Babuska and B.DeSchutte.D.Ernst, Reinforcement learning and dynamic programming using function approximators, Florida,USA: FL:CRC Press,Baca Raton, 2010.

[65] C.Druet, D.Ernst and L.Wehenkel, "Application of Reinforcement Learning to Electrical Power Systems Closed-Loop Emergency Control," in *4th European Conference on Principles and Practice of Knowledge Discovery in Databases (PKDD 2000)*, Lyon, 2000.

[66] Y.Chompoobutrgool and L.Vanfretti, "A fundamental study on damping control design using PMU signals from dominant inter-area oscillation paths," *2012 North American Power Symposium (NAPS),* pp. 1-6, 2012.

[67] M.Djukanovic, M.Khammas and V.Vittal, "Sequential synthesis of structural singular value based decentralized controllers in power systems "," *Power Systems, IEEE Transactions,* vol. 14, no. 2, pp. 635 - 641, 1999.

[68] H.Xin, Z.Huang, K.Zhuang and L.Cao, "Applications of Stability-Constrained Optimal Power Flow in East China syatem," *IEEE,* vol. 25, no. 3, pp. 1423-1433, 2010.

[69] M.Kahl and T.Leibfried, "Decentralized Model Predictive Control oflectrical power syatems".

[70] M.Peyvandi, M.Zafarani and E.Nasr, "Comparison of Particle Swarm Optimization and the Genetic algoritmn in the Improvement of power system stability of the SSSC based controller," *Journal of Electrical Engineering & Technology,* vol. 6, no. 2, pp. 182-191, 2011.

[71] O.Antoine and J.Maun, "Inter-area oscillations: Identifying causes of poor damping using phasor measurement units," in *Power and Energy Society General Meeting,2012,IEEE*, San Diego,CA, 2012.

[72] G.Zwe-Lee, "A particle swarm optimization approach for optimum design of PID controller in AVR system," *Energy Conversion,IEEE Transaction on,* vol. 19, no. 2, pp. 384 - 391, 2004.

[73] Q.Zhoa and J.Jiang, "A TCSC damping controller design using robust control theory," *Electrical Power & Energy Systems,,* vol. 20, no. 1, pp. 25-33, 1998.

[74] A.C.Zolotas, B.Chaudhuri, I.M.Jaimoukha and P.Korba, "A study on LQG/LTR Control loop for damping Inter area Oscillatons in Power Systems," *Control Systems Technology, IEEE Transactions on,* vol. 15, pp. 151-160, 2007.

[75] L.Vanfretti and J.H.Chow, "Analysis of power system oscillations for developing synchrophasor data applications," in *Bulk Power System Dynamics and Control (iREP) - VIII (iREP),2010 iREP Symposium*, Rio de Janeiro, 2010.

[76] B. Kuo and M.F.Golnaraghi, Automatic control systems, 9th ed./, Illinois: Wiley & Sons, 2010.

[77] N.P.Padhy and S.Panda, "Comparison of particle swarm optimization and genetic algorithm for FACTS-based controller design," *Applied Soft Computing,* vol. 8, pp. 1418-1427, 2008.

[78] B.Kouvaritakis and J.A.Rossiter, "constraint stable generalised Predictive Control," *Control Theory and Applications:IEE Proceedings D,* vol. 140, no. 4, pp. 243-254, 1993.

[79] D.Q.Mayne and J.B.Rawlings, Model predictive control: theory and design, Madison Wis:Nob Hill Pub, 2009.

[80] A.Pizano-Martinez, C.R.Fuerte-Esquivel, H.Ambriz-Perez and E.Acha, "Modeling of VSC-Based HVDC Systems for a Newton-Raphson OPF Algorithm," *Power Systems, IEEE Transactions on,* vol. 22, pp. 1794-1803, 2007.

[81] M.Larsson, P.Korba, W.Sattinger and P.Owen, "Monitoring and Control of Power System Oscillations using FACTS/HVDC and wide area phasor measurements," *Cigre,* vol. B5, no. 119, 2012.

[82] R.L.Cresap, W.A.Mittelstadt, D.N.Scott, W.A.Mittelstadt and C.W.Taylor, "Operating experience with Modulation of the Pacific HVDC intertie," *IEEE,* Vols. PAS-97, no. 4, pp. 1053-1057, 1978.

[83] J.Shiau, G.N.Taranto, J.H.Chow and G.Boukarim, "Power Swing Damping Controller Design Using an Iterative Linear Matrix Inequality Algorithm," *IEEE Transactions on Control Systems Technology,* vol. 7, no. 3, pp. 371 - 381, 1999.

[84] F.Capitanescu, J. M. Ramos, P.Panciatici, D.Kirshen and M.Marcolini, "State-of-the-art,challenges,and future trends in security constrained optimal power flow," *Electric Power systems Research,* vol. 81, no. 8, pp. 1731-1741, 2011.

[85] G.Farmer and E.Kyriakidesr, "The modelling of damping for power system stability analysis," *Electric Power Components and Systems,* vol. 32, no. 8, pp. 827-837, 2004.

[86] G.S.Zhai, M.S.Ikeda and Y.Fujisaki, "Decentralized H (Infinity) controller design: a matrix inequality approach using a homotopy method," *Automica,* vol. 37, no. 4, p. 565 –572, 2001.

[87] A.N.Hussain, F.Malek, M. A.Rashid and M. F.Haji Abd Malek, "Performance Improvement of Power of System Stability by Using Multiple Damping Controllers Based on PSS and the," *International Journal of Engineering and TechnologyISSN : 0975-4024,* vol. 5, no. 4, pp. 3258-3269, 2013.

8 Appendix A – State Space Model Details

The HVDC system properties for this study are as follows:

- Monopolar ,Twelve pulse converter at both the rectifier and Inverter
- Transmitting Power ∓ 100 MW ,
- Inverter properties: DC voltage of 504.3 kV, with a gamma /extinction angle of 18 deg
- Line current of 0.2 A
- Rectifier properties: DC voltage of 504.466 kV, Alpha angle of 29.3212deg

Table 11 includes the input and output values in the state space model and nominal values used for the controller design where the base is 100 MVA.

Table 11: State Space Model Inputs and Outputs

Details		**Signal Name**	**Description**	**Nominal value pu**
Input				
		b_dcr	DC Line current	0.2
		b_lmod	Load modulation	0
Output				
Location of signal	**Buses**	**Signal Name**	**Description**	**Nominal value pu**
Bus 7 – Bus 9		Vang (3-9)	Voltage angle diff	18.0416
Line110km	B7 to B8	Pf1_6	Line Real power Tx line(i)	1.4607
Line110km2	B7 to B8	Pf1_7	Line Real power Tx line(i)	1.4607
Line10km	B6 to B7	Pf2_5	Line Real power Tx line(j)	14.9139
Line110km1	B8 to B9	Pf2_13	Line Real power Tx line(j)	1.4345
Line110km3	B8 to B9	Pf2_14	Line Real power Tx line(j)	1.4345
Bus 7		V3	Voltage	1
Bus 9		V13	Voltage	1.0518
Bus 7		Vdci	DC Voltage(Inverter)	504.267 kV
Bus 9		Vdcr	DC Voltage(Rectifier)	504.466 kV

9 Appendix B – Controller Design Code

```
% PST Method

% Create statespace model
%a=a_mat; b = b_dcr; c=c_pf2(13,:); d=0; % Power in AC line between bus 7 and 9
a=a_mat; b = b_dcr; c=c_ang(3,:)-c_ang(9,:); d=0; % Angle between bus 7 and 9
%a=a_mat; b = b_dcr; c=c_spd(1,:); d=0;

spssd = stsp(a,b,c,d);
lz = zeros(spssd);

f = linspace(.01,2,100);
[f,mag,ang]=fr_stsp(spssd,f);

% Define the transfer function
% K(1+T1s)/(1+T2s) = ldlg_stsp(K,T2,T1)
% Corner frequencies f1 = 1/T1 f2 = 1/T2
% Kunder uses T1 = 0.55 and T2 = 0.2

T1 = 0.05;
T2 = 0.02;
w1 = 1/T1
w2=1/T2
A = T1/T2;
phase_max = asind((A-1)/(A+1));
omega_m = 1/T2/sqrt(A);
gain_m = sqrt(A);
G = 2.4;

spss1=wo_stsp(10).*ldlg_stsp(G,T2,T1).*ldlg_stsp(1,T2,T1);
```

```
% Determine the Stability of the System with Feedback
sfb=fb_aug(spssd,spss1);

stab_plot(spssd);
stab_plot(sfb);

% Determine the root locus
rlpss=rtlocus(spssd,spss1,0,0.2,10);

% Plot root locus
figure,plot(l,'k+')
hold
plot(lz,'ko')
plot(rlpss,'k.')
axis([-5 1 0 10])
grid
plot(l,'k+')
plot(rlpss,'k.')
dr_plot(0,20,0.05,'k');
plot(rlpss(:,12),'r*')
labxyarg
title('Root Locus with Feedback Gain')

% Step response
r = cell2mat(residue(spssd)');
l2 = l;
r(imag(l2)==0) =[];
l2(imag(l2)==0) =[];

[l2(11:12) r(11:12)];
```

```
r_ang = angle(r(11:12))*180/pi;

cr_ang = r_ang-180;


sys = stsp2ss(spssd);

sys_ss = stsp2ss(spss1);

sys_fb = stsp2ss(sfb);


% C = pid(10,0,2,1/3.1);

% CL1 = feedback(sys,C,1);

CL2 = feedback(sys,sys_ss,1);


figure,step(sys,CL2,10);

figure,step(CL2,20);

figure,impulse(sys,CL2,10);

figure,impulse(CL2,30);

figure,bode(sys,sys_fb,sys_ss),xlim([10^-1 10^2]),grid

%figure,bode(sys),xlim([10^-1 10^2]),grid

% Plant Model

a=a_mat; b = [b_dcr, b_lmod(:,2)]; c=[c_ang(3,:)-c_ang(9,:);
c_pf1(6:7,:);c_pf2(5,:);c_pf2(13:15,:);c_spd(1:4,:);c_v(3,:);c_v(9,:);c_v(13,:);c_Vdci;c_Vdcr]; d=0;

SIMO = ss(a,b,c,d);

SIMO.InputName = {'dcr','lmod'};

%SIMO.OutputName =
{'ang3_9','dcii','dcir','pf1_5','pf1_6','pf1_7','pf1_13','pf1_14','pf2_5','pf2_6','pf2_7','pf2_13','pf2_14','sp
d_1','spd_2','spd_3','spd_4','spd_5','spd_6','spd_7','spd_8','spd_9','v3','v9','v13','Vdci','Vdcr'};

SIMO.OutputName =
{'ang3_9','pf1_6','pf1_7','pf2_5','pf2_13','pf2_14','pf2_15','spd_1','spd_2','spd_3','spd_4','v3','v9','v13','
Vdci','Vdcr'};

SIMO.InputGroup.MV = 1;

SIMO.InputGroup.UD = 2;

SIMO.OutputGroup.UO = [2:4,6:16];

SIMO.OutputGroup.MO = [5];
```

```
% Controller
MPC = mpc(SIMO,1,10,3);

% Constraints
MPC.MV.Min = 0;
MPC.MV.Max = 20;
MPC.MV.RateMin = -1;
MPC.MV.RateMax = 1;

% Weighting
MPC.Weights.MV = {1};
MPC.Weights.ManipulatedVariablesRate = {0.1};

% Nominal
MPC.Model.Nominal.Y = [18.0416 1.46 1.46 14.9 1.43 1.43 14.03 1 1 1 1 1 1 1.05 504.27 504.47]
MPC.Model.Nominal.U = [1 0]

display(MPC)

% Setpoints
refs = [18.0416 1.46 1.46 14.9 1.43 1.43 14.03 1 1 1 1 1 1 1.05 504.27 504.47];

% Disturbance
fault = 0*ones(30,1);
fault(1,1) = 1;

options = mpcsimopt(MPC);
%options.PlantInitialState;
options.UnmeasuredDisturbance = fault;
options.model = SIMO;

% Simulation
```

```
sim(MPC,30,refs,options)
[Y,T,U] = sim(MPC,30,refs,options);
figure,impulse(SIMO)
[y,t,u] = impulse(SIMO,10);
```